Spring 2019

# RESOURCE ESTIMATION AND SIMULATION AT WEST BUTTE IN THE MCDONALD GOLD DEPOSIT NEAR LINCOLN, MONTANA

Jonathan Szarkowski

# RESOURCE ESTIMATION AND SIMULATION AT WEST BUTTE IN THE MCDONALD GOLD DEPOSIT NEAR LINCOLN, MONTANA

by

Jonathan Szarkowski

A thesis submitted in partial fulfillment of the
requirements for the degree of

Master of Science in Geosciences

Montana Tech

2019

# Abstract

The McDonald gold deposit is located in Lewis and Clark County near Lincoln, Montana and is divided into two regions: East Butte and West Butte. Approximately 90% of gold mineralization at McDonald is hosted by quartz-adularia-altered lithic tuff. Low-grade, stratabound, disseminated mineralization within permeable volcanic tuff is the dominant style of mineralization at McDonald. Higher-grade mineralization at West Butte is interpreted to be controlled by subvertical, intersecting vein systems that occur along the 9800' E-W fault. Preliminary gold estimates at West Butte indicated the possibility of a 500 koz gold orebody at an average grade of 7.2 grams per ton or 0.21 troy ounces per ton (opt). The purpose of this project is to develop a gold resource estimate and simulated model of West Butte at the McDonald gold deposit using Maptek Vulcan. A drillhole database was provided for this project, however, previous work indicated significant downhole contamination in reverse circulation (RC) drilling. Domains could not be defined based on logged geologic information, so a grade shell was used to define estimation domains. The grade shell was defined based on a 0.04 Au opt cutoff and only core drilling was considered. Resource estimation of gold at West Butte was conducted in three passes. At a cutoff of 0.06 Au opt, conservative estimates indicate the existence of a 2.75 Mt orebody at an average grade of 0.171 Au opt and a total of approximately 470 koz. Metal loss reports indicate potentially-substantial increases in total ounces if more core drilling takes place to replace contaminated RC drilling. Sequential Gaussian simulation (SGS) was conducted in conjunction with resource estimation of gold at West Butte. Visual discrepancies between the estimated model and the averages of the simulated models delineated regions of high uncertainty within West Butte. It is recommended that more core drilling takes place at West Butte. Angled core drilling should be conducted to better characterize subvertical orientations outlined by previous company geologists, and new exploration drilling should take place to the east and below the project area. It is likely that additional core drilling and replacement of contaminated RC drilling will result in a higher-tonnage orebody at West Butte through the expansion of the grade shell.

# Dedication

*To Pete Knudsen and Chris Gammons,*

*Two professors, two mentors, who I consider to be,*

*Two of my greatest friends.*

## Acknowledgements

# Table of Contents

## List of Tables

## List of Figures

# 1. Introduction

## 1.1. Location

The McDonald gold deposit is located in west-central Montana in Lewis and Clark County, approximately 8 miles east of Lincoln, Montana and 40 miles northwest of Helena, Montana (Figure 1). The McDonald deposit lies near the confluence of Lander's Fork and the Blackfoot River, and can be divided into two regions: East Butte and West Butte (Figure 2).
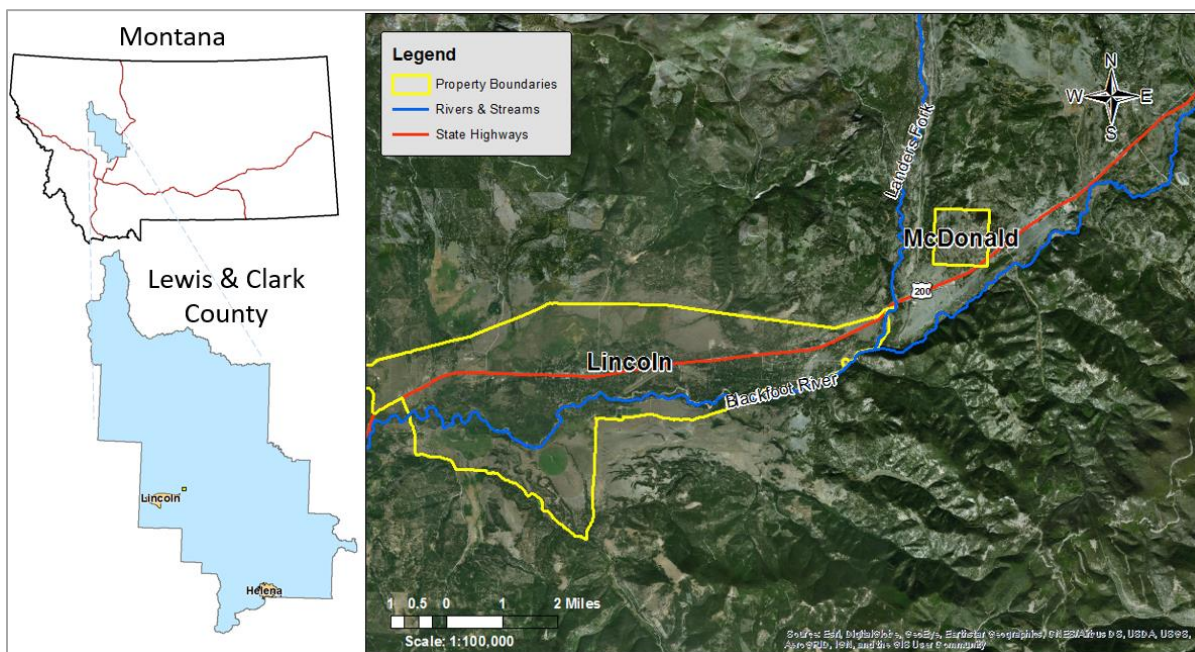


**Figure 1: Location map of the McDonald gold deposit near Lincoln, Montana**
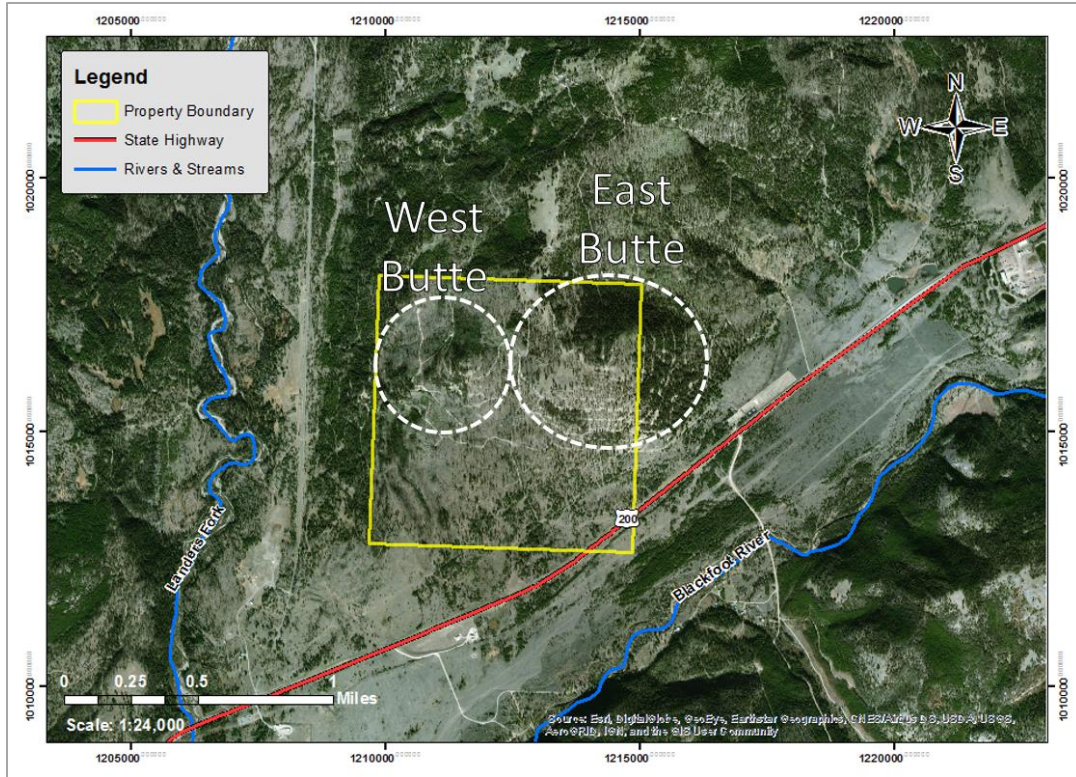
**Figure 2: Site map of the McDonald gold deposit**

## 1.2.    Deposit Geology at West Butte

The following information on the geologic setting and history of the McDonald deposit comes from Bartlett, Enders, Volberding, & Wilkinson's *The Geology of the McDonald Gold Deposit, Lewis and Clark County, Montana* (Bartlett et al., 1995), except where otherwise stated.

### 1.2.1.  Description of Significant Lithologies

The McDonald deposit is hosted within a sequence of layered Tertiary volcanics which overly Precambrian Belt Supergroup rocks (Figure 3 and 4). These layered volcanics dip 20° to the north and include lithologies such as andesite and others (Ta), lithic tuff (Trtl), crystal-rich tuff (Trtcr), and volcaniclastic sedimentary rocks and sinter (Tvs-l and Tvs-u). Overlying these units are biotitic rhyolite tuffs (Trb) that post-date mineralization at the McDonald deposit and Quaternary glacial tills and alluvium (Qal).

EXPLANATION

Contact - mapped or projected, dashed where concealed.

Fault - dashed where mapped or projected, dot-dashed where concealed, ball and pin on downthrown side

| Qal | Quaternary alluvium |
| Qg | Quaternary glacial deposits |
| Tvs-u | Tertiary upper volcaniclastic sediments-predominatelyh conglomerate |
| Trb | Tertiary biotie rhyolite |
| Tvs-ls | Tertiary lower volcaniclastic sediments-Sinter |
| Tvs-l | Tertiary lower volcaniclatic sedimetns-primarily mudstone and siltstone |
| Trtcr | Tertiary crystal-rich rhyolite tuff |
| Trtl | Tertiary lithic-rich rhyolite tuff |
| Ta | Tertiary andesite |
| pC | Precambrian sediments |

27 ⟋ Strike and dip of foliation

**Figure 3: Geologic map of the McDonald site location. Taken from (CAM, 2003)**
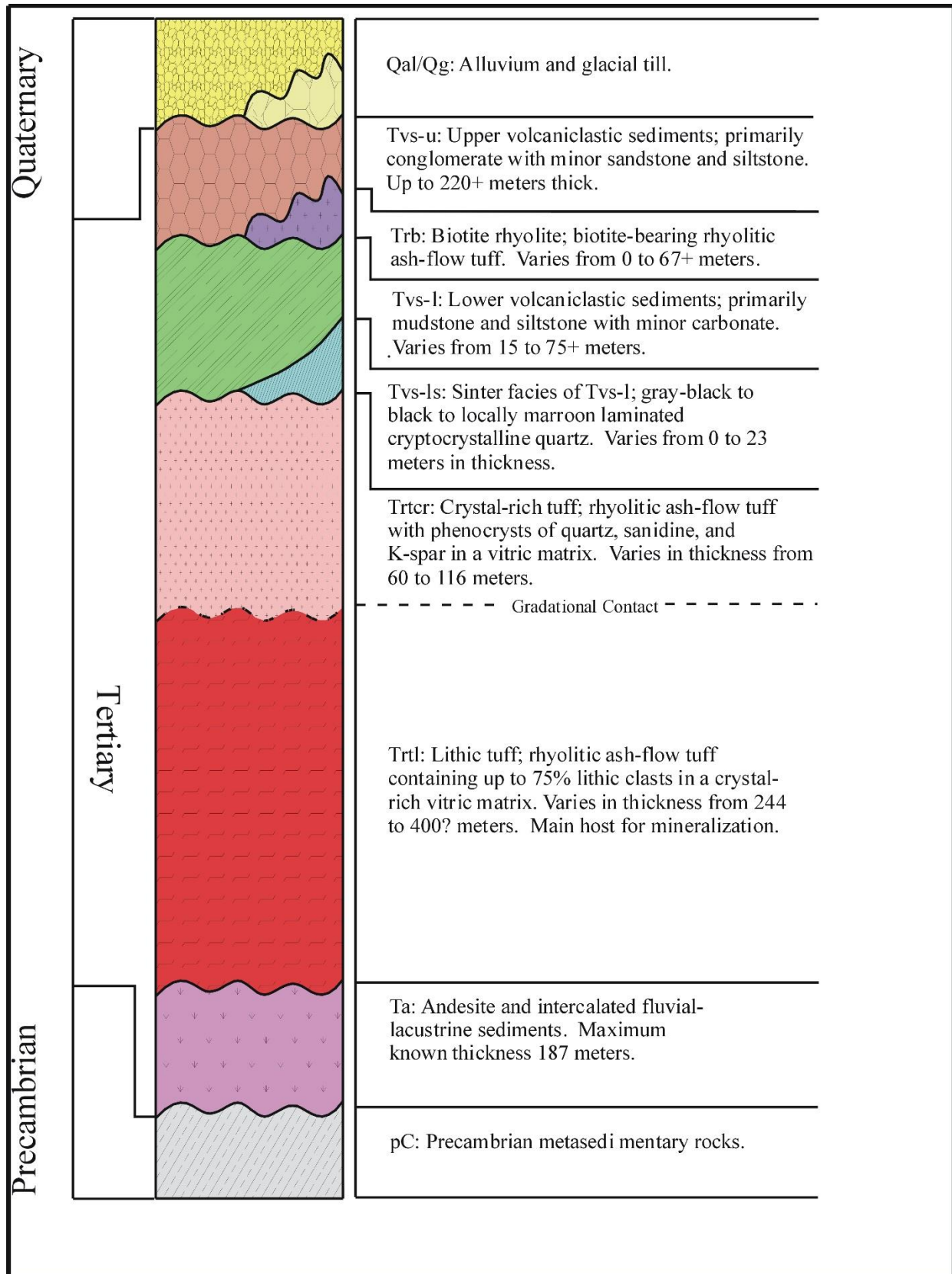
**Figure 4: Stratigraphic section of rocks at the McDonald deposit site location. Taken from (CAM, 2003)**

### 1.2.1.1. Andesite and others (Ta)

Andesite, latite porphyry, and volcaniclastic rocks overlie Precambrian Belt rocks at McDonald, with a thickness of roughly 180 m. The volcaniclastic rocks within this unit are deposited laterally adjacent to the andesite and latite porphyry. This lithology hosts approximately 3% of gold mineralization sampled at the McDonald deposit.

### 1.2.1.2. Lithic tuff (Trtl)

The Tertiary lithic tuff unit is the thickest and most significant lithology present at the McDonald deposit, reaching up to 400 m in thickness and hosting approximately 90% of all gold mineralization sampled at the McDonald deposit. The rhyolitic lithic tuff unconformably overlies Tertiary andesites, is moderately- to strongly-welded, and contains up to 35% lithic fragments, which decrease gradually in abundance up-section. Additionally, the lithic tuff contains up to 20% pumice lapilli and up to 20% quartz and sanidine phenocrysts. The remaining fraction is comprised of vitroclastic matrix. Lithic tuff at McDonald is relatively permeable, exhibiting leaching within pumice layers and containing well-developed joints along bedding planes and vertical orientations.

### 1.2.1.3. Crystal Rich Tuff (Trtcr)

The crystal-rich tuff at McDonald overlies the lithic tuff unit and only slightly differs in composition from the lithic tuff, having a lesser fraction of lithic fragments. This unit is up to 116 m thick and contains approximately 7% of gold mineralization sampled at the McDonald deposit. The contact between the crystal-rich tuff and the lithic tuff is rarely well defined and is often delineated by a 3 – 5% change in the percentage of lithic fragments down-section.

### 1.2.2.  Ore Mineralogy

The McDonald deposit is almost entirely oxidized to a depth of 300 to 350 m below the surface, with minor to no sulfide logged in drillholes. Sulfide-bearing material is generally restricted to highly-silicified veins or deeply-emplaced, unoxidized mineralization. Common oxidation products include a variety of iron oxide and manganese oxide minerals (Table I).

Gold mineralization at McDonald is comprised mainly of electrum (Au,Ag), native gold, and minor gold-silver-sulfide minerals (Table I). Electrum grains range in size from 0.5 to 350 microns with compositions varying between 55 and 60 wt% gold.

Electrum is often accompanied by pyrite, goethite, hematite, acanthite, and adularia; with goethite replacing pyrite. Silver at the McDonald deposit is present mostly in the form of acanthite ($Ag_2S$), but lesser quantities are hosted by electrum and Ag-sulfosalts such as pearceite-polybasite ($[(Ag,Cu)_6As_2S_7][Ag_9CuS_4]$ to $[(Ag,Cu)_6Sb_2S_7][Ag_9CuS_4]$) and proustite-pyrargyrite ($Ag_3AsS_3$ to $Ag_3SbS_3$).

**Table I: Ore and Gangue Mineralogy of the McDonald Deposit**

| Mineralogy | Mineral | Formula |
|---|---|---|
| Ore | acanthite | $Ag_2S$ |
| | electrum | Ag,Au |
| | native gold | Au |
| Gangue | quartz | $SiO_2$ |
| | chalcedony | $SiO_2$ |
| | calcite | $CaCO_3$ |
| | adularia | $KAlSi_3O_8$ |
| | pyrite | $FeS_2$ |
| | marcasite | $FeS_2$ |
| | hematite | $Fe_3O_4$ |
| | goethite | $Fe^{3+}O(OH)$ |
| | jarosite | $KFe^{3+}_3(SO_4)_2(OH)_6$ |
| | cryptomelane | $K(Mn^{4+}_7Mn^{3+})O_{16}$ |
| Uncommon | chalcopyrite | $CuFeS_2$ |
| | covellite | CuS |
| | digenite | $Cu_9S_5$ |
| | galena | PbS |
| | pyrrhotite | $Fe_7S_8$ |
| | sphalerite | ZnS |
| | stromeyerite | $AgCuS_2$ |
| Rare | famatinite | $Cu_3SbS_4$ |
| | pearceite | $[Ag_9CuS_4][(Ag,Cu)_6As_2S_7]$ |
| | polybasite | $[Ag_9CuS_4][(Ag,Cu)_6Sb_2S_7]$ |
| | proustite | $Ag_3AsS_3$ |
| | pyrargyrite | $Ag_3SbS_3$ |
| | petrovskaite | AuAgS |
| | uytenbogaardtite | $Ag_3AuS_2$ |

### 1.2.3. Hydrothermal Alteration

The McDonald deposit exhibits some zonation in hydrothermal alteration with depth. Intense quartz-adularia alteration with minor chalcedony and kaolinite is the most dominant style of alteration within mineralized zones at McDonald. This alteration exists at depth (between 60 and 200 m) and grades vertically into more chalcedony-dominated silicic alteration at shallower depths and at the surface in the form of silica sinter. Gold mineralization at McDonald is observed to be mostly confined to zones of quartz-adularia alteration.

Argillic alteration exists as halos around mineralized zones and within favorable volcanic units. Kaolinite is the more prevalent alteration product immediately adjacent to mineralized zones, while alteration to montmorillonite and minor chlorite, epidote, and calcite is more distally related.

### 1.2.4. Structure

At least two subparallel, subvertical faults striking approximately N 60° E exist at West Butte (Figure 3). The Eclipse Fault, which bounds West Butte to the north, exhibits post-mineral displacement of 180 m downward to the north. The other two faults also display post-mineral displacement, but movement is minor. Also present at West Butte is a north-northeast striking fault on the western flank and the 9800' E-W fault which strikes approximately N 80° W.

### 1.2.5. Modes of Gold Mineralization

Higher-grade gold mineralization at the McDonald deposit is present predominantly as steeply-dipping, intersecting veins. These veined zones appear to correlate with the 9800' E-W fault, which is interpreted to be a mineralizing structure. Lower-grade regions at McDonald consist of stratabound, disseminated mineralization. This lower-grade material is preferentially mineralized within the lithic tuff unit, and to a lesser degree the andesite and crystal-rich tuff unit, due to high relative permeability.

## 1.3. Exploration History

Exploration of the McDonald deposit began in the 1980s by the Anaconda Company, who discovered it during exploration of the adjacent Keep Cool area to the west. In 1986, the Western Energy Company conducted surface mapping at the McDonald deposit and drilled two shallow holes. In 1989, Addwest Gold optioned the property and drilled 11 shallow holes, totaling 1,720 m. Shortly after, Phelps Dodge Mining Company and CR Montana Corporation coordinated to create the Seven-Up Pete Joint Venture, which lasted until 1992. This Joint Venture eventually included Echo Bay Mining, who were brought in to evaluate the property. Echo Bay Mining conducted a close-spaced, angled-core drilling program at West Butte, which demonstrated the existence of high-grade, high-angle veins (Paul & Guimard, 2011). By the end of the Joint Venture in 1992, 494 drillholes were drilled, with the majority being reverse circulation (RC) drilling. Permitting applications for an open pit mine at McDonald were accepted in 1996 by Montana state regulators. However, in 1998, Initiative 137 passed, banning open-pit, cyanide-leach (vat or heap leaching), gold-and-silver mining in Montana. By 2003, the McDonald deposit was estimated to be the largest gold deposit in Montana, with an open pit potential in excess of 10 Moz of gold at 0.016 Au opt (CAM, 2003).

In 2007, Newmont Mining Corporation acquired the McDonald property through an exchange of assets; and in 2011, conducted a reevaluation of the property to determine the potential of a high-grade, structurally-controlled orebody amenable to underground mining methods (Paul & Guimard, 2011). In 2017, Newmont transferred all remaining core, chip boards, and documentation pertaining to the McDonald Project to Montana Tech (Rosenthal & Rosenthal, 2017).

## 1.4. Project Scope

The McDonald deposit is interpreted to be the largest gold deposit in Montana, with an open pit potential in excess of 10 Moz of gold at 0.5 grams per ton (Newmont Mining Corporation, 2014). Preliminary resource estimates produced by Newmont suggest the existence of a 500 koz gold orebody at West Butte with a grade of 0.21 troy ounces per ton (Newmont Mining Corporation, 2014). The purpose of this thesis is to utilize existing drilling data and geologic information on the McDonald deposit to produce a resource model and simulated model of gold at West Butte which reflects the two modes of mineralization described by Bartlett et al. and Newmont geologists.

## 2. Exploratory Data Analysis

Maptek Vulcan version 11.0.0 and Leapfrog Geo version 4.3.1 were used in tasks related to exploratory data analysis (EDA). The dimensions used in this project are represented in feet, and grades are represented as ounces per ton.

### 2.1. Drill Hole Database & Variables List

The drillhole data for the McDonald deposit are comprised of three Microsoft Excel comma separated values (.csv) files which contain collar, survey, and assay tables for the drilling data. This drillhole database consists of 55 diamond core holes, 447 reverse circulation drillholes, and 100 monitoring wells (Table II); and at West Butte, consists of 18 diamond core holes, 122 reverse circulation drillholes, and 7 monitoring wells (Table III).

**Table II: Breakdown of McDonald Drillhole Database by Drilling Type**

| Type of Drillhole | Count |
|---|---|
| Diamond Core | 55 |
| Reverse Circulation (RC) | 447 |
| Monitoring Wells | 100 |
| Total | 602 |

**Table III: Breakdown of West Butte Drillhole Database by Drilling Type**

| Type of Drillhole | Count |
|---|---|
| Diamond Core | 18 |
| Reverse Circulation (RC) | 122 |
| Monitoring Wells | 7 |
| Total | 147 |

Samples in reverse circulation were taken on 5 ft. intervals. Diamond core holes were logged and sampled based on geology, but were generally taken on 5 ft. intervals. Samples were assayed for gold (Au) and silver (Ag) and logged for a suite of geologic parameters (Table IV). Missing or non-assayed samples were assigned placeholder values of -99.0.

**Table IV: Logged Geologic Parameters**

| Variable | Description |
|----------|-------------|
| fm | formation |
| lth | lithology |
| alt_t | alteration type |
| alt_i | alteration intensity |
| ox | oxidation intensity |
| pyabd | pyrite abundance |
| pytyp | pyrite type |
| vabd | vein abundance |
| vtyp | vein type |
| grc | geotechnical rock classification |
| str | structures |

## 2.2.  Compositing Methodology

Compositing is a method of processing samples in a drilling database into a database of equivalent samples. By taking length-weighted averages down each hole at a constant length, compositing converts sampled intervals of varying lengths into samples of equivalent length called composite samples. Compositing methodologies can vary widely to accommodate different geological attributes (E.g. breaking composite intervals by lithology) or spatial parameters (e.g. bench height composites), but they must also address short intervals found at the ends of drillholes. These "leftover" intervals are shorter than the compositing length and may be left in, discarded, or processed in other ways.

The drilling data for the McDonald deposit were composited down-hole using composite intervals of 10 ft., and short composite samples were kept. Figures 5 and 6 summarize lengths and gold grades of short composites. Gold and silver concentrations in troy ounces per ton (opt) were composited as assay fields, and the majority geology codes for each compositing interval were recorded. Missing and non-sampled data were assigned placeholder values of -99.0 and were excluded from compositing calculations.
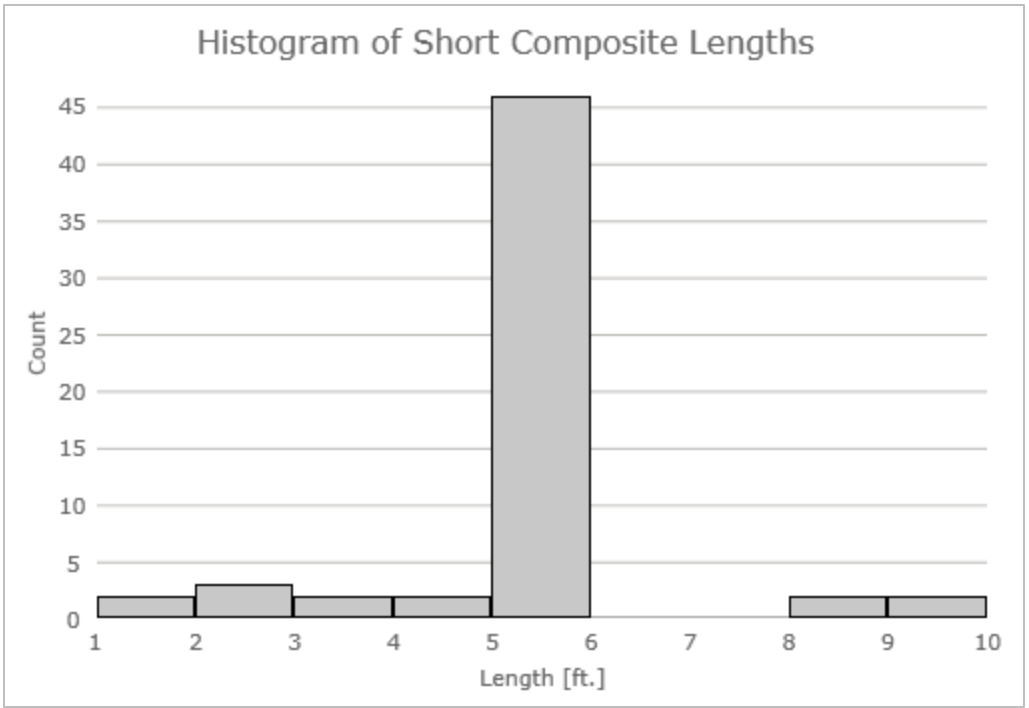
**Figure 5: Histogram of short composite lengths**
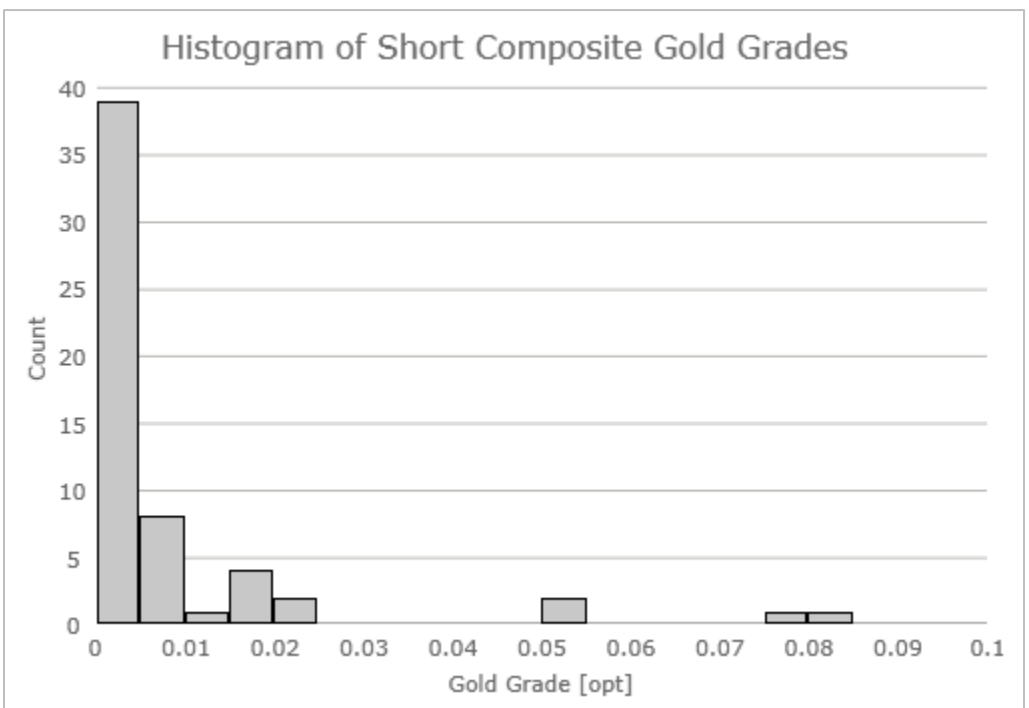


**Figure 6: Histogram of short composite gold grades**

## 2.3.   Domains and Statistics

Domains are relatively-stationary subsets of data that are critical to the estimation

process. Domains must be defined such that each domain contains sufficient data to characterize

its statistical behavior, and they are often defined by the mineralizing controls within a deposit

(Rossi & Deutch, 2014).  At the McDonald deposit, two geographic domains exist: East Butte

and West Butte. For this project, only data from West Butte was considered.

### 2.3.1.  Downhole Contamination

Downhole contamination or "smearing" is a form of bias found in some reverse

circulation drilling that can lead to the recording of longer, mineralized intercepts than what is

actually present. Downhole contamination is often thought of as a form of dilution and is

attributed to vertical mixing of cuttings over an interval larger than the sampling interval. If not

addressed, downhole-contaminated data may lead to an overestimation or bias in mineable tons.

Bias in the form of downhole contamination of gold grades in reverse circulation (RC)

drilling at the McDonald deposit has been noted by Newmont geologists. A 2014 internal

presentation by Newmont outlines that "potential exists for bias in RC gold assay data > 0.05

opt, with ~70% RC drilling in West Butte underground target and ~90% in East Butte"

(Newmont Mining Corporation, 2014).

Visual inspection and analysis of sampling intervals in RC drillhole PRM-94-557

(Figures 45 and 46 in Appendix A) suggests the presence of downhole contamination in RC

drilling data. To further assess if downhole contamination exists, a quantile-quantile (Q-Q) plot

of deposit-wide, gold composite data was created using pairs of RC and core samples (Figure 7).
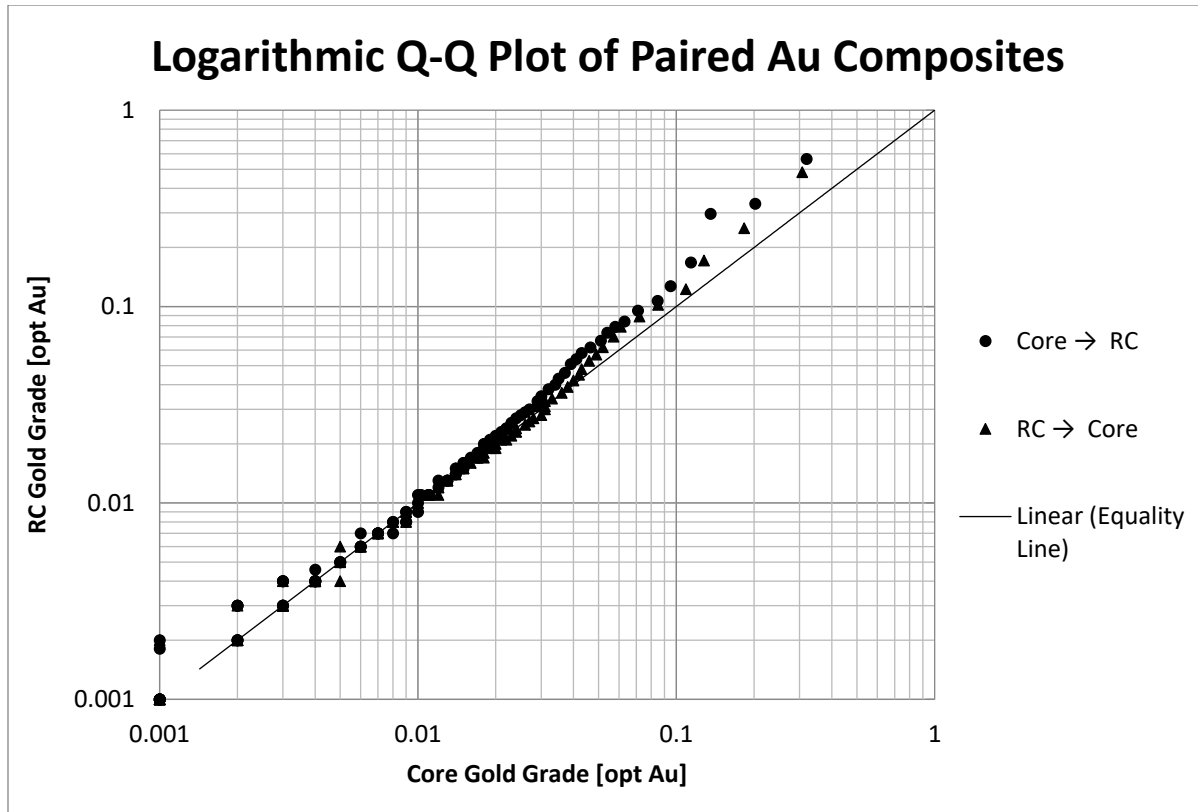
**Figure 7: Quantile-Quantile plot of gold composite pairs for the McDonald deposit**

The Q-Q plot in Figure 7 compares equivalent grade distributions at close distances between RC and core data. Data pairs generated for the Q-Q plot were comprised of one RC and one core sample with a maximum spacing of 100 feet. Data pairs were defined twice, as different data pairs are generated depending on which type of data is considered first.

Deviation from the equality line in the Q-Q plot indicates deposit-scale downhole contamination in RC drilling at higher grade values. In addition, the Q-Q plot suggests a positive correlation between downhole contamination and gold grades beyond 0.02 Au opt. However, it is impossible to quantify the nature and extent of contamination in grade values in downhole-contaminated RC drilling, as the Q-Q plot is only indicative.

### 2.3.2. Geologic Domains

Statistics of gold grades by alteration styles and lithology (see Appendix A for gold statistics) agree with Bartlett et al. (1995), who stated that, "Silicification and adularization are the dominant forms of alteration within the mineralized zones" and that "The lithic tuff (Trtl) [hosts] approximately 90 percent of all the known gold mineralization…" However, the lithic tuff lithology and silicic alteration were not ideal attributes for domain definition, as these parameters were inherent of the majority of data at West Butte. Vein type, vein abundance, pyrite type, and pyrite abundance did not show any significant visual or statistical correlation to gold grades and were not used to define domains.

### 2.3.3. Grade Shelling

It is the author's opinion that grade shelling is a controversial technique in the field of resource estimation. It is a method that defines domains based on grade cutoffs that should only be employed when no other methods exist to define estimation domains. Grade shells often inflate block grade statistics inside the shelled volume by artificially creating hard boundaries within estimated models (Jewbali, Elenbaas, & Roos, 2015). Despite this, grade shells have found success in the estimation of some gold deposits, where grade shells are used primarily to constrain estimated tonnages within structurally-controlled orebodies where the orebody edges may be ambiguous. It is the author's opinion that grade shells can be used to constrain estimated tonnages in areas of sparse drilling where a hard grade boundary is expected. Grade shells constructed for this purpose should honor grade data as well as geologic data, and should be free of spikes and "one-hole wonders" (discontinuous pod-like shapes sometimes also referred to as "leapblobs").

Grade shelling was conducted using Seequent Leapfrog Geo version 4.3.1, a 3D geologic

modeling tool and implicit modeler. Grade shelling was selected as a method of defining

estimation domains at the McDonald deposit because logged geologic attributes in the composite

database failed to provide a means of defining higher-grade, vertical vein systems characterized

by Bartlett et al., Echo Bay Mining, and Newmont geologists. In addition, choosing not to

domain higher-grade mineralization would likely lead to "…falsely smearing the grade laterally

along volcanic stratigraphy" (Paul & Guimard, 2011). The grade shell was produced at a gold

grade cutoff of 0.04 troy ounces per ton (opt) using Leapfrog Geo's radial basis function (RBF)

indicator interpolant feature. The parameters used to construct the grade shell are outlined in

Table V.

**Table V: Grade Shell Parameters**

| Grade Shell Parameters | |
|---|---|
| Composite data used | Core Data Only |
| Grade cutoff (Au opt) | 0.04 |
| Iso value | 0.35 |
| Resolution | 20 |
| Interpolant type | Spheroidal |
| Total sill | 1 |
| Nugget | 0.1 |
| Base range (ft) | 350 |
| Volume filter (ft³) | 1,000,000 |

Only core data were used to construct the shell, as the usage of contaminated RC data

may overinflate the shelled volume and lead to a subsequent overestimation of higher-grade

tonnages. After initial construction, internal discontinuities in the shell were observed; so a

structural trend was added at a northwesterly trend, producing a continuous, en-echelon,

vertically-oriented orebody that strikes roughly N 80º W (Figure 8 and 9).
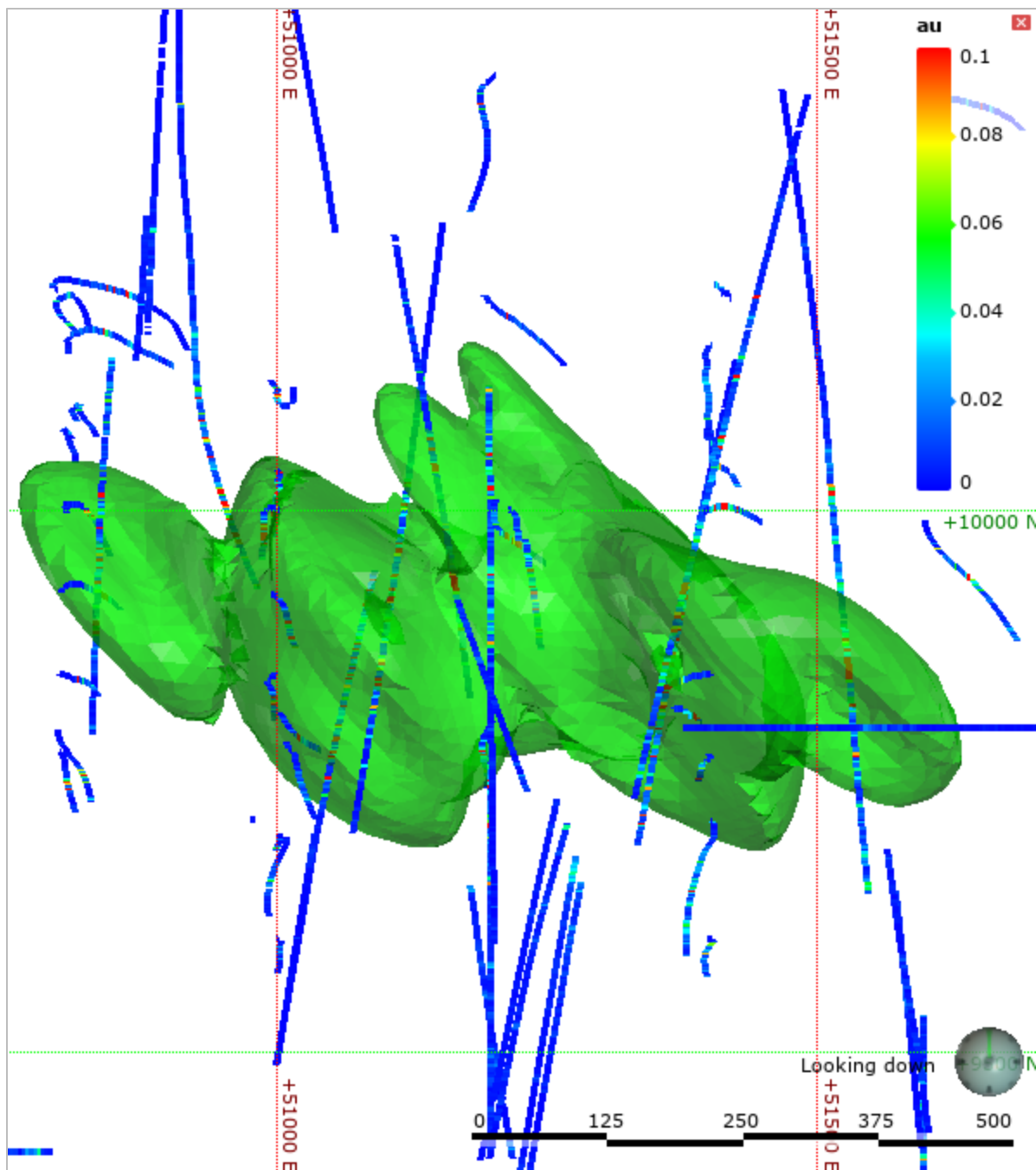
**Figure 8: Plan view of the 0.04 Au opt grade shell (green) with gold drilling data**
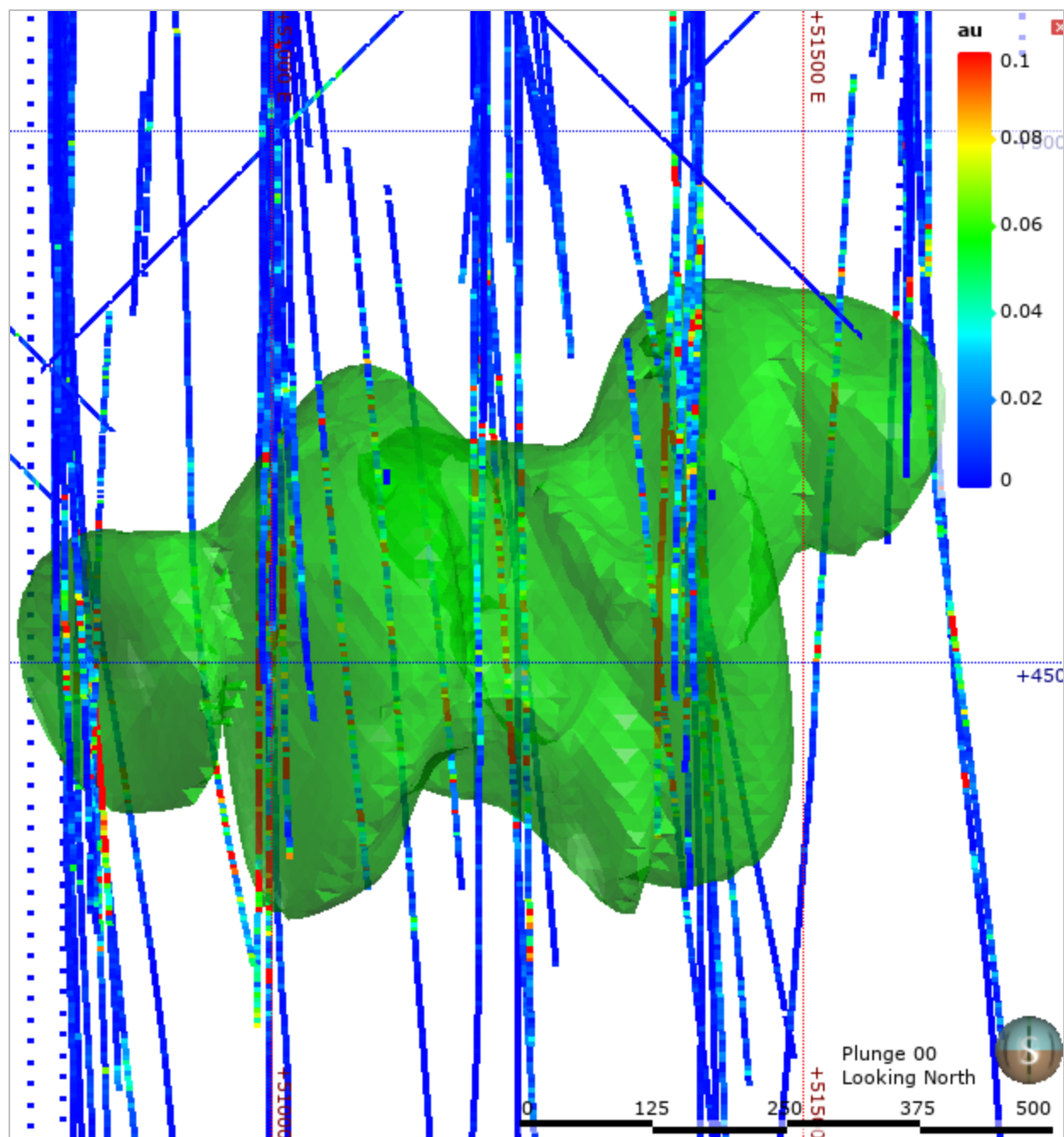
**Figure 9: Side view looking north at the 0.04 Au opt grade shell (green) with gold drilling data**

Gold statistics inside and outside the shell (Table VI) show that the shelling process was effective, however some high grade samples present in reverse circulation drilling were not captured within the shelled volume.

**Table VI: Grade shell statistics of gold grade (Au opt)**

|  | Location (within West Butte) | |
|---|---|---|
|  | Inside of shell | Outside of shell |
| Count | 556 | 41,554 |
| Mean | 0.142 | 0.010 |
| Variance | 0.140 | 0.002 |
| Standard deviation | 0.374 | 0.041 |
| Max | 6.826 | 4.260 |
| Upper quartile | 0.117 | 0.010 |
| Median | 0.050 | 0.004 |
| Lower quartile | 0.024 | 0.001 |
| Min | 0.002 | 0.000 |

### 2.3.4. Estimation Domains

Estimation domains (Table VII) were defined within West Butte based on the 0.04 Au opt grade shell. The grade shell effectively represents a higher-grade, higher-confidence volume within an otherwise nebulous, low-grade, stratabound deposit. Additionally, the grade shell defines a maximum volume which will limit estimated tonnages of high-grade material and minimize "…smearing [of] grade laterally along volcanic stratigraphy" as recognized by Paul and Guimard (Paul & Guimard, 2011).

**Table VII: Estimation domains for the McDonald deposit**

| Geographic Zone | Au Zone | Notes |
|---|---|---|
| West Butte | Inside Shell | Inside 0.04 Au opt grade shell |
|  | Outside Shell | Outside 0.04 Au opt grade shell |
| East Butte | Not modeled | Not modeled |

## 2.4. Variography

Variography provides a method of quantifying spatial variability of sample data in space. "The variogram is a central parameter for many geostatistical techniques. Kriging, Gaussian simulation, and indicator methods all require a variogram model for each variable in each domain" (Deutsch J. L., 2019). In its purest definition, the variogram is defined as half of the average squared difference between two attribute values approximately separated by a vector **h** (Deutsch & Journel, Geostatistical Software Library and User's Guide, 1992). Many mining and geostatistical programs published today offer a variety of methods to calculate and model variograms. Many of these software packages have the ability to produce variogram "fans" or "maps", which allow the user to view numerous variograms calculated at different orientations at once. Additionally, each software package accommodates different suites of variogram and model types.

Variography at the McDonald deposit was conducted to ascertain the orientation and continuity of gold grade within each estimation domain and to produce variogram models that would be later used in ordinary kriging. Variograms were calculated on a declustered composite database using correlograms standardized to 1 and modeled using two-structure, spherical models with a nugget value. Nugget values were approximated using downhole variograms (Figure 10 and 11) and the major, semi-major, and minor orientations (Figure 12 - Figure 17) were guided by orientations described by Bartlett et al. (1995), especially inside the grade shell, due to the paucity of the composite data. Table VIII summarizes the variogram models for the estimation domains.
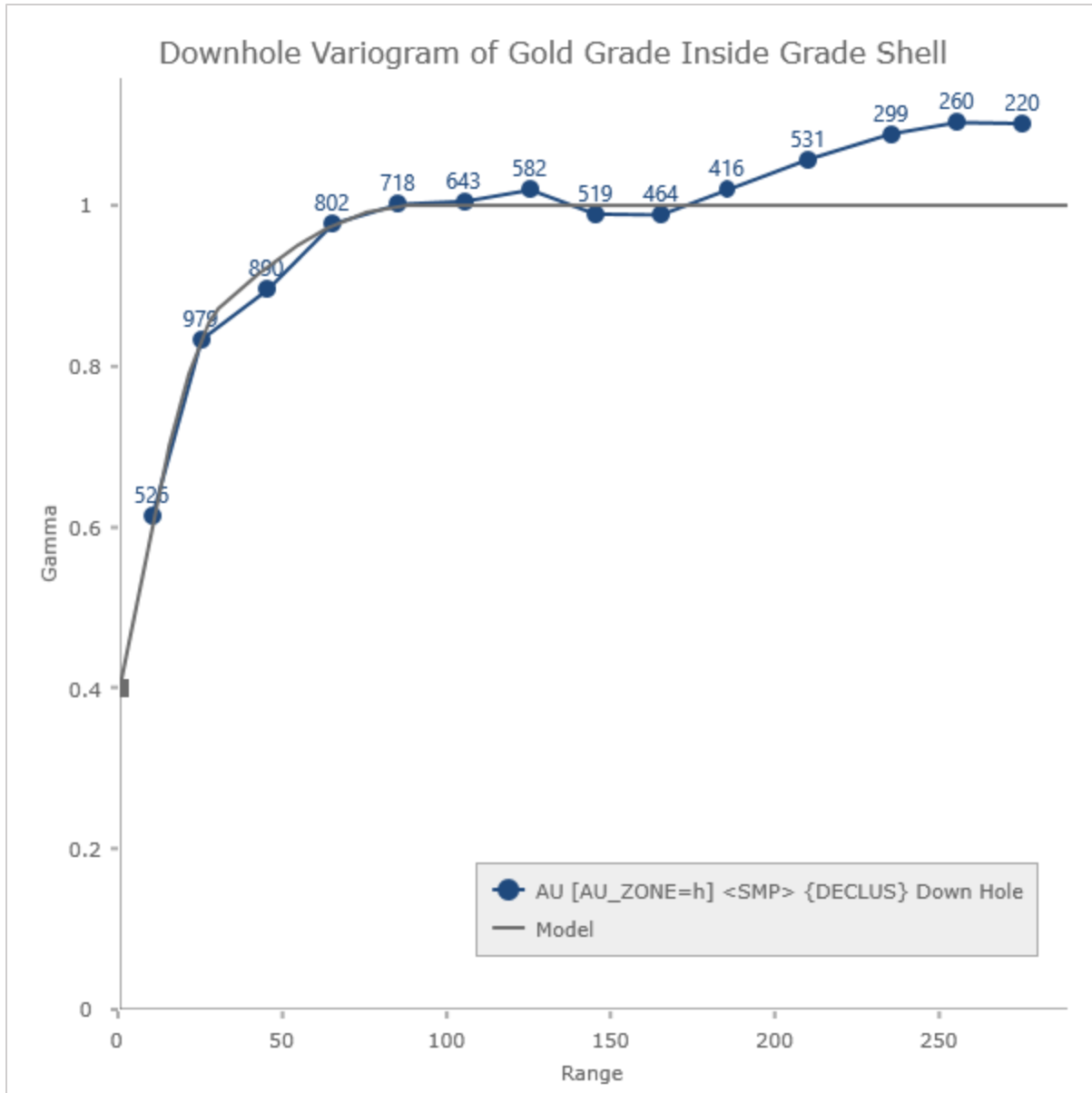
**Figure 10: Downhole variogram of gold grades inside the grade shell**
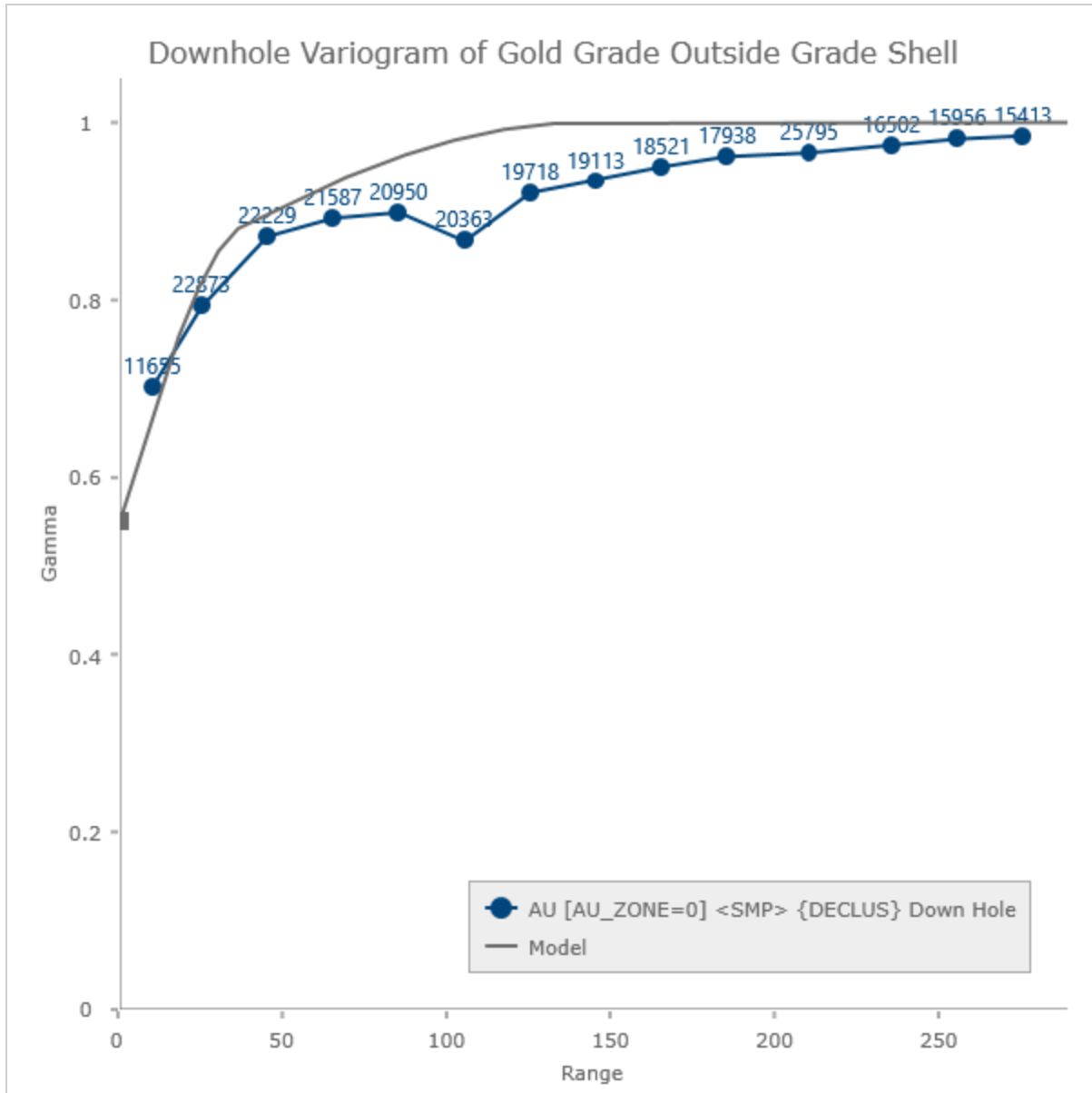
**Figure 11: Downhole variogram of gold grades outside the grade shell**
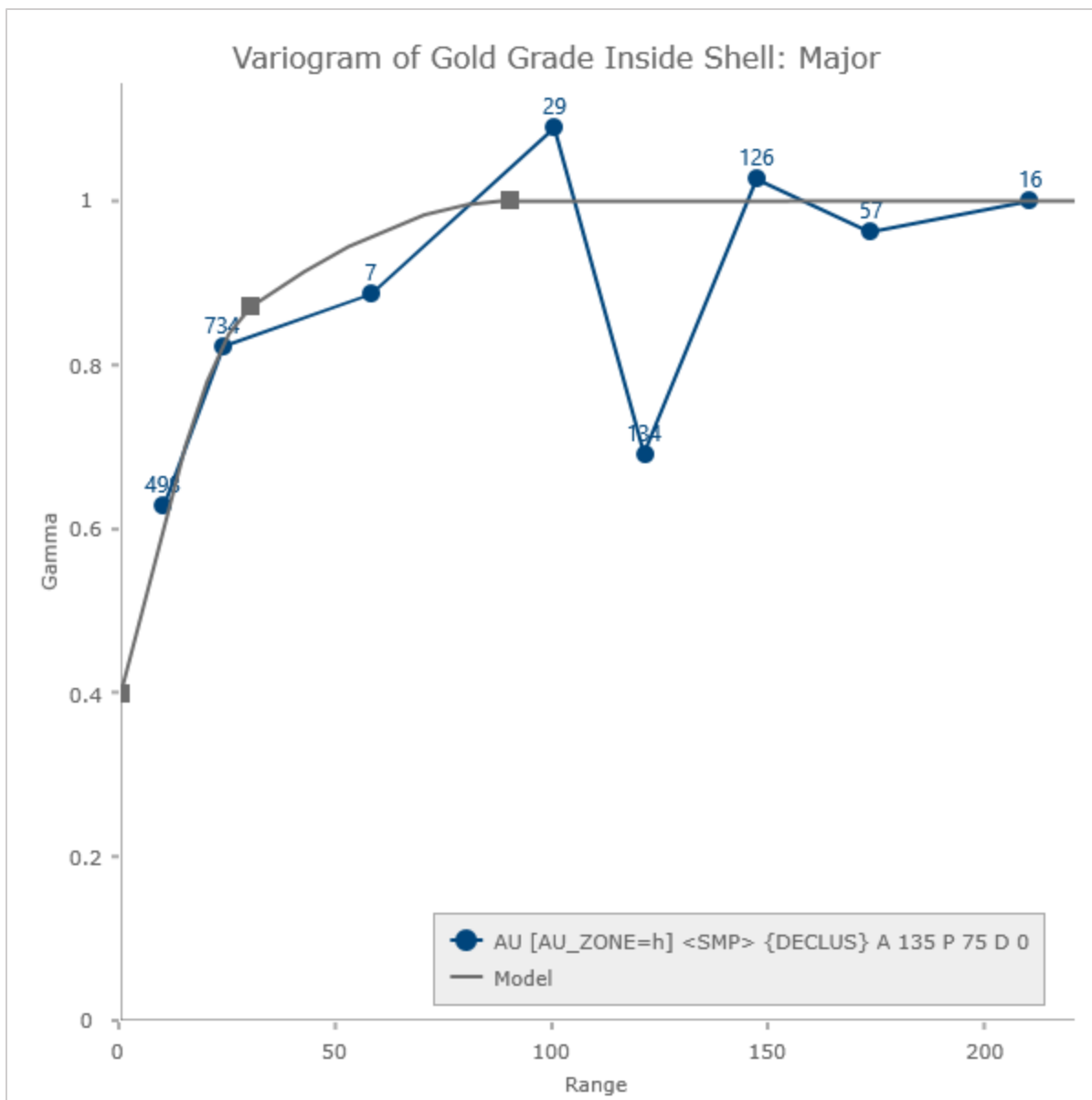
**Figure 12: Major variogram of gold grades inside the grade shell**
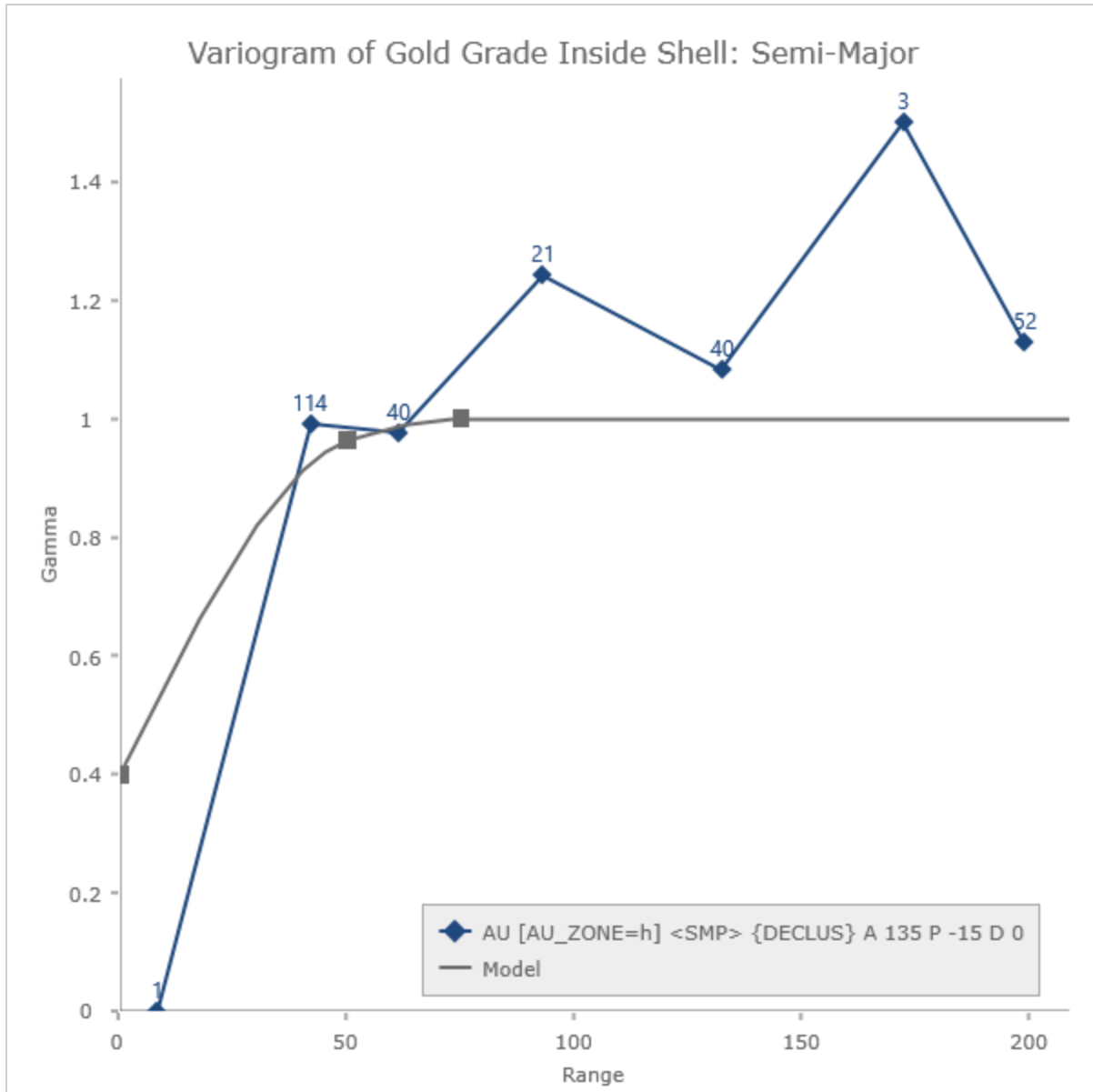
**Figure 13: Semi-major variogram of gold grades inside the grade shell**
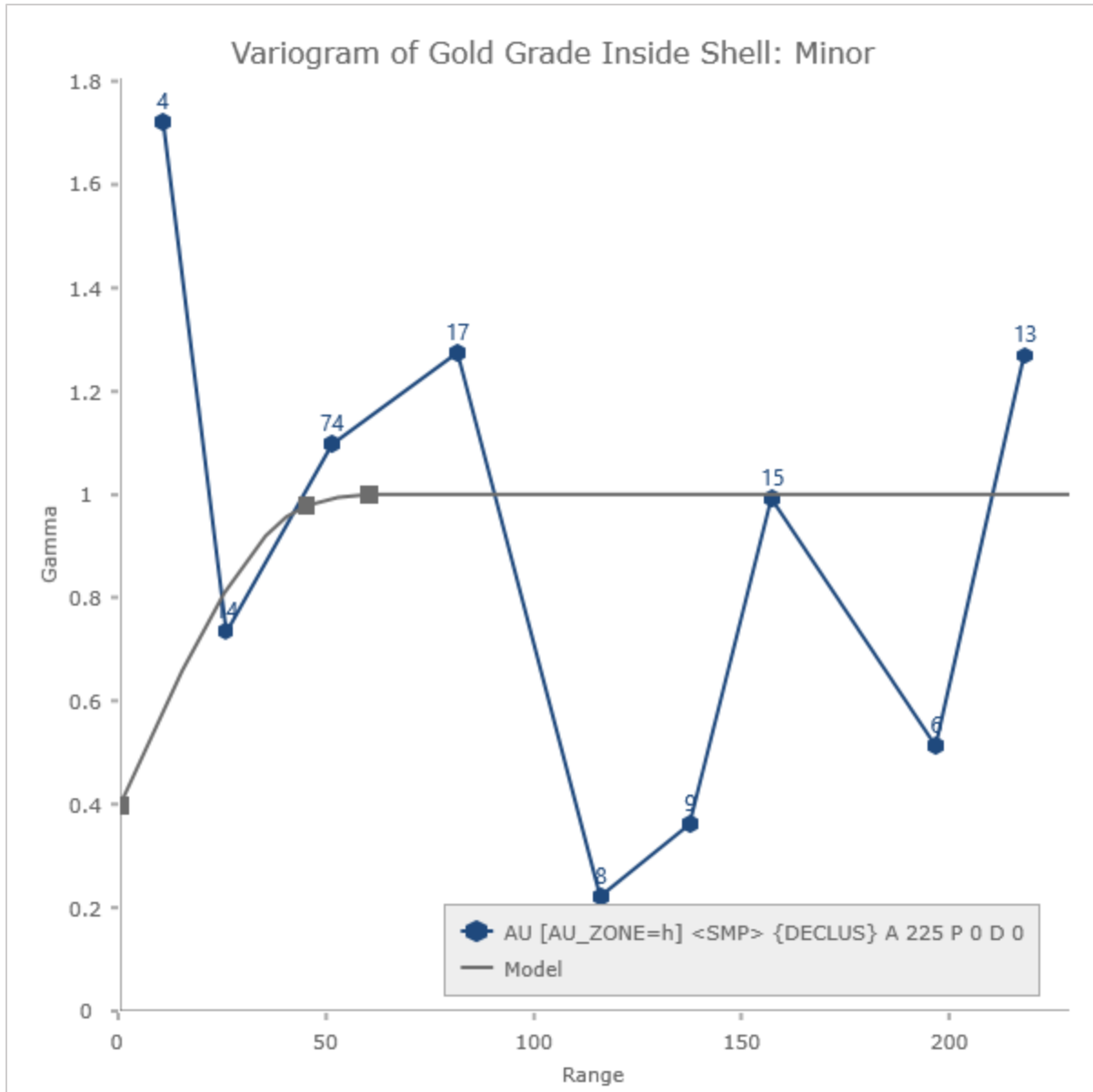
**Figure 14: Minor variogram of gold grades inside the grade shell**
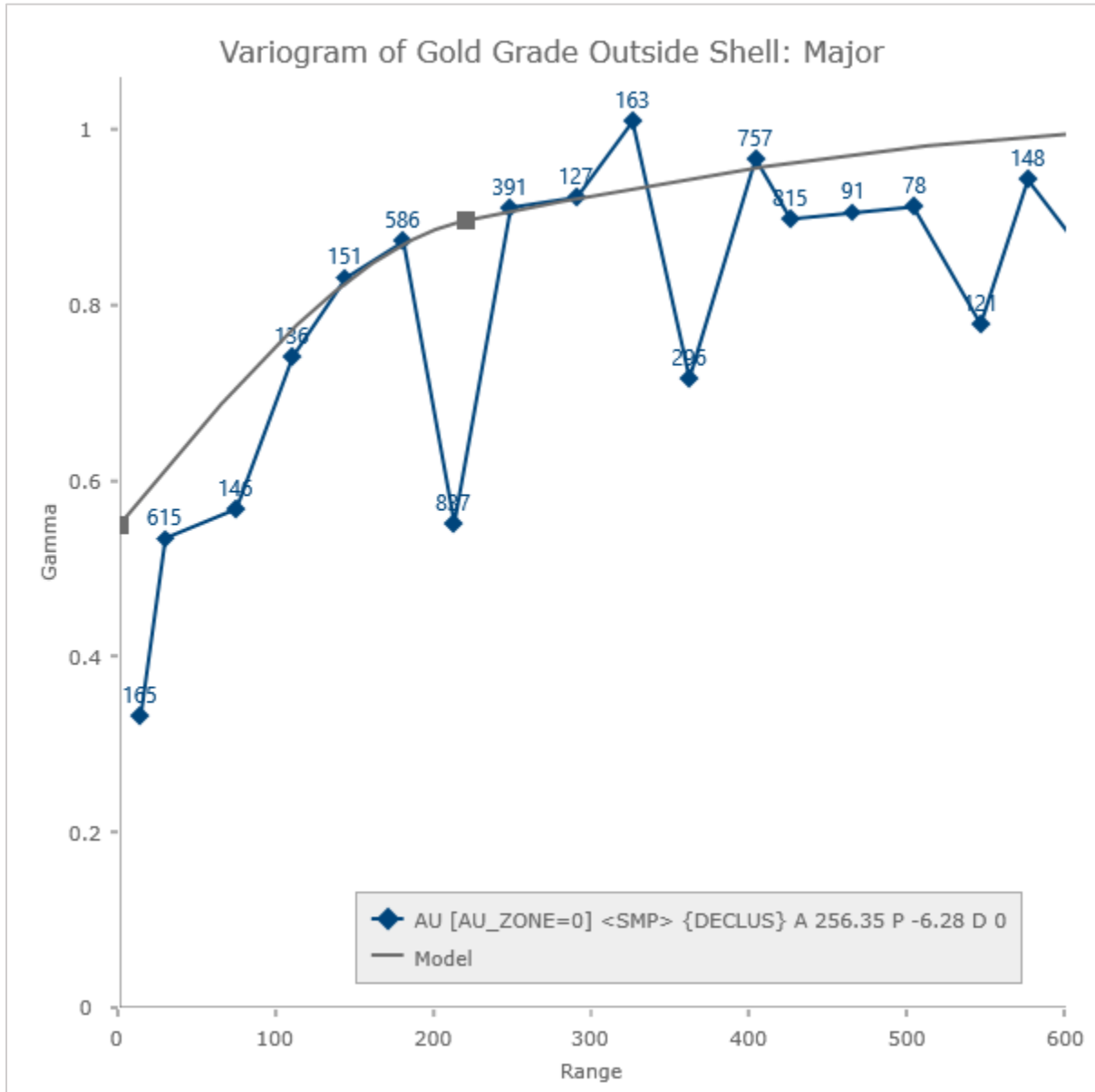
**Figure 15: Major variogram of gold grades outside the grade shell**
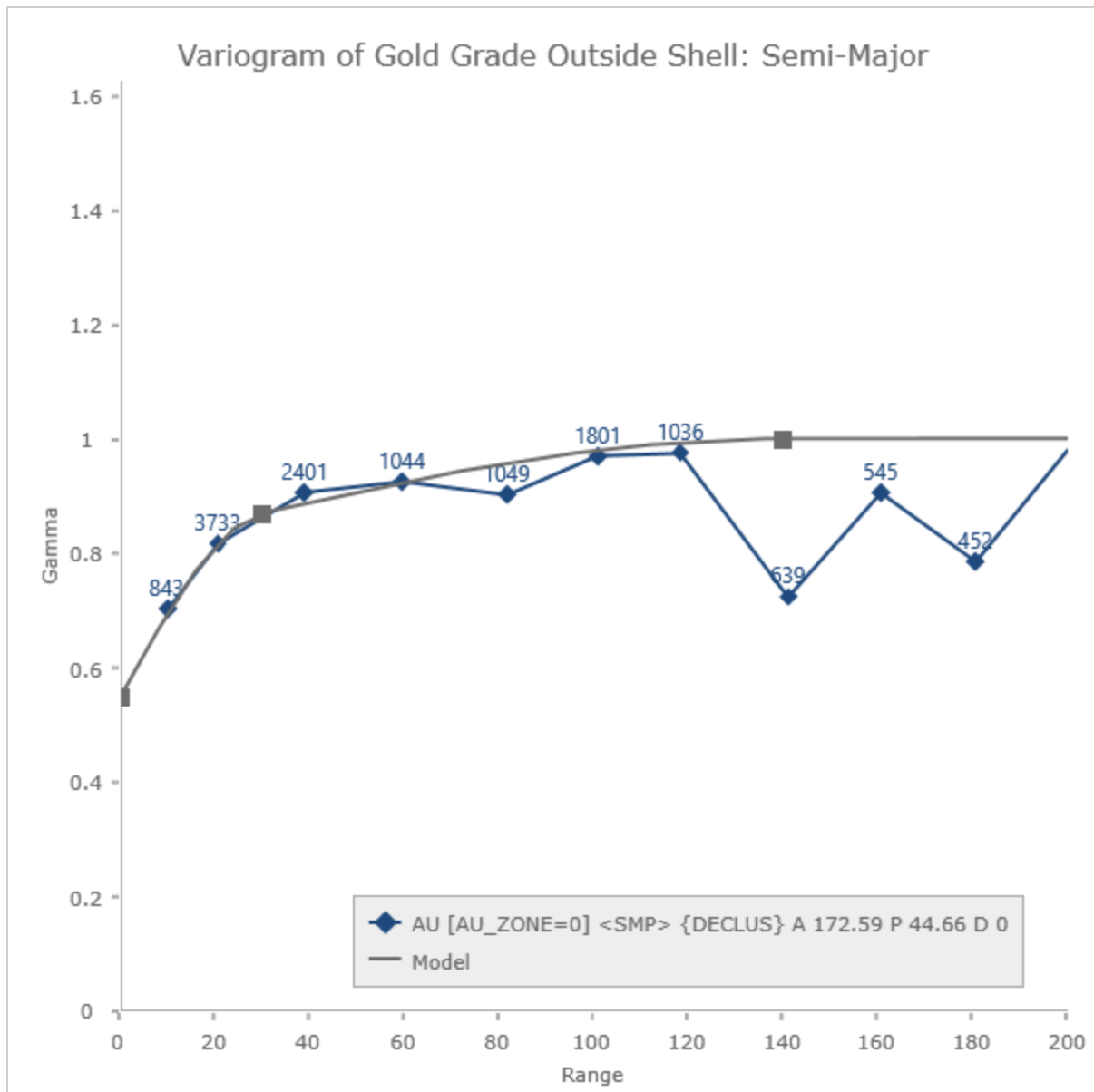
**Figure 16: Semi-major variogram of gold grades outside the grade shell**
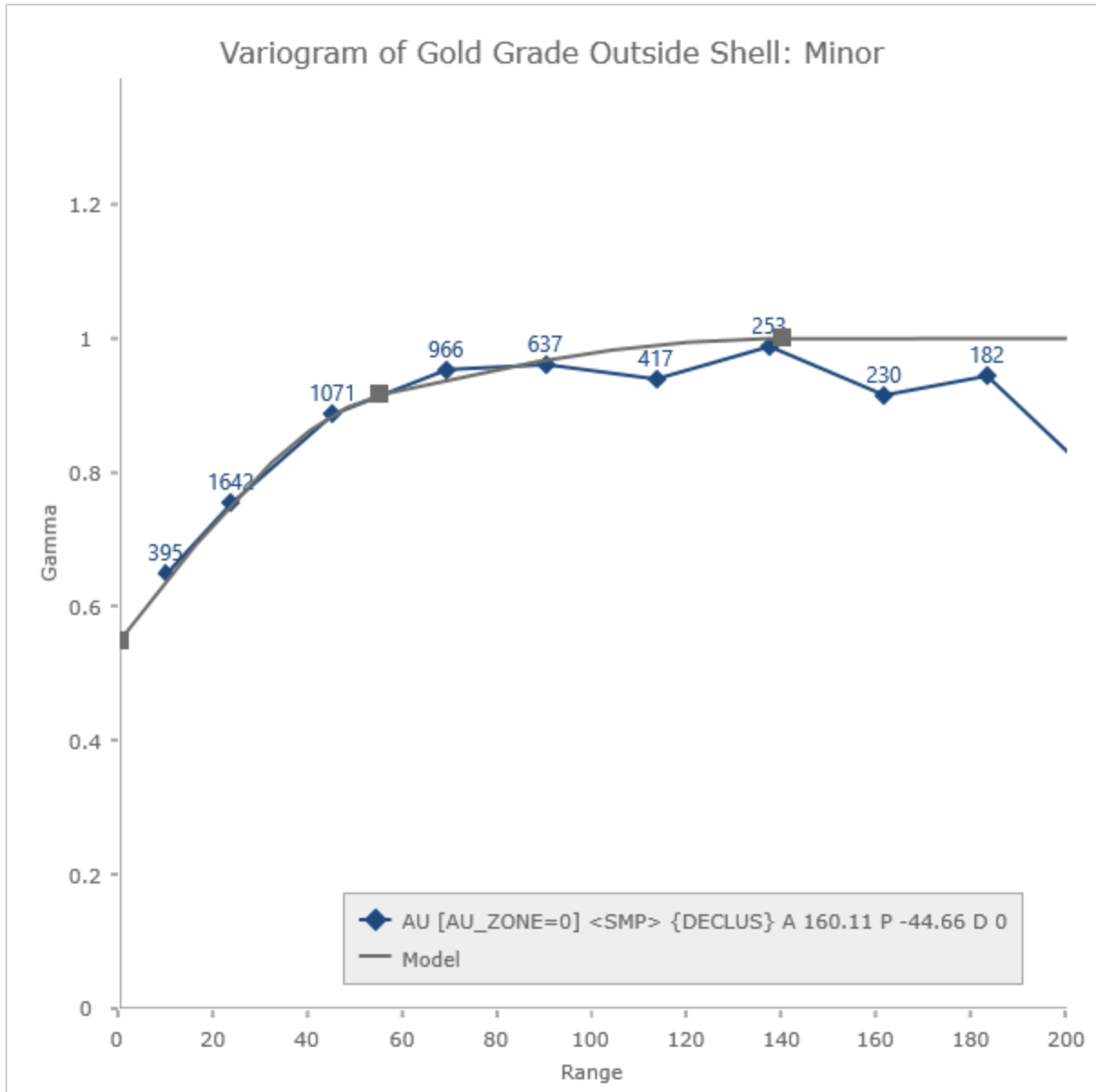
**Figure 17: Minor variogram of gold grades outside the grade shell**

**Table VIII: Variogram Model Parameters for Estimation**

| | Estimation Domain | | | |
| --- | --- | --- | --- | --- |
| | Inside Grade Shell | | Outside Grade Shell | |
| Total Sill | 1 | | 1 | |
| Nugget | 0.4 | | 0.6 | |
| Structure | 1 | 2 | 1 | 2 |
| Structure Type | Spherical | Spherical | Spherical | Spherical |
| Bearing | 135 | 135 | 256.35 | 256.35 |
| Plunge | 75 | 75 | -6.28 | -6.28 |
| Dip | 90 | 90 | -45 | -45 |
| Sill | 0.35 | 0.25 | 0.26 | 0.14 |
| Major Range | 30 | 90 | 250 | 1200 |
| Semi-Major Range | 50 | 75 | 35 | 400 |
| Minor Range | 45 | 60 | 70 | 300 |

# 3.  Resource Estimation

The goal of resource estimation is to provide a reasonable prediction of tonnages and grade of material within a deposit. Many estimation techniques have been adapted for such purposes and have been well-documented in texts such as Knudsen (1988) *A Short Course on Geostatistical Ore Reserve Estimation*, Goovaerts (1997) *Geostatistics for Natural Resources Evaluation* and Rossi & Deutch (2014) *Mineral Resource Estimation*. Resource estimation of the McDonald gold deposit was conducted using Maptek Vulcan 11.0.0.

## 3.1.  Block Model Construction

The block model construction parameters are outlined in Table IX. The orientation of the model was set at a bearing, plunge, and dip of 90°, 0°, and 0° respectively.

**Table IX: Block Model Construction Parameters (ft.)**

|   | Origin | Start Offsets | End Offsets | Block Size |
|---|--------|---------------|-------------|------------|
| X | 48,700 | 0 | 4,000 | 20 |
| Y | 8,300 | 0 | 2,800 | 20 |
| Z | 3,000 | 0 | 3,000 | 20 |

The block size of 20 x 20 x 20 feet was selected based on the anticipated selectable mining unit (SMU) for an underground mine at West Butte. All blocks within the model and below topography were coded with a density value of 0.074 tons per cubic foot based on the bulk density report of silicically-altered lithic tuff (Trtl) and crystal-rich tuff (Trtcr) (Fuller, 1998). It is not an ideal practice to assign all blocks the same density value; but it is reasonable within the scope of this project, as most gold mineralization at West Butte is confined within silicically-altered lithic and crystal-rich tuffs. The block model variables are summarized in Table X.

**Table X: Block Model Variables**

| Variable | Data Type | Default Value | Description |
|---|---|---|---|
| density | Double (Real * 8) | 0 | density |
| au_zone | Integer (Integer * 4) | 0 | domain variable, 1 = inside shell, 0 = outside shell |
| id_flag | Float (Real * 4) | -99 | inverse distance estimate flag |
| ok_flag | Float (Real * 4) | -99 | ordinary kriging estimate flag |
| au_id | Double (Real * 8) | -99 | au opt - inverse distance |
| au_ok | Double (Real * 8) | -99 | au opt - ordinary kriging |
| au_nn | Double (Real * 8) | -99 | au opt - nearest neighbor |
| nsamp_id | Float (Real * 4) | -99 | samples per estimate id |
| nsamp_ok | Float (Real * 4) | -99 | samples per estimate ok |
| nhole_id | Float (Real * 4) | -99 | holes per estimate id |
| nhole_ok | Float (Real * 4) | -99 | holes per estimate ok |
| kvar_ok | Double (Real * 8) | -99 | kriging variance ok |
| keff_ok | Double (Real * 8) | -99 | kriging efficiency |
| dist_id | Float (Real * 4) | -99 | distance to closest sample |
| dist_ok | Float (Real * 4) | -99 | distance to closest sample |
| dist_nn | Float (Real * 4) | -99 | distance to closest sample |

## 3.2.  Estimation Plan

Resource estimation of gold at the McDonald deposit was conducted using ordinary kriging (OK) and inverse distance squared (IDS) estimation methods. A nearest-neighbor (NN) estimate was also produced for validation purposes. Estimates were carried out in three passes:

1.  In-shell estimate using samples only inside the grade shell

2.  In-shell, infill estimate using samples inside and outside the grade shell; and

3.  Out-of-shell estimate using samples only outside the grade shell

Estimation parameters (Table XI - XII) between OK and IDS estimates were held constant with few exceptions. A cap of 2.0 Au opt was used for all estimates, and a high-yield limit of 0.1 Au opt was used to further limit the influence of high-grade samples outside the shell. Ordinary kriging estimates used the variogram models outlined in Table VIII.

**Table XI: Search Ellipsoid Parameters for Estimation**

| Estimate Type | Description | Orientation (°) | | | Search Ellipsoid Ranges (ft.) | | |
|---|---|---|---|---|---|---|---|
| | | Bearing | Plunge | Dip | Major | Semi-Major | Minor |
| IDS | Inside | 135 | 75 | 90 | 200 | 120 | 80 |
| IDS | Infill | 135 | 75 | 90 | 200 | 120 | 80 |
| IDS | Outside | 256.35 | -6.28 | -45 | 700 | 150 | 150 |
| NN | Inside | 135 | 75 | 90 | 200 | 120 | 80 |
| NN | Infill | 135 | 75 | 90 | 200 | 120 | 80 |
| NN | Outside | 256.35 | -6.28 | -45 | 700 | 150 | 150 |
| OK | Inside | 135 | 75 | 90 | 200 | 120 | 80 |
| OK | Infill | 135 | 75 | 90 | 200 | 120 | 80 |
| OK | Outside | 256.35 | -6.28 | -45 | 700 | 150 | 150 |

**Table XII: Sample Parameters for Estimation**

| Estimate Type | Description | Sample Parameters | | |
|---|---|---|---|---|
| | | Minimum | Maximum | Maximum per Drillhole |
| IDS | Inside | 3 | 6 | 0 |
| IDS | Infill | 3 | 6 | 0 |
| IDS | Outside | 3 | 6 | 2 |
| NN | Inside | 1 | 1 | 0 |
| NN | Infill | 1 | 1 | 0 |
| NN | Outside | 1 | 1 | 2 |
| OK | Inside | 3 | 6 | 0 |
| OK | Infill | 3 | 6 | 0 |
| OK | Outside | 3 | 6 | 2 |

## 3.3. Model Validation

### 3.3.1. Summary Statistics

"The histograms and basic statistics may be compared to the original, declustered drillhole data used to estimate the grades for each domain. This is to check… that overall means (without applying a cutoff) are very similar, since the estimated grades should be unbiased" (Rossi & Deutch, 2014). If capping strategies were used, the mean of the resource estimate may be lower than the declustered mean. Generally, most estimates will exhibit "smoother" distributions than the sample database. This smoothing effect may be observed by a decrease in

variability (variance, standard deviation, etc.) when comparing statistics between the block

model and sample database. Table XIII - XV summarize sample and block statistics of the

estimates inside the shell, outside the shell, and overall.

**Table XIII: Sample and Block Statistics of Gold Inside the Grade Shell**

|                    | Sample Database | Nearest-Neighbor | Inverse Distance Squared | Ordinary Kriging |
|--------------------|----------------:|-----------------:|-------------------------:|-----------------:|
| Count              | 556             | 6,639            | 6,639                    | 6,639            |
| Mean               | 0.141           | 0.112            | 0.120                    | 0.123            |
| Variance           | 0.140           | 0.040            | 0.017                    | 0.018            |
| Standard deviation | 0.374           | 0.200            | 0.132                    | 0.133            |
| Max                | 6.826           | 2.000            | 1.445                    | 1.252            |
| Upper quartile     | 0.117           | 0.099            | 0.152                    | 0.154            |
| Median             | 0.050           | 0.047            | 0.074                    | 0.075            |
| Lower quartile     | 0.024           | 0.024            | 0.043                    | 0.042            |
| Min                | 0.002           | 0.002            | 0.003                    | 0.004            |

**Table XIV: Sample and Block Statistics of Gold Outside the Grade Shell**

|                    | Sample Database | Nearest-Neighbor | Inverse Distance Squared | Ordinary Kriging |
|--------------------|----------------:|-----------------:|-------------------------:|-----------------:|
| Count              | 11,900          | 1,304,383        | 857,702                  | 857,702          |
| Mean               | 0.007           | 0.006            | 0.007                    | 0.007            |
| Variance           | 0.001           | 0.000            | 0.000                    | 0.000            |
| Standard deviation | 0.024           | 0.012            | 0.009                    | 0.008            |
| Max                | 3.175           | 2.000            | 1.164                    | 0.669            |
| Upper quartile     | 0.006           | 0.005            | 0.008                    | 0.009            |
| Median             | 0.002           | 0.002            | 0.004                    | 0.004            |
| Lower quartile     | 0.000           | 0.001            | 0.001                    | 0.002            |
| Min                | 0.000           | 0.001            | 0.000                    | 0.000            |

**Table XV: Sample and Block Statistics of Gold in West Butte**

|                    | Sample Database | Nearest-Neighbor | Inverse Distance Squared | Ordinary Kriging |
|--------------------|----------------:|-----------------:|-------------------------:|-----------------:|
| Count              | 12,456          | 1,311,022        | 864,341                  | 864,341          |
| Mean               | 0.008           | 0.006            | 0.007                    | 0.008            |
| Variance           | 0.002           | 0.000            | 0.000                    | 0.000            |
| Standard deviation | 0.046           | 0.020            | 0.018                    | 0.018            |
| Max                | 6.826           | 2.000            | 1.445                    | 1.252            |
| Upper quartile     | 0.006           | 0.006            | 0.008                    | 0.009            |
| Median             | 0.002           | 0.002            | 0.004                    | 0.004            |
| Lower quartile     | 0.001           | 0.001            | 0.001                    | 0.002            |
| Min                | 0.000           | 0.001            | 0.000                    | 0.000            |

### 3.3.2. Swath Plots

Swath plots (Figures 18 - 23) are valuable tools in resource model validation which allow spatial trends in grade to be evaluated. These plots divide composite data and block models into slices along each coordinate axis, and calculate average grades within each slice. Generally, resource estimates should follow nearest-neighbor estimates closely on swath plots, since nearest-neighbor estimates approximate the sample database and honor the sample data at close distances.
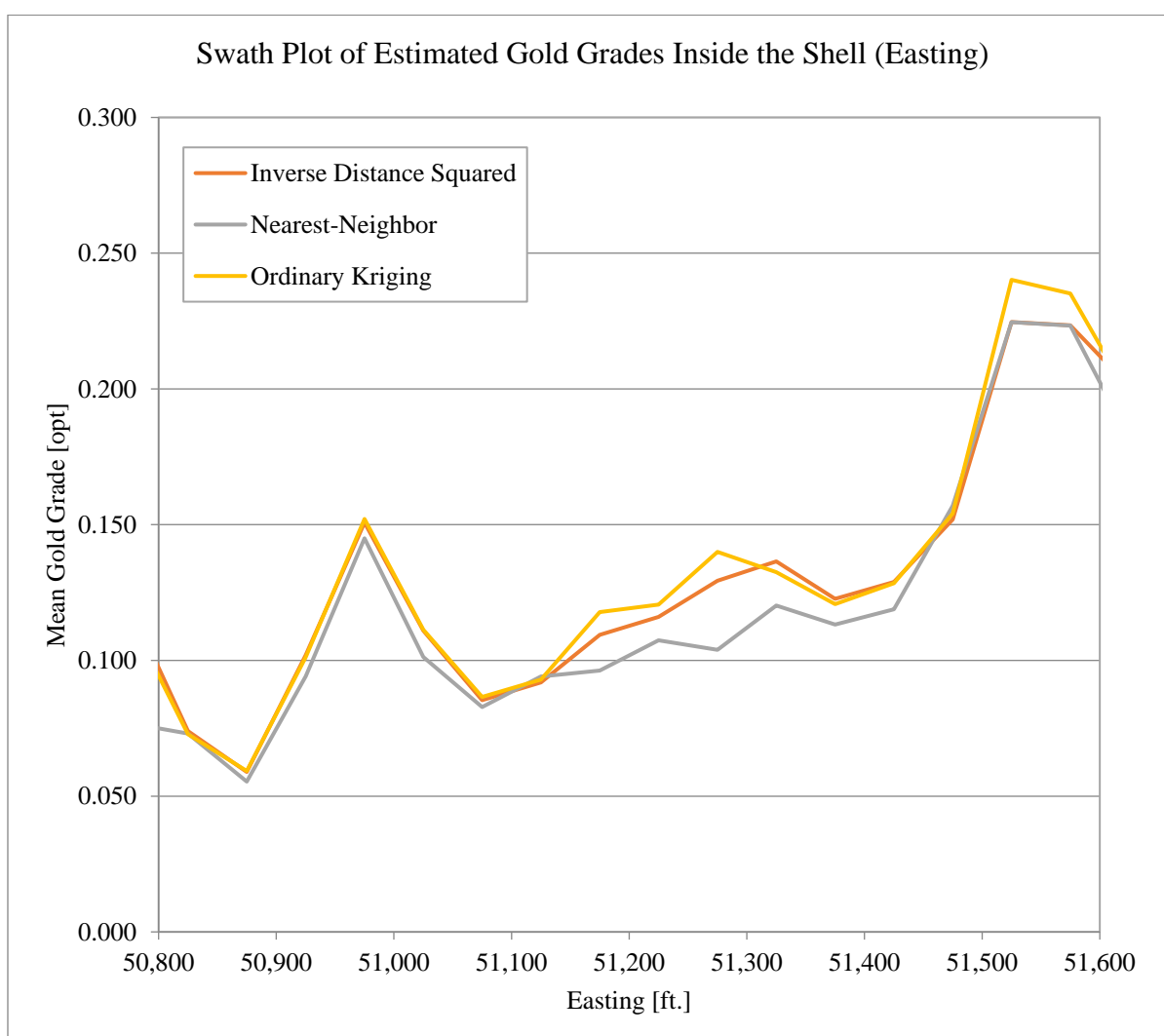


**Figure 18: Swath plot of estimated gold grades inside the shell (Easting)**
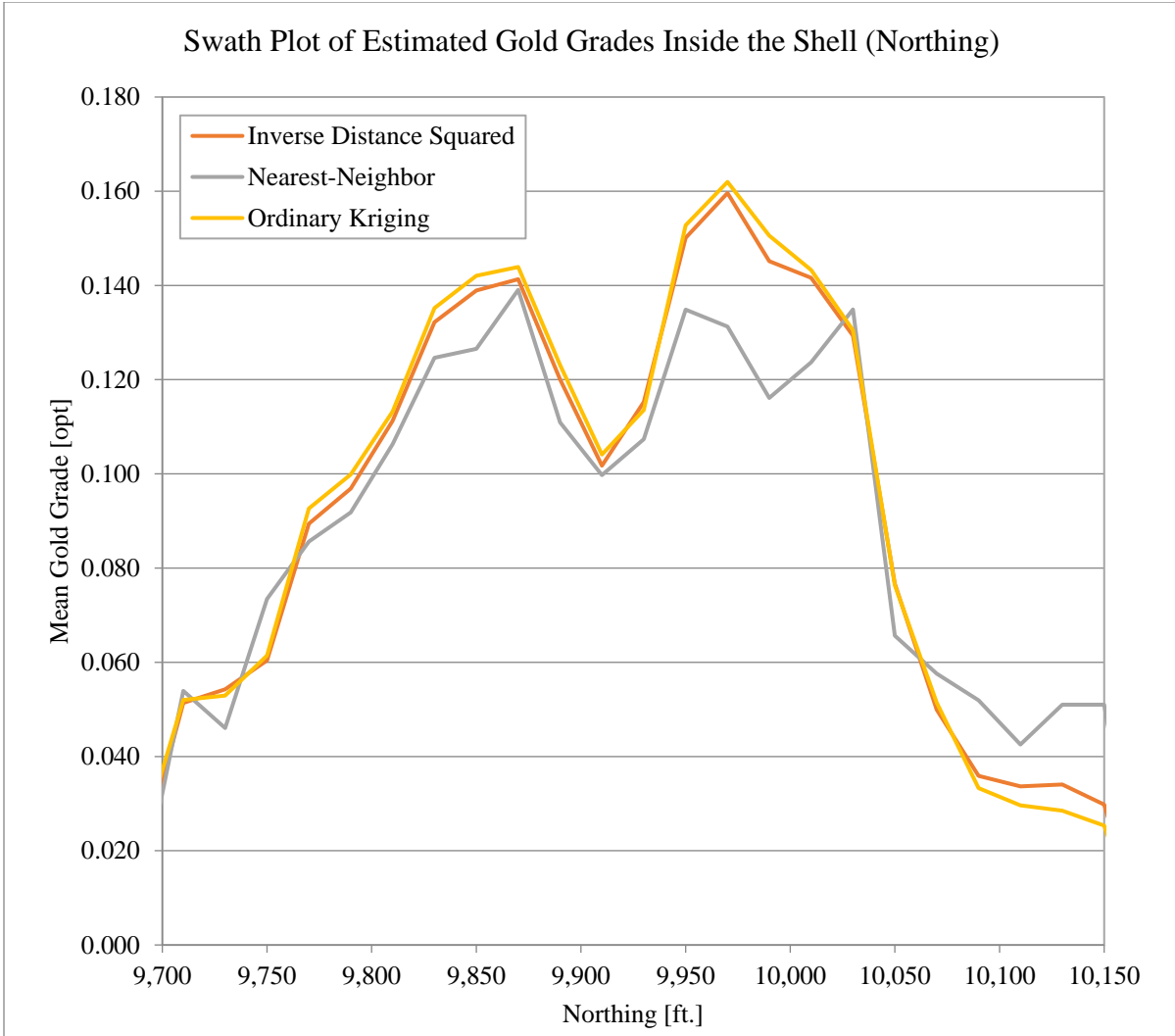
**Figure 19: Swath Plot of Estimated Gold Grades Inside the Shell (Northing)**
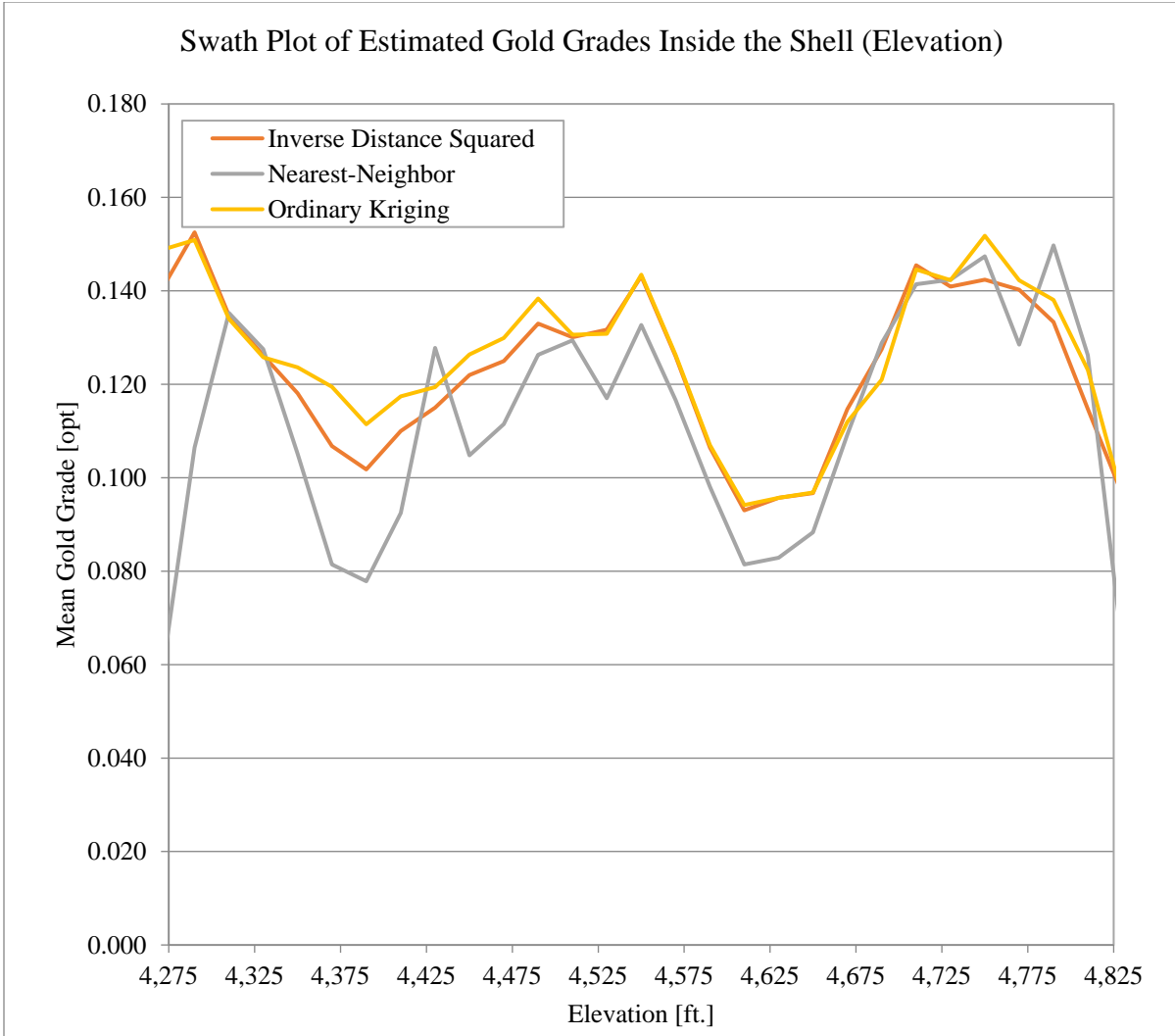
**Figure 20: Swath Plot of Estimated Gold Grades Inside the Shell (Elevation)**
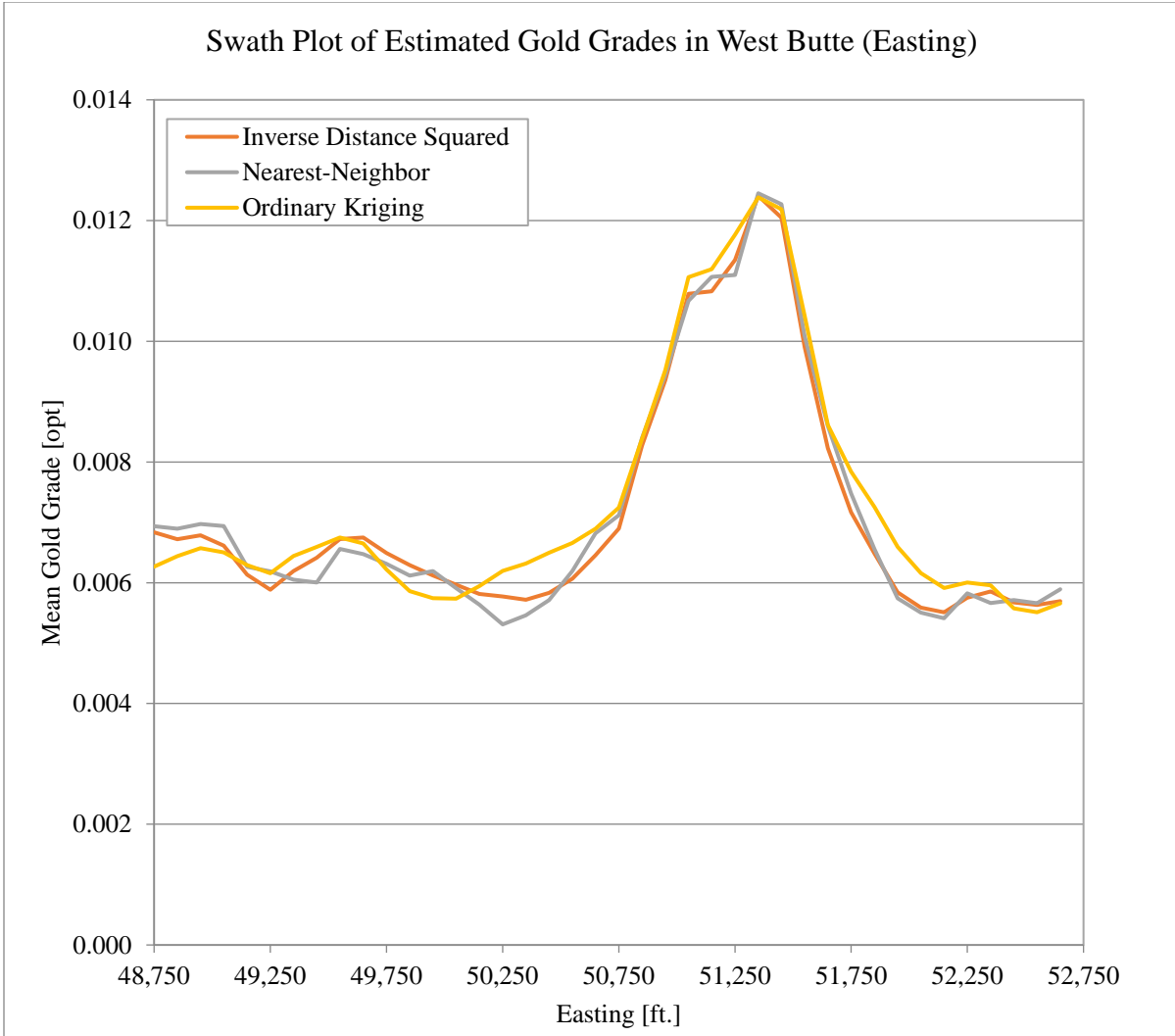
**Figure 21: Swath Plot of Estimated Gold Grades in West Butte (Easting)**
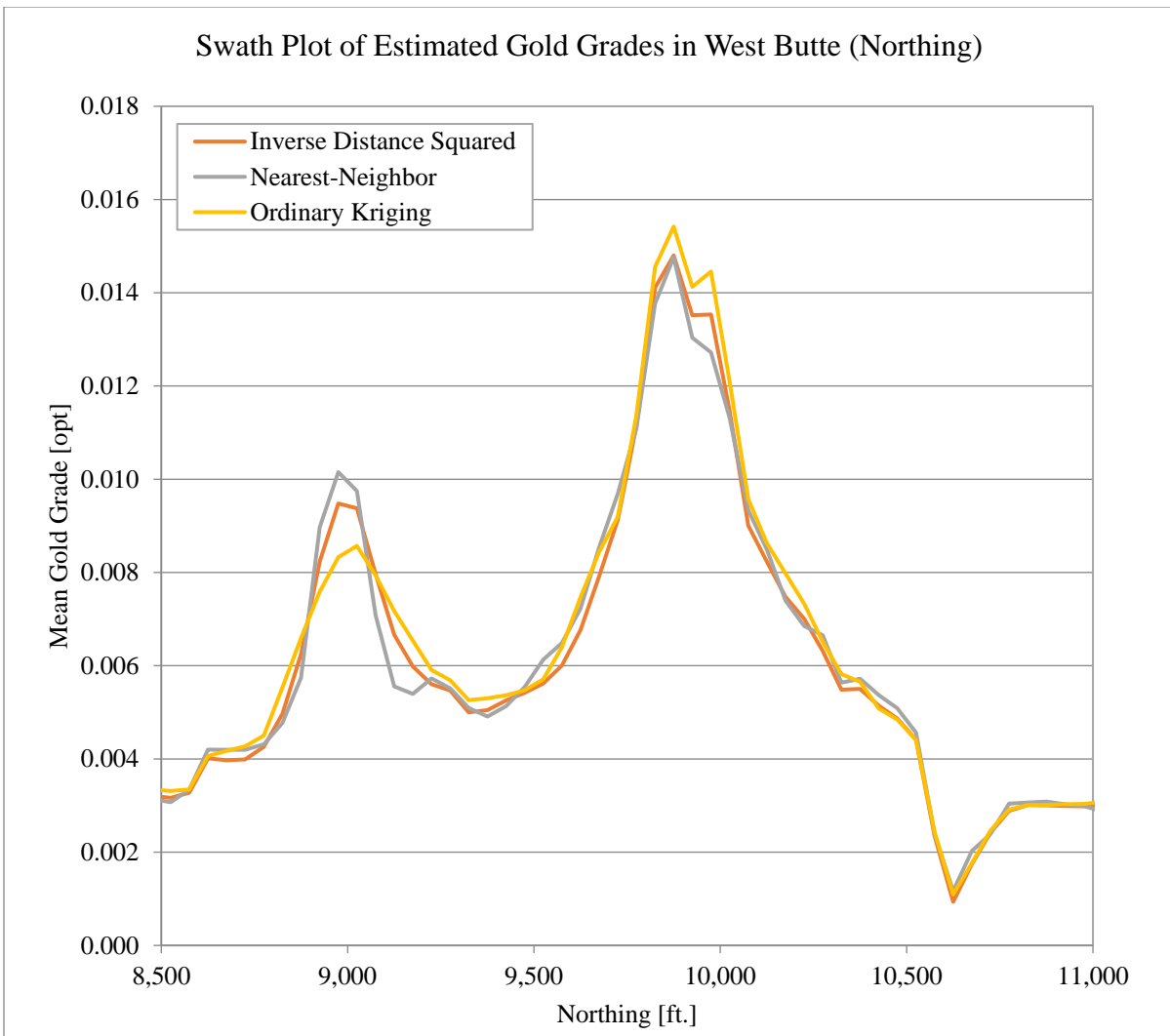
**Figure 22: Swath Plot of Estimated Gold Grades in West Butte (Northing)**
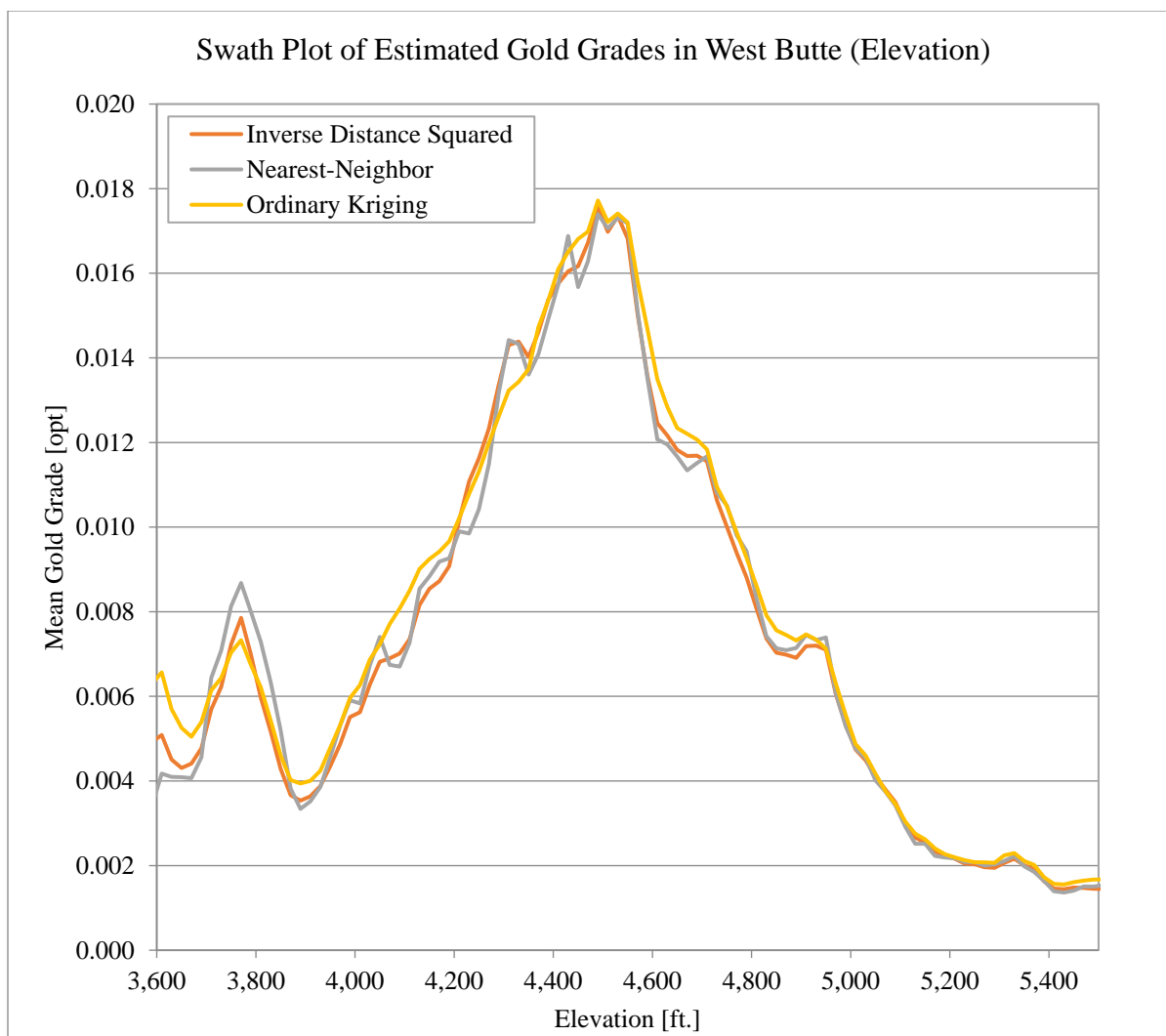
**Figure 23: Swath Plot of Estimated Gold Grades in West Butte (Elevation)**

### 3.3.3. Visual Inspection

Visual inspection is essential in the validation of a resource model to ensure that estimated block grades are similar to the sample grades nearby and that the distribution of estimated grades matches orientations described by the variogram model. See Appendix A for selected plan-view sections of the ordinary-kriged gold estimate.

## 3.4. Model Results

### 3.4.1. Grade-Tonnage Curves

Grade-tonnage curves are graphs that report tonnages and average grades of material at different cutoffs. These curves are used to assess sensitivity and selectivity of mineable material as mining cutoffs change. Grade-tonnage curves were generated for inverse-distance-squared (IDS) and ordinary kriged (OK) estimates (Table XVI - XX and Figure 24 - 26).

**Table XVI: Grade, Tons, and Metal of IDS and OK Estimate in West Butte**

| Cutoff [opt] | Inverse Distance Squared (IDS) Estimate | | | Ordinary Kriging (OK) Estimate | | |
|---|---|---|---|---|---|---|
| | Grade [opt] | Tonnage [t] | Metal [oz t] | Grade [opt] | Tonnage [t] | Metal [oz t] |
| 0.006 | 0.017 | 181,430,832 | 3,049,852 | 0.016 | 196,063,296 | 3,174,265 |
| 0.01 | 0.023 | 104,823,664 | 2,454,970 | 0.022 | 114,517,072 | 2,542,279 |
| 0.02 | 0.042 | 36,275,984 | 1,509,444 | 0.039 | 38,369,296 | 1,478,753 |
| 0.04 | 0.088 | 8,679,904 | 767,390 | 0.106 | 5,745,360 | 610,502 |
| 0.06 | 0.155 | 3,336,512 | 517,026 | 0.171 | 2,750,432 | 469,581 |
| 0.08 | 0.197 | 2,251,376 | 442,868 | 0.204 | 2,074,368 | 423,379 |
| 0.1 | 0.227 | 1,759,424 | 399,512 | 0.233 | 1,656,416 | 386,127 |
| 0.2 | 0.336 | 780,848 | 262,435 | 0.340 | 769,008 | 261,693 |
| 0.5 | 0.727 | 91,168 | 66,286 | 0.690 | 100,640 | 69,403 |

The results of both estimates show lower average grades and less metal than preliminary models produced by Newmont; however, the estimated grades and tonnages were constrained in effort to limit the influence of bias in RC data, resulting in more conservative estimates. The grade shell used to define estimation domains was derived not only from a grade cutoff of 0.04 Au opt but also from proximity to core data. As such, the grade shell not only represents a high-grade volume, but also a more-confident and more-selective volume. Additionally, estimates of high grade blocks were capped; and a high-yield limit of 0.1 Au opt was imposed outside the shell, further limiting the influence and spread of high-grade outside the grade shell.
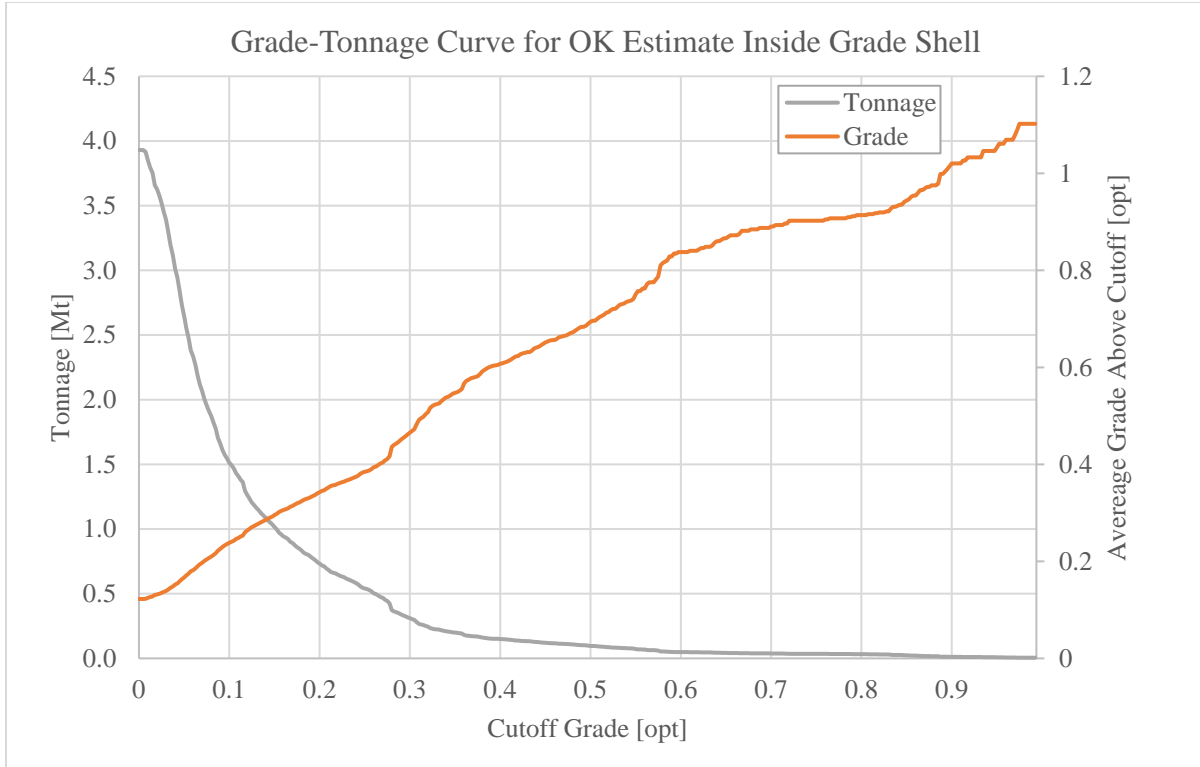
**Figure 24: Grade-Tonnage curve for the ordinary kriging (OK) estimate inside the grade shell**

**Table XVII: Grade, Tonnage, and Metal of the OK Inside-Shell Estimate at Selected Cutoffs**

| Cutoff [opt] | Grade [opt] | Tonnage [t] | Metal [oz t] |
|---|---|---|---|
| 0.006 | 0.123 | 3,929,104 | 481,630 |
| 0.01 | 0.125 | 3,849,776 | 480,953 |
| 0.02 | 0.132 | 3,627,776 | 477,633 |
| 0.04 | 0.152 | 3,012,096 | 458,290 |
| 0.06 | 0.182 | 2,333,072 | 424,619 |
| 0.08 | 0.210 | 1,875,456 | 393,152 |
| 0.1 | 0.238 | 1,513,744 | 360,998 |
| 0.2 | 0.342 | 732,896 | 250,958 |
| 0.5 | 0.694 | 96,496 | 66,961 |
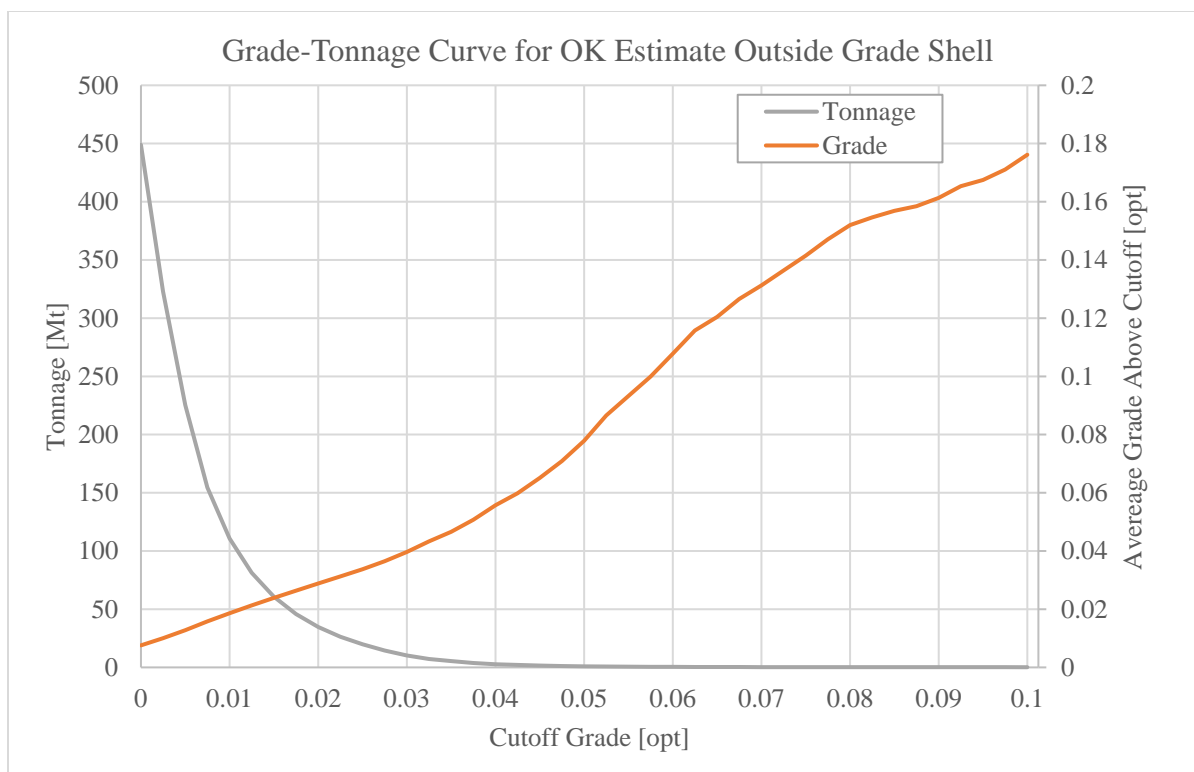
**Figure 25: Grade-Tonnage curve for the ordinary kriging (OK) outside-shell estimate**

**Table XVIII: Grade, Tonnage, and Metal of the OK Outside-Shell Estimate at Selected Cutoffs**

| Cutoff [opt] | Grade [opt] | Tonnage [t] | Metal [oz t] |
|---|---|---|---|
| 0.006 | 0.014 | 192,134,192 | 2,691,800 |
| 0.01 | 0.019 | 110,667,296 | 2,060,625 |
| 0.02 | 0.029 | 34,741,520 | 1,001,251 |
| 0.04 | 0.056 | 2,733,264 | 152,243 |
| 0.06 | 0.108 | 417,360 | 44,975 |
| 0.08 | 0.152 | 198,912 | 30,235 |
| 0.1 | 0.176 | 142,672 | 25,132 |
| 0.2 | 0.297 | 36,112 | 10,733 |
| 0.5 | 0.589 | 4,144 | 2,443 |
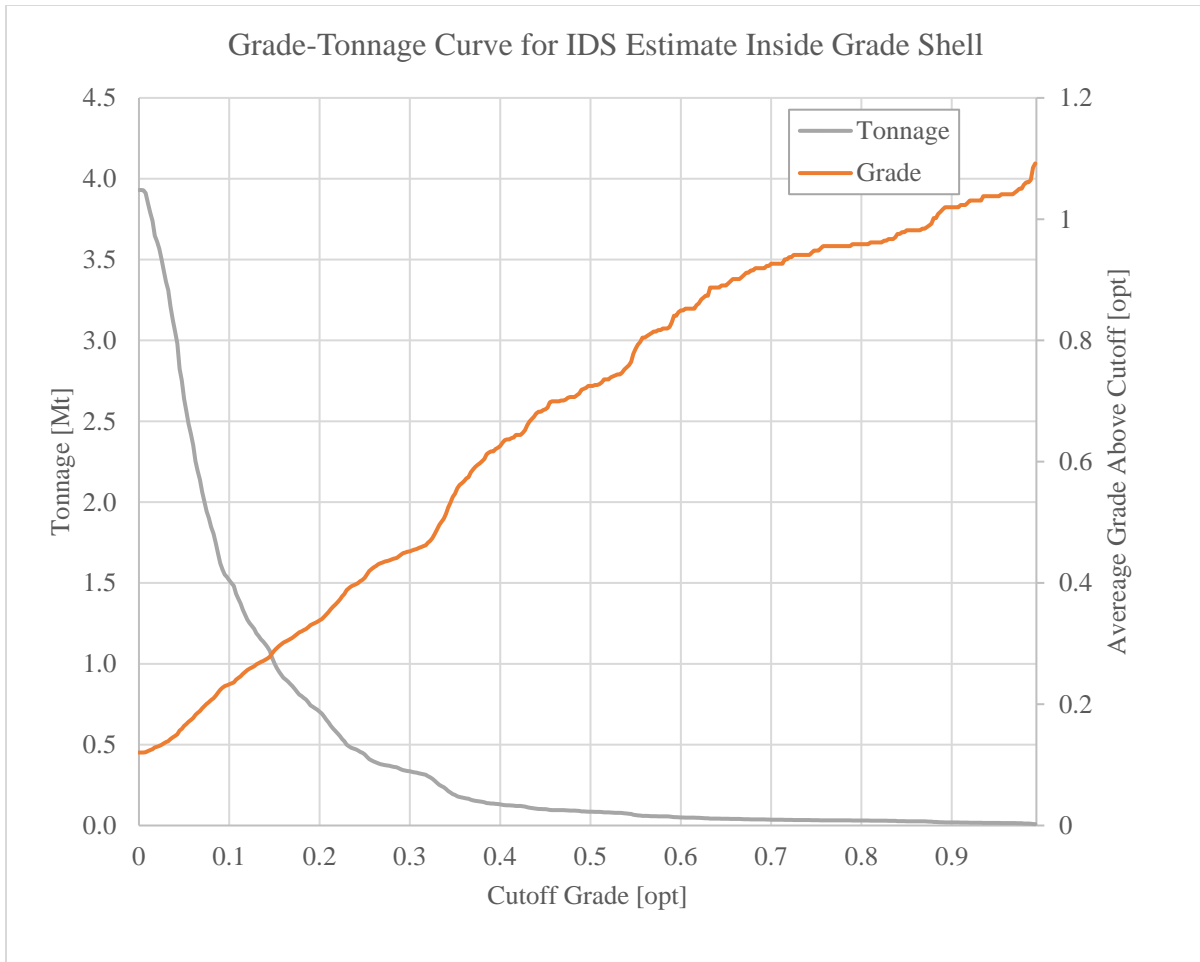
**Figure 26: Grade-Tonnage curve for the Ordinary Kriging (IDS) Inside-shell estimate**

**Table XIX: Grade, Tonnage, and Metal of the IDS Inside-Shell Estimate at Selected Cutoffs**

| Cutoff [opt] | Grade [opt] | Tonnage [t] | Metal [oz t] |
|---|---|---|---|
| 0.006 | 0.120 | 3,927,328 | 472,968 |
| 0.01 | 0.123 | 3,849,776 | 472,329 |
| 0.02 | 0.130 | 3,611,792 | 468,847 |
| 0.04 | 0.148 | 3,053,536 | 451,649 |
| 0.06 | 0.177 | 2,352,016 | 417,224 |
| 0.08 | 0.207 | 1,847,040 | 382,356 |
| 0.1 | 0.233 | 1,517,296 | 353,318 |
| 0.2 | 0.338 | 703,296 | 237,883 |
| 0.5 | 0.725 | 85,248 | 61,798 |
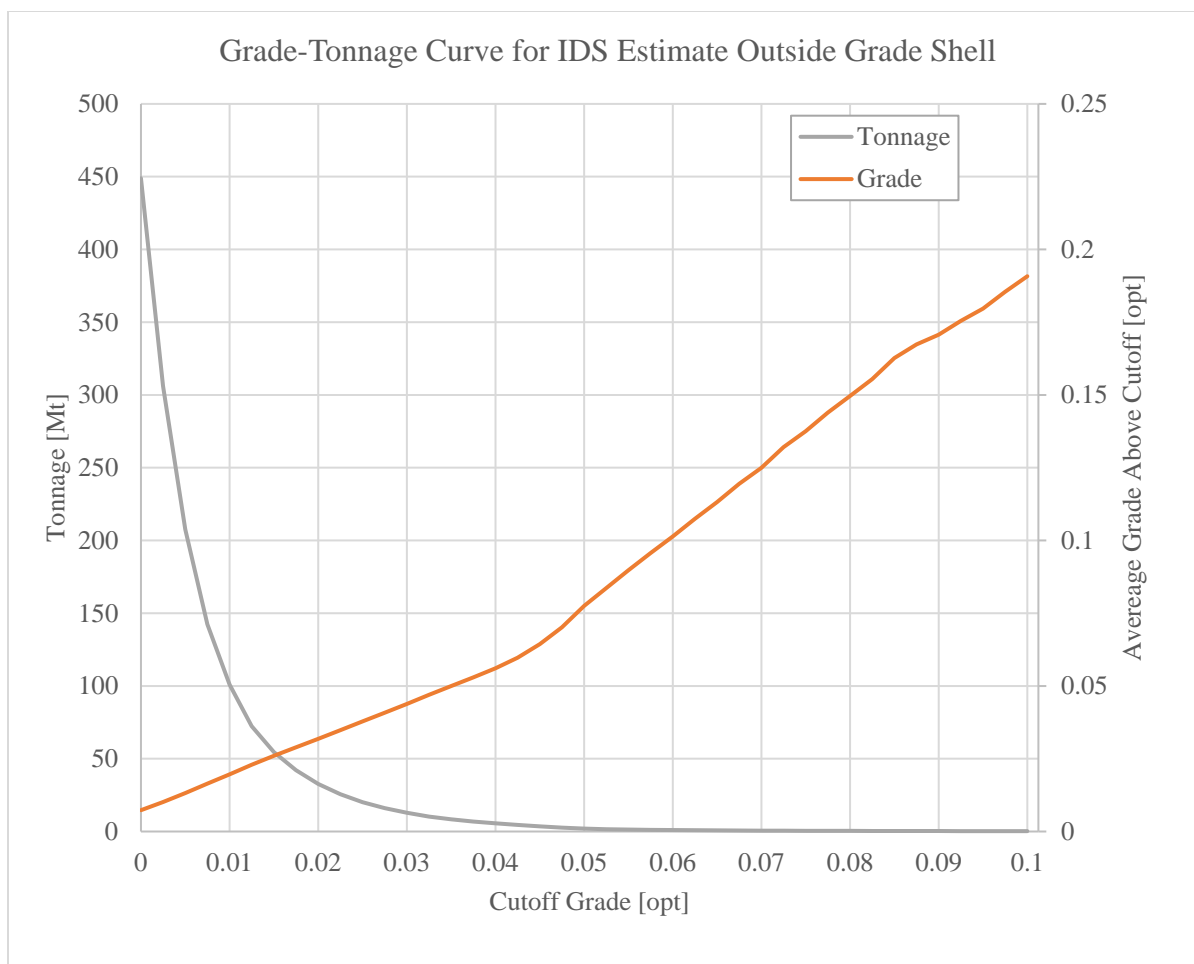
**Figure 27: Grade-Tonnage curve for the Ordinary Kriging (IDS) outside-shell estimate**

**Table XX: Grade, Tonnage, and Metal of the IDS Outside-Shell Estimate at Selected Cutoffs**

| Cutoff [opt] | Grade [opt] | Tonnage [t] | Metal [oz t] |
|---|---|---|---|
| 0.006 | 0.015 | 177,503,504 | 2,577,351 |
| 0.01 | 0.020 | 100,973,888 | 1,982,117 |
| 0.02 | 0.032 | 32,664,192 | 1,040,681 |
| 0.04 | 0.056 | 5,626,368 | 315,696 |
| 0.06 | 0.101 | 984,496 | 99,798 |
| 0.08 | 0.150 | 404,336 | 60,509 |
| 0.1 | 0.191 | 242,128 | 46,193 |
| 0.2 | 0.317 | 77,552 | 24,551 |
| 0.5 | 0.758 | 5,920 | 4,487 |

### 3.4.2. Metal Loss Due to Capping

Capping strategies are often used to prevent the overstatement of grades and tonnages within a deposit by limiting the influence of high-grade samples during the estimation process. It is an industry-best practice to provide metal loss reports with resource estimates to quantify the amount of additional metal that may exist as a result of conservative estimation. It is the author's opinion that a conservative estimate with metal loss reports is more valuable than an optimistic, unconstrained estimate. Table XXI Table XXVI characterize metal loss due to capping at West Butte. Table XXIII andTable XXIV suggest the presence of a significant gold resource outside the grade shell in West Butte; however, the magnitude of resource outside the shell may not be accurately represented. It is likely that the gold resources are overstated in the uncapped estimates outside the shell, due to high-grade samples being unrestricted within a generally-low-grade domain.

**Table XXI: Metal Loss Report for IDS Inside the Grade Shell**

| Cutoff [opt] | Capped | | | Uncapped | | |
|---|---|---|---|---|---|---|
| | Grade [opt] | Tonnage [t] | Metal [oz t] | Grade [opt] | Tonnage [t] | Metal [t oz] |
| 0.006 | 0.120 | 3,927,328 | 472,968 | 0.128 | 3,927,328 | 502,070 |
| 0.01 | 0.123 | 3,849,776 | 472,329 | 0.130 | 3,849,776 | 501,433 |
| 0.02 | 0.130 | 3,611,792 | 468,847 | 0.138 | 3,612,384 | 497,931 |
| 0.04 | 0.148 | 3,053,536 | 451,649 | 0.157 | 3,058,272 | 480,883 |
| 0.06 | 0.177 | 2,352,016 | 417,224 | 0.189 | 2,356,160 | 446,422 |
| 0.08 | 0.207 | 1,847,040 | 382,356 | 0.222 | 1,850,000 | 411,477 |
| 0.1 | 0.233 | 1,517,296 | 353,318 | 0.252 | 1,519,072 | 382,320 |
| 0.2 | 0.338 | 703,296 | 237,883 | 0.379 | 704,480 | 266,829 |
| 0.5 | 0.725 | 85,248 | 61,798 | 1.037 | 88,208 | 91,482 |

**Table XXII: Metal Loss Report for OK Inside the Grade Shell**

| | Capped | | | Uncapped | | |
|---|---|---|---|---|---|---|
| Cutoff [opt] | Grade [opt] | Tonnage [t] | Metal [oz t] | Grade [opt] | Tonnage [t] | Metal [t oz] |
| 0.006 | 0.123 | 3,929,104 | 481,630 | 0.130 | 3,929,104 | 510,784 |
| 0.01 | 0.125 | 3,849,776 | 480,953 | 0.133 | 3,849,776 | 510,134 |
| 0.02 | 0.132 | 3,627,776 | 477,633 | 0.140 | 3,627,776 | 506,800 |
| 0.04 | 0.152 | 3,012,096 | 458,290 | 0.162 | 3,016,832 | 487,611 |
| 0.06 | 0.182 | 2,333,072 | 424,619 | 0.194 | 2,336,624 | 453,866 |
| 0.08 | 0.210 | 1,875,456 | 393,152 | 0.225 | 1,878,416 | 422,362 |
| 0.1 | 0.238 | 1,513,744 | 360,998 | 0.257 | 1,516,112 | 390,156 |
| 0.2 | 0.342 | 732,896 | 250,958 | 0.381 | 734,080 | 279,956 |
| 0.5 | 0.694 | 96,496 | 66,961 | 0.970 | 100,048 | 97,011 |

**Table XXIII: Metal Loss Report for IDS Outside the Grade Shell**

| | Capped | | | Uncapped | | |
|---|---|---|---|---|---|---|
| Cutoff [opt] | Grade [opt] | Tonnage [t] | Metal [oz t] | Grade [opt] | Tonnage [t] | Metal [t oz] |
| 0.006 | 0.015 | 177,503,504 | 2,577,351 | 0.017 | 193,518,288 | 3,297,552 |
| 0.01 | 0.020 | 100,973,888 | 1,982,117 | 0.024 | 113,964,144 | 2,681,576 |
| 0.02 | 0.032 | 32,664,192 | 1,040,681 | 0.039 | 43,031,296 | 1,695,003 |
| 0.04 | 0.056 | 5,626,368 | 315,696 | 0.075 | 10,866,752 | 818,484 |
| 0.06 | 0.101 | 984,496 | 99,798 | 0.110 | 4,802,304 | 529,118 |
| 0.08 | 0.150 | 404,336 | 60,509 | 0.136 | 2,949,936 | 402,224 |
| 0.1 | 0.191 | 242,128 | 46,193 | 0.163 | 1,861,248 | 303,867 |
| 0.2 | 0.317 | 77,552 | 24,551 | 0.404 | 215,488 | 87,126 |
| 0.5 | 0.758 | 5,920 | 4,487 | 0.607 | 76,960 | 46,717 |

**Table XXIV: Metal Loss Report for OK Outside the Grade Shell**

| | Capped | | | Uncapped | | |
|---|---|---|---|---|---|---|
| Cutoff [opt] | Grade [opt] | Tonnage [t] | Metal [oz t] | Grade [opt] | Tonnage [t] | Metal [t oz] |
| 0.006 | 0.014 | 192,134,192 | 2,691,800 | 0.017 | 193,518,288 | 3,297,552 |
| 0.01 | 0.019 | 110,667,296 | 2,060,625 | 0.024 | 113,964,144 | 2,681,576 |
| 0.02 | 0.029 | 34,741,520 | 1,001,251 | 0.039 | 43,031,296 | 1,695,003 |
| 0.04 | 0.056 | 2,733,264 | 152,243 | 0.075 | 10,866,752 | 818,484 |
| 0.06 | 0.108 | 417,360 | 44,975 | 0.110 | 4,802,304 | 529,118 |
| 0.08 | 0.152 | 198,912 | 30,235 | 0.136 | 2,949,936 | 402,224 |
| 0.1 | 0.176 | 142,672 | 25,132 | 0.163 | 1,861,248 | 303,867 |
| 0.2 | 0.297 | 36,112 | 10,733 | 0.404 | 215,488 | 87,126 |
| 0.5 | 0.589 | 4,144 | 2,443 | 0.607 | 76,960 | 46,717 |

**Table XXV: Metal Loss Report for IDS in West Butte**

| Cutoff [opt] | Capped | | | Uncapped | | |
|---|---|---|---|---|---|---|
| | Grade [opt] | Tonnage [t] | Metal [oz t] | Grade [opt] | Tonnage [t] | Metal [t oz] |
| 0.006 | 0.017 | 181,430,832 | 3,049,852 | 0.020 | 183,416,992 | 3,600,476 |
| 0.01 | 0.023 | 104,823,664 | 2,454,970 | 0.028 | 108,857,552 | 3,020,797 |
| 0.02 | 0.042 | 36,275,984 | 1,509,444 | 0.049 | 43,068,000 | 2,115,069 |
| 0.04 | 0.088 | 8,679,904 | 767,390 | 0.090 | 14,955,696 | 1,349,452 |
| 0.06 | 0.155 | 3,336,512 | 517,026 | 0.135 | 7,267,392 | 981,171 |
| 0.08 | 0.197 | 2,251,376 | 442,868 | 0.173 | 4,609,312 | 798,886 |
| 0.1 | 0.227 | 1,759,424 | 399,512 | 0.207 | 3,290,928 | 681,946 |
| 0.2 | 0.336 | 780,848 | 262,435 | 0.352 | 1,076,848 | 378,727 |
| 0.5 | 0.727 | 91,168 | 66,286 | 1.023 | 100,640 | 102,954 |

**Table XXVI: Metal Loss Report for OK in West Butte**

| Cutoff [opt] | Capped | | | Uncapped | | |
|---|---|---|---|---|---|---|
| | Grade [opt] | Tonnage [t] | Metal [oz t] | Grade [opt] | Tonnage [t] | Metal [t oz] |
| 0.006 | 0.016 | 196,063,296 | 3,174,265 | 0.019 | 197,447,392 | 3,808,760 |
| 0.01 | 0.022 | 114,517,072 | 2,542,279 | 0.027 | 117,813,920 | 3,191,579 |
| 0.02 | 0.039 | 38,369,296 | 1,478,753 | 0.047 | 46,659,072 | 2,201,842 |
| 0.04 | 0.106 | 5,745,360 | 610,502 | 0.094 | 13,883,584 | 1,306,168 |
| 0.06 | 0.171 | 2,750,432 | 469,581 | 0.138 | 7,138,928 | 983,030 |
| 0.08 | 0.204 | 2,074,368 | 423,379 | 0.171 | 4,828,352 | 824,586 |
| 0.1 | 0.233 | 1,656,416 | 386,127 | 0.205 | 3,377,360 | 694,014 |
| 0.2 | 0.340 | 769,008 | 261,693 | 0.387 | 949,568 | 367,084 |
| 0.5 | 0.690 | 100,640 | 69,403 | 0.812 | 177,008 | 143,727 |

## 4. Conditional Simulation

Estimation methods such as inverse distance weighting and some forms of kriging are deterministic processes that provide "a value that is, on average, as close as possible to the actual (unknown) value…" (Rossi & Deutch, 2014). In a resource model, an estimate provides a singular, estimated value for each block within the model. Metrics such as kriging efficiency and kriging variance help to characterize uncertainty within an estimated model, but these metrics are limited and do not completely describe the distribution of possible values. Simulated models offer a stochastic solution that not only incorporates a single expected value at each block, but also provides each block with a distribution of possible outcomes. Simulated models aim to reproduce the statistics and spatial variability (variograms) of the sample data (Goovaerts, 1997). Conditional simulation has become a popular geostatistical technique in the mining industry "…[having] been used as grade control tools in daily operations, to analyze risk related to resource classifications, to assess the uncertainty of minable reserves at the project's feasibility stage, and to assess mineralization potential in certain settings" (Rossi & Deutch, 2014). Simulation methods and validations are discussed in depth in literature such as Goovaerts (1997) *Geostatistics for Natural Resources Evaluation*, Rossi & Deutch (2014) *Mineral Resource Estimation*, and Leuangthong et al. (2004) "Minimum acceptance criteria for geostatistical realizations".

## 4.1.    Data Transformation and Variography

Prior to performing sequential Gaussian simulations (SGS), the composite data set was transformed to standard normal distributions. Data transformations were performed on each estimation domain separately, and the normal-scored domain statistics were reviewed to ensure the data were standard normal. Variogram models (Table XXVII and Figure 28 - 35) were derived from normal-scored, declustered composite data, and were fixed to the same orientations used in the estimated models.

**Table XXVII: Variogram Model Parameters for SGS**

|  | Estimation Domain | | | | |
|---|---|---|---|---|---|
|  | Inside Grade Shell | | Outside Grade Shell | | |
| Total Sill |  | 1 |  |  | 1 |
| Nugget |  | 0.2 |  |  | 0.1 |
| Structure | 1 | 2 | 1 | 2 | 3 |
| Structure Type | Spherical | Spherical | Spherical | Spherical | Spherical |
| Bearing | 135 | 135 | 256.35 | 256.35 | 256.35 |
| Plunge | 75 | 75 | -6.28 | -6.28 | -6.28 |
| Dip | 90 | 90 | -45 | -45 | -45 |
| Sill | 0.25 | 0.55 | 0.16 | 0.24 | 0.5 |
| Major Range | 25 | 200 | 40 | 350 | 2500 |
| Semi-Major Range | 60 | 100 | 25 | 350 | 525 |
| Minor Range | 40 | 65 | 25 | 250 | 680 |

**Figure 28: Downhole variogram of normal-scored gold grades inside the grade shell**

**Figure 29: Downhole variogram of normal-scored gold grades outside the grade shell**

**Figure 30: Major variogram of normal-scored gold grades inside the grade shell**
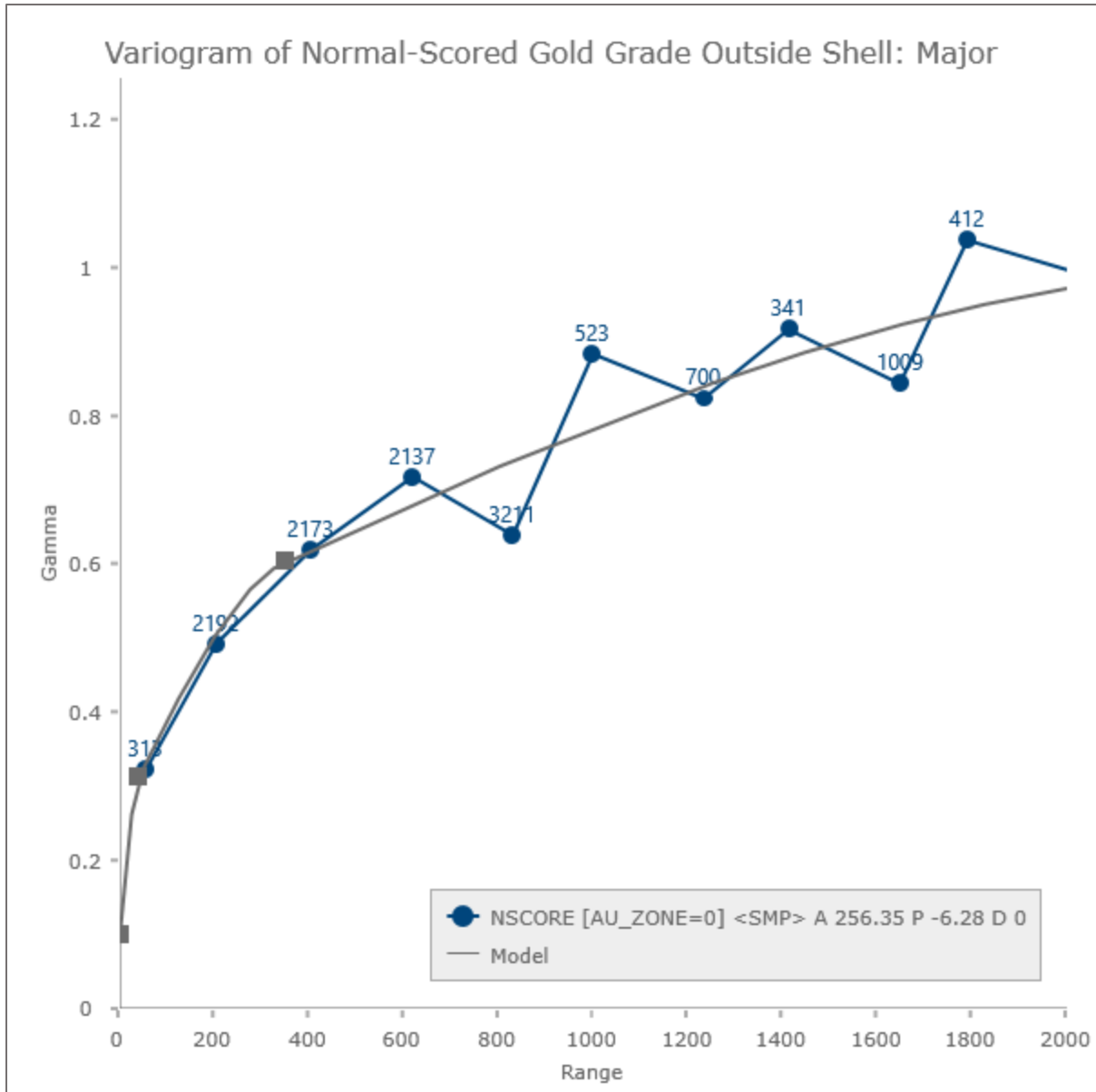
**Figure 31: Major variogram of normal-scored gold grades outside the grade shell**
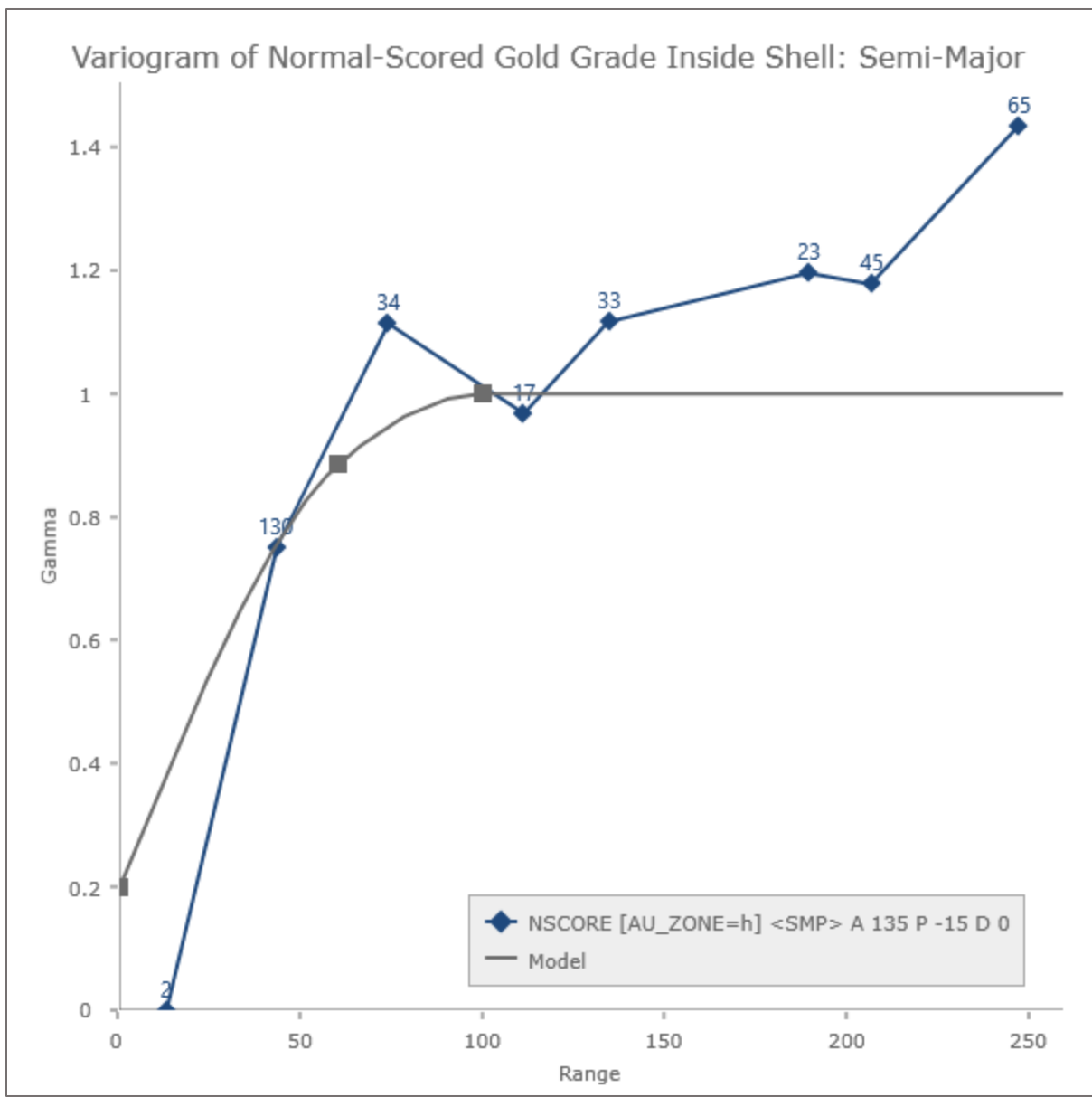
**Figure 32: Semi-Major variogram of normal-scored gold grades inside the grade shell**

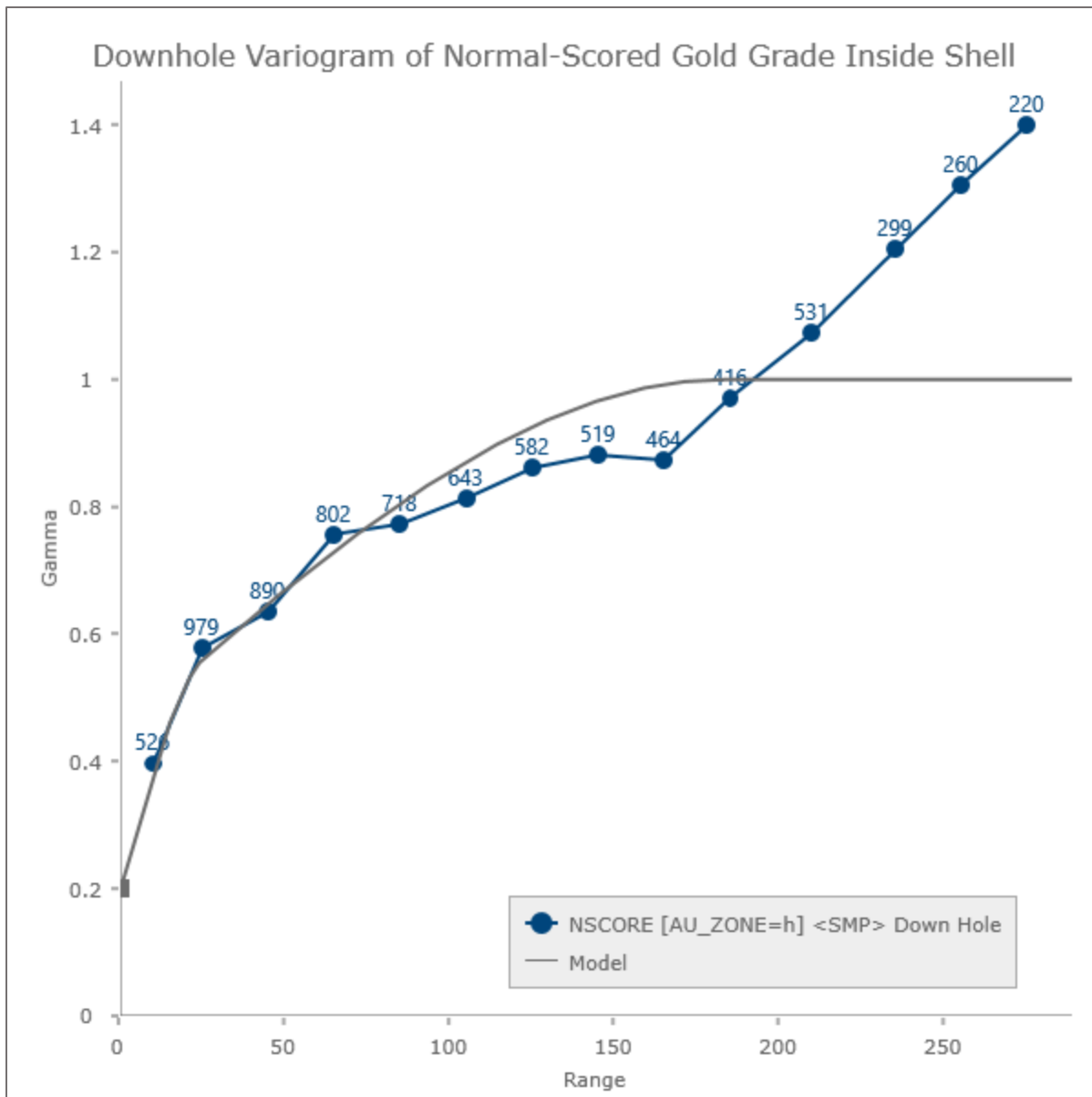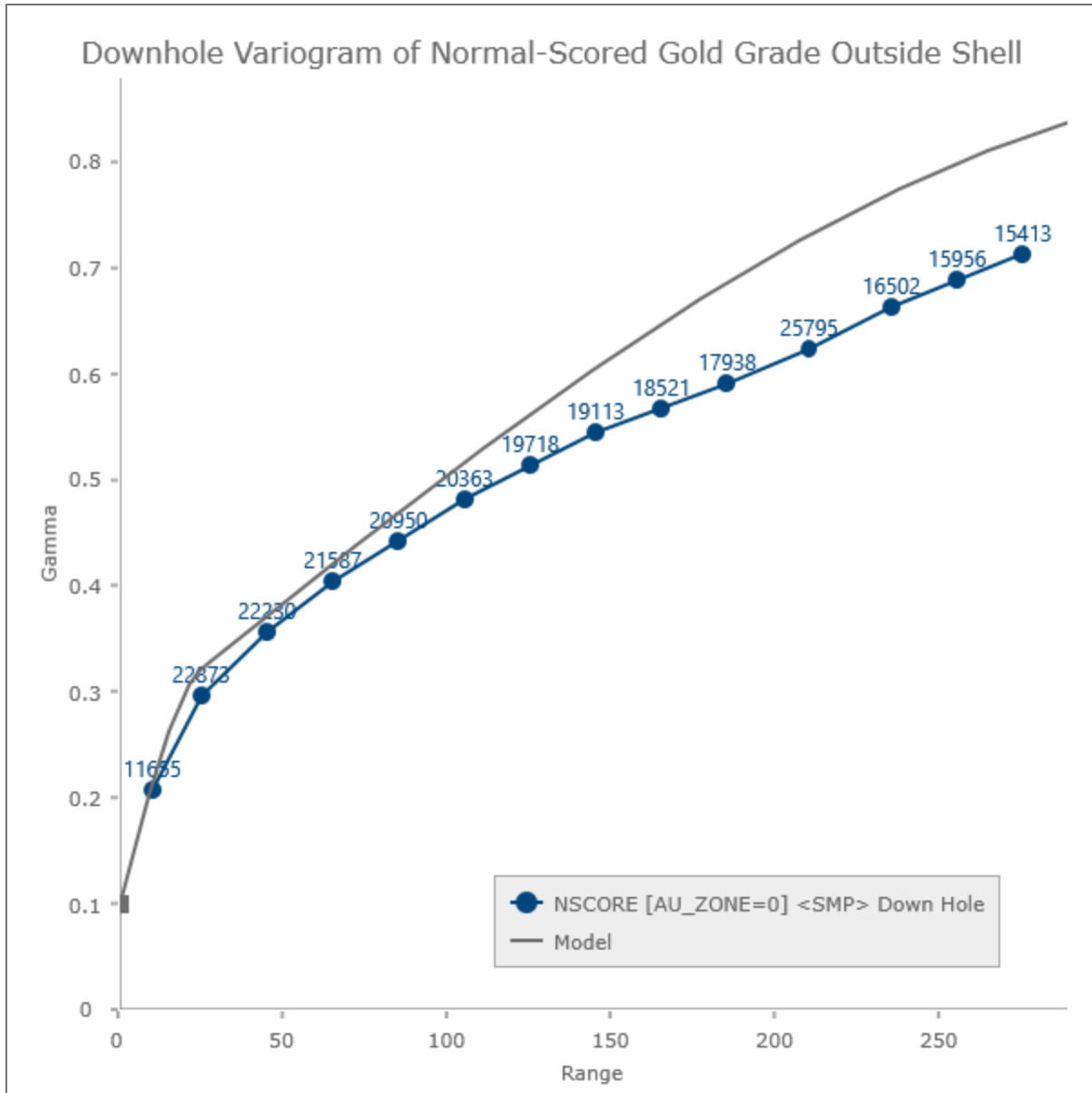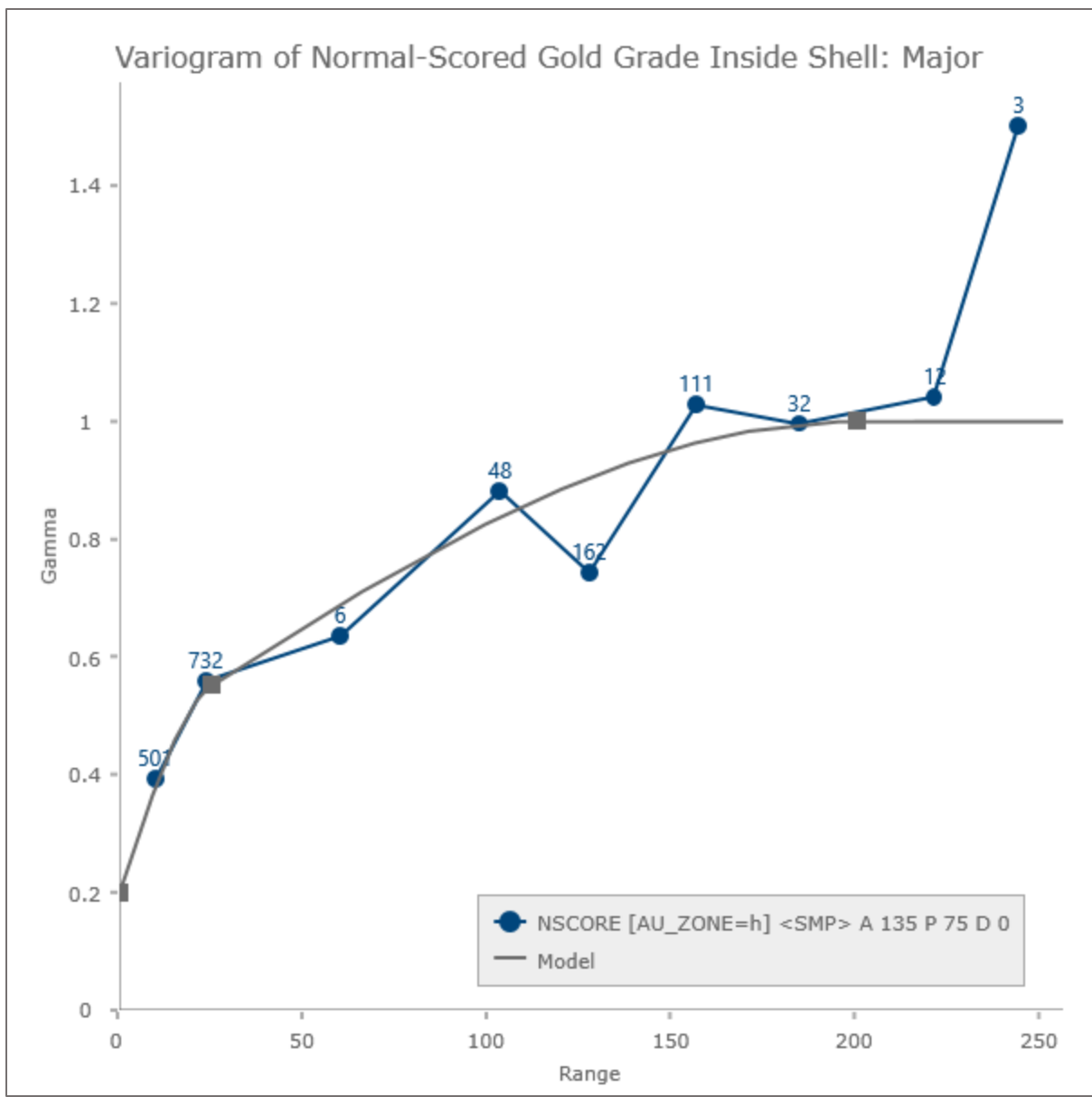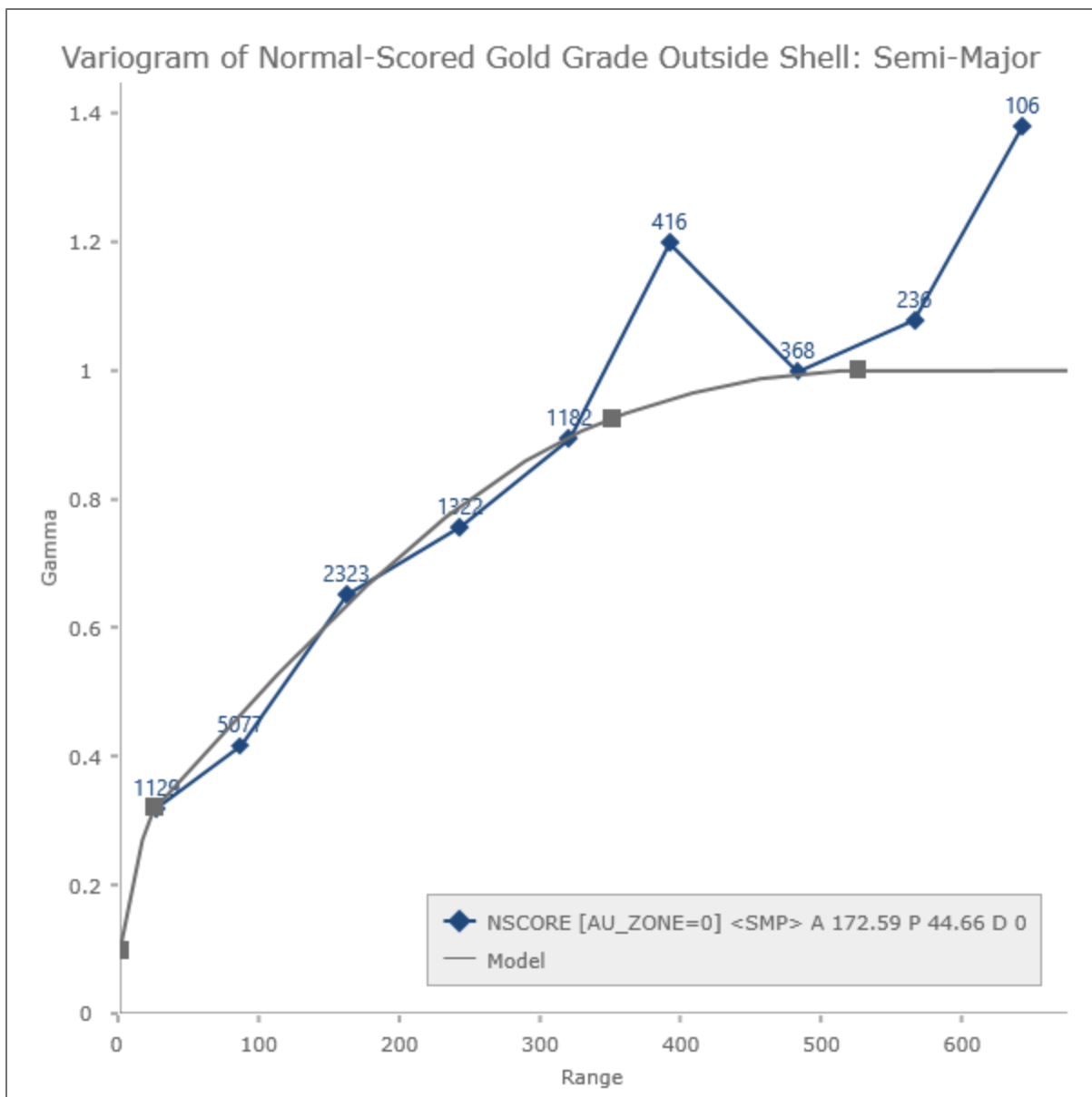**Figure 33: Semi-Major variogram of normal-scored gold grades outside the grade shell**
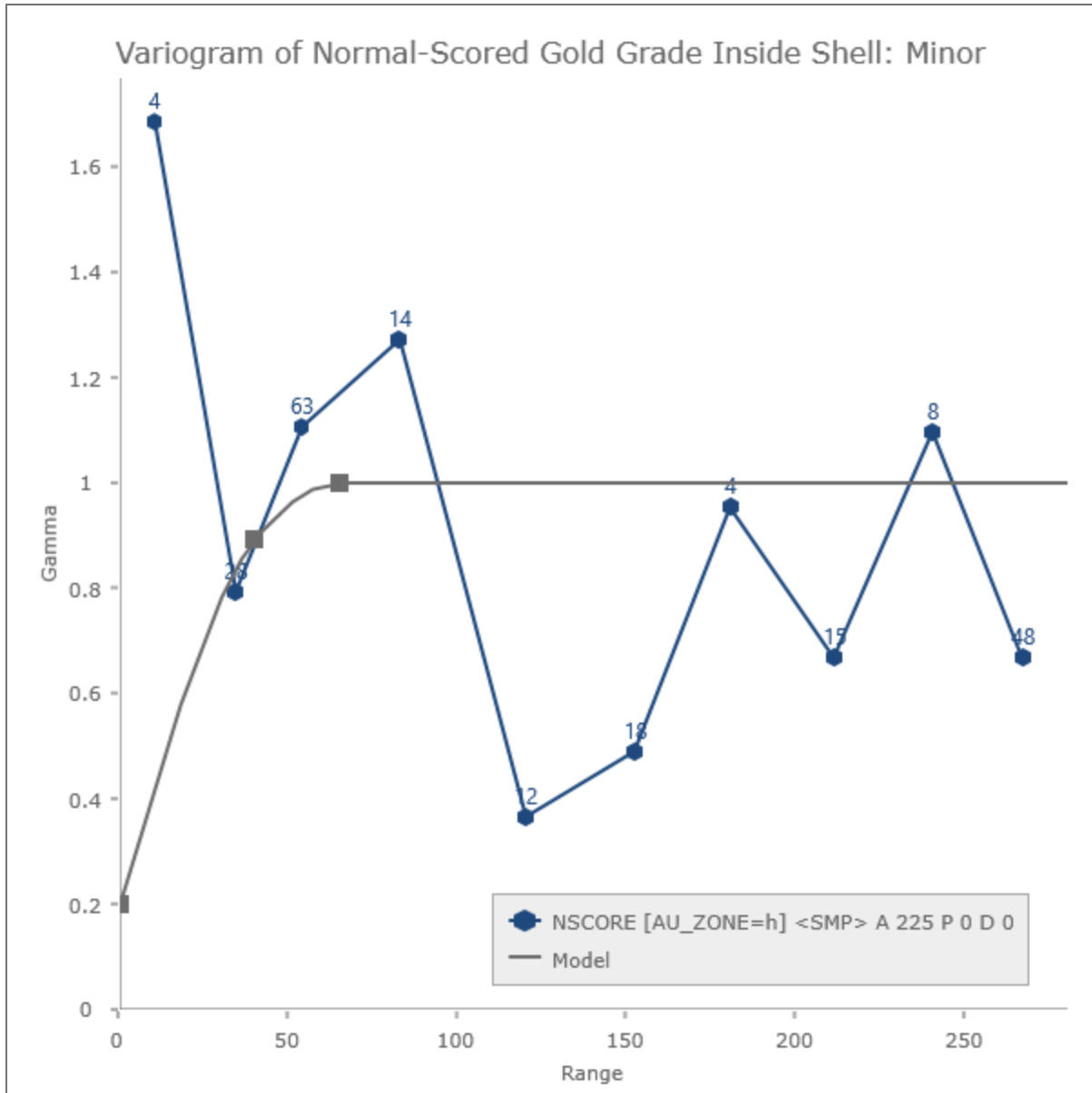
**Figure 34: Minor variogram of normal-scored gold grades inside the grade shell**
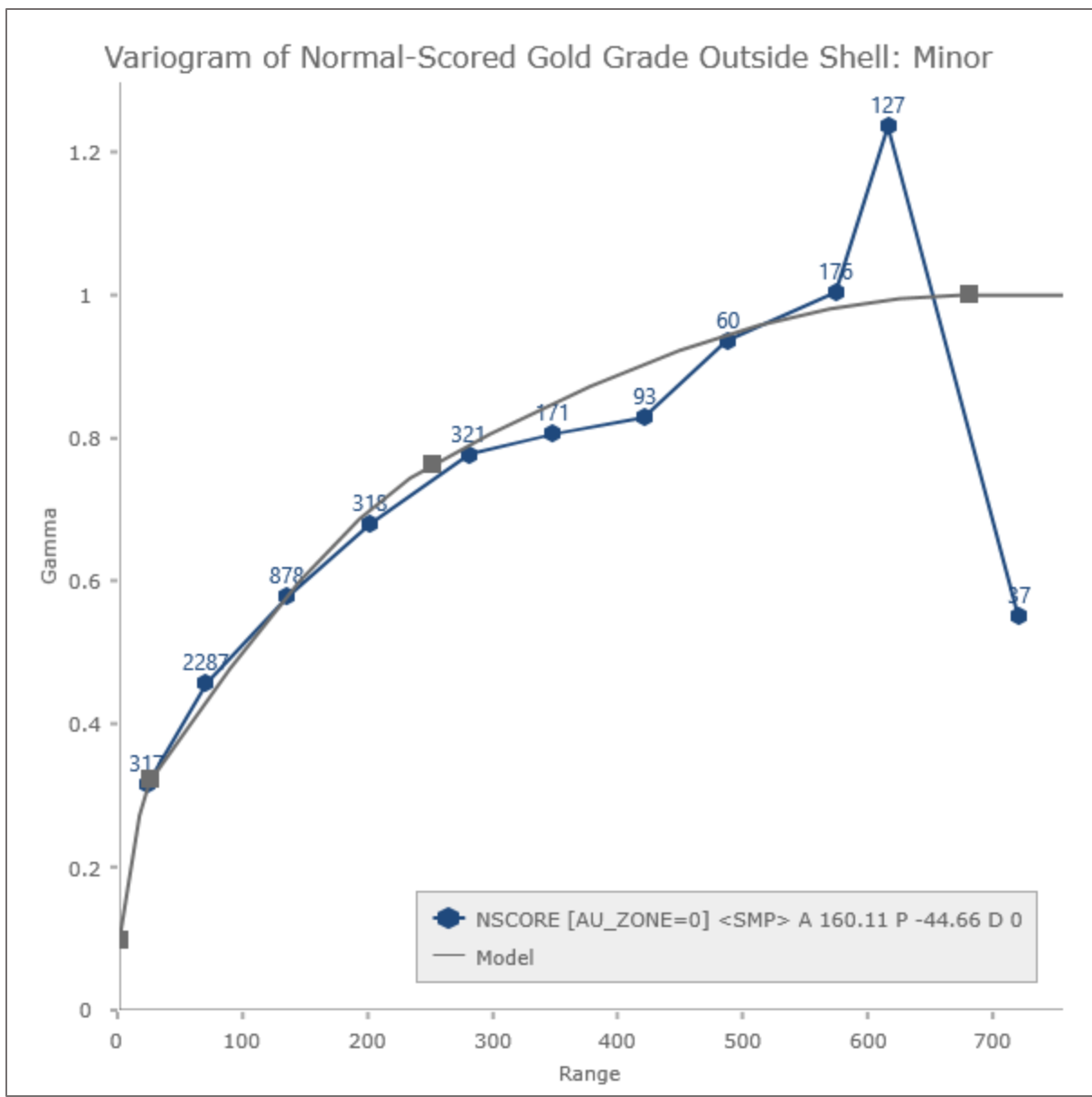
**Figure 35: Minor variogram of normal-scored gold grades outside the grade shell**

## 4.2. Simulation Plan

Conditional simulation of gold at the McDonald deposit was conducted using sequential Gaussian simulation. Simulated models were created using 30, 50, and 100 realizations. The simulated models were carried out using the same parameters outlined in sections 3.1 – 3.2, with some exceptions: normal-score and gold variables were added to each simulated model based on the number of realizations used, capping strategies were removed, maximum sample limits were increased to 50, and normal-scored variogram models (Table XXVII) were used.

## 4.3. Model Validation

Validation of simulated models can be carried out using a variety of metrics as outlined in Leuangthong et al. (2004) "Minimum acceptance criteria for geostatistical realizations" and Deutsch (2017) "Checking Simulated Realizations – Mining". In effort to reduce redundancy, model validation will be restricted to the 30 realization simulated model.

### 4.3.1. Summary Statistics

The statistics of individual realizations of a simulated model should closely match the declustered database used. The average of all realizations in a simulated model should also reasonably match a corresponding kriged estimate. Table XXVIII – XXX compare selected realizations against the declustered database, and Table XXX compares the average of all realizations against a corresponding ordinary kriged estimate. Appendix A contains cumulative density functions of selected realizations for each estimation domain.

**Table XXVIII: Sample and Selected Realization Statistics of Gold Inside the Shell**

|  | Sample Database | au_005 | au_010 | au_015 | au_020 | au_025 | au_030 |
|---|---|---|---|---|---|---|---|
| Count | 556 | 6,639 | 6,639 | 6,639 | 6,639 | 6,639 | 6,639 |
| Mean | 0.141 | 0.132 | 0.128 | 0.149 | 0.129 | 0.137 | 0.132 |
| Variance | 0.140 | 0.094 | 0.085 | 0.118 | 0.078 | 0.131 | 0.087 |
| Standard deviation | 0.374 | 0.306 | 0.292 | 0.344 | 0.279 | 0.362 | 0.296 |
| Max | 6.826 | 6.827 | 6.827 | 6.827 | 6.827 | 6.827 | 6.827 |
| Upper quartile | 0.117 | 0.114 | 0.109 | 0.128 | 0.110 | 0.115 | 0.117 |
| Median | 0.050 | 0.050 | 0.047 | 0.052 | 0.049 | 0.051 | 0.050 |
| Lower quartile | 0.024 | 0.024 | 0.022 | 0.025 | 0.024 | 0.024 | 0.024 |
| Min | 0.002 | 0.000 | 0.001 | 0.001 | 0.000 | 0.001 | 0.001 |

**Table XXIX: Sample and Selected Realization Statistics of Gold Outside the Shell**

|  | Sample Database | au_005 | au_010 | au_015 | au_020 | au_025 | au_030 |
|---|---|---|---|---|---|---|---|
| Count | 11,900 | 1,262,314 | 1,262,314 | 1,262,314 | 1,262,314 | 1,262,314 | 1,262,314 |
| Mean | 0.007 | 0.006 | 0.006 | 0.007 | 0.006 | 0.007 | 0.006 |
| Variance | 0.001 | 0.000 | 0.000 | 0.000 | 0.000 | 0.000 | 0.000 |
| Standard deviation | 0.024 | 0.018 | 0.019 | 0.022 | 0.019 | 0.022 | 0.018 |
| Max | 3.175 | 5.602 | 5.690 | 4.672 | 5.042 | 5.307 | 5.553 |
| Upper quartile | 0.006 | 0.006 | 0.006 | 0.006 | 0.006 | 0.006 | 0.006 |
| Median | 0.002 | 0.003 | 0.003 | 0.003 | 0.003 | 0.003 | 0.003 |
| Lower quartile | 0.000 | 0.001 | 0.001 | 0.001 | 0.001 | 0.001 | 0.001 |
| Min | 0.000 | 0.000 | 0.000 | 0.000 | 0.000 | 0.000 | 0.000 |

**Table XXX: Kriged Estimate and Average Realization Statistics**

|  | Inside Grade Shell | | Outside Grade Shell | |
|---|---|---|---|---|
|  | Kriged Estimate | Average of Realizations | Kriged Estimate | Average of Realizations |
| Count | 6,639 | 6,639 | 1,262,314 | 1,262,314 |
| Mean | 0.132 | 0.140 | 0.007 | 0.006 |
| Variance | 0.011 | 0.017 | 0.000 | 0.000 |
| Standard deviation | 0.105 | 0.131 | 0.009 | 0.009 |
| Max | 2.165 | 6.827 | 0.612 | 0.619 |
| Upper quartile | 0.158 | 0.167 | 0.009 | 0.008 |
| Median | 0.105 | 0.119 | 0.004 | 0.004 |
| Lower quartile | 0.072 | 0.084 | 0.001 | 0.002 |
| Min | 0.007 | 0.003 | 0.000 | 0.000 |

### 4.3.2. Visual Inspection

Visual inspection of simulated models, like in estimated models, should be conducted to ensure that simulated grades are similar to sample grades nearby. Individual realizations are expected to visually appear noisy, however, simulated grades should honor sample grades at close spacing. The average of the realizations, referred to as the "E-type" or the expected value estimate (Goovaerts, 1997), should also honor sample grades at close spacing, but would ideally also match an unrestricted kriged estimate. Visual discrepancies between the kriged estimate and the E-type indicate regions of relatively-high uncertainty. See Appendix A for selected plan-view sections of the simulated model.

## 4.4. Model Results

In the context of simulation, grade-tonnage curves may be used to evaluate the relationship between individual realizations, the E-type or average realization, and the unrestricted kriged estimate. Ideally, the E-type and kriged estimates should follow each other closely on the grade-tonnage curve. Grade-tonnage curves were generated for the 30 realization model inside the grade shell (Figure 36). Values in Table XXXI will differ from the estimation results presented in section 3.4.1, due to the removal of capping strategies and sample restrictions.

**Table XXXI: Grade, Tons, and Metal of the 30 Realization Simulated Model Inside the Grade Shell**

| Cutoff [opt] | E-Type Grade [opt] | E-Type Tonnage [t] | Metal [oz t] | Kriged Grade [opt] | Kriged Tonnage [t] | Metal [oz t] |
|---|---|---|---|---|---|---|
| 0.005 | 0.140 | 3,926,736 | 548,997 | 0.132 | 3,930,288 | 517,501 |
| 0.01 | 0.140 | 3,920,224 | 548,949 | 0.132 | 3,927,328 | 517,504 |
| 0.02 | 0.141 | 3,885,888 | 548,415 | 0.133 | 3,897,728 | 516,995 |
| 0.04 | 0.145 | 3,752,688 | 544,327 | 0.137 | 3,747,952 | 512,233 |
| 0.06 | 0.153 | 3,470,304 | 530,020 | 0.148 | 3,321,712 | 491,049 |
| 0.08 | 0.164 | 3,049,984 | 500,472 | 0.166 | 2,703,072 | 447,737 |
| 0.1 | 0.179 | 2,531,392 | 453,676 | 0.188 | 2,089,168 | 392,638 |
| 0.2 | 0.309 | 587,264 | 181,271 | 0.315 | 575,424 | 181,506 |
| 0.5 | 0.915 | 36,112 | 33,036 | 0.750 | 34,928 | 26,179 |
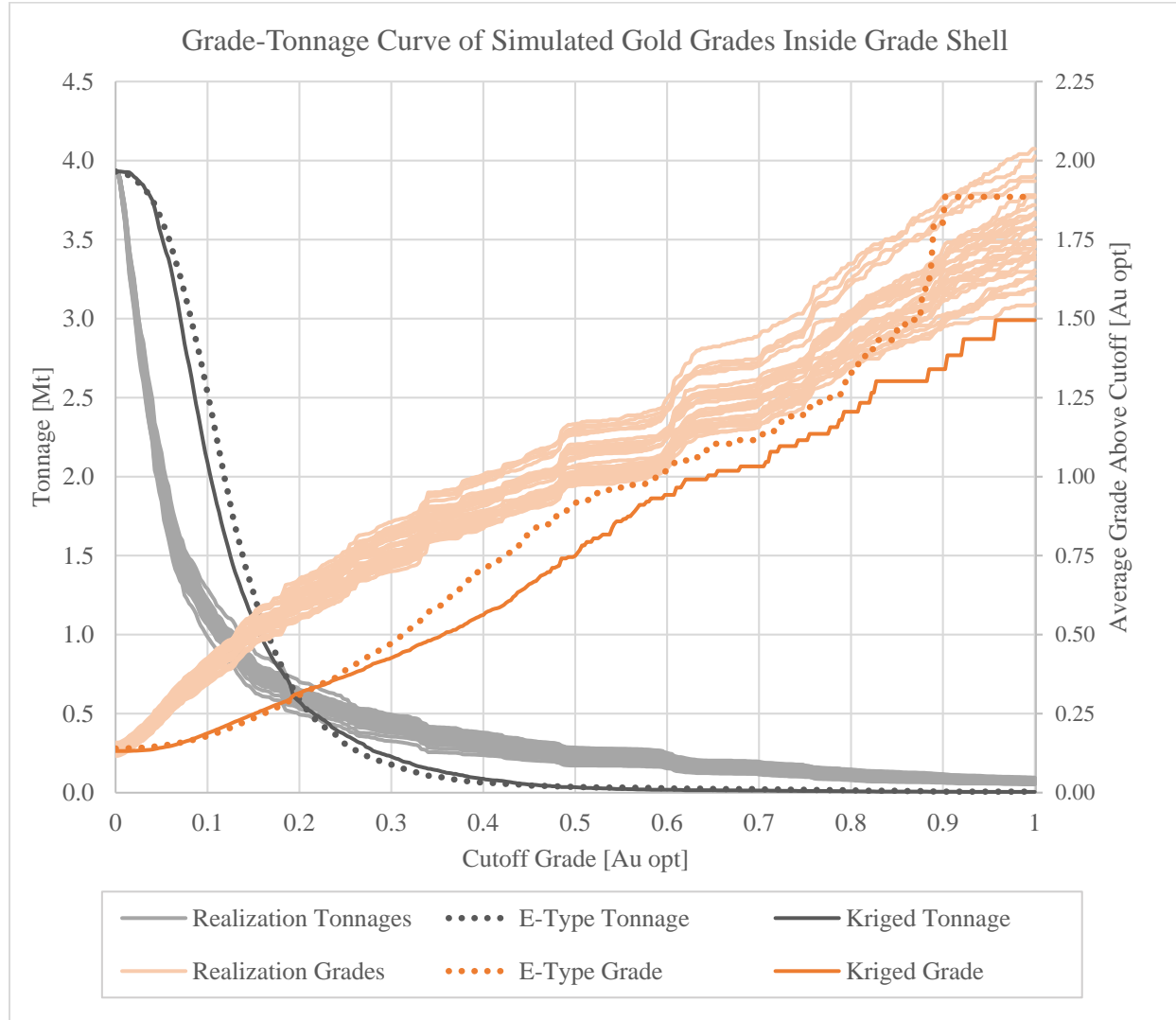
**Figure 36: Grade-Tonnage curve of simulated gold grades inside the grade shell. 30 realizations shown**

## 5. Additional Work

During the course of this study, the author was involved in two small mineralogy projects related to the McDonald deposit. In the first project, a high-grade sample from McDonald (PCM-91-173, at a depth of 790.4 ft.) provided by Bill Fuchs (a mineralogist who did work on the McDonald deposit in the 1980s) was set in epoxy, polished, and analyzed by scanning electron microscopy/energy-dispersive X-ray spectroscopy (SEM-EDS) at the Center for Advanced Mineral, Metallurgical, and Materials Processing (CAMP) laboratory at Montana Tech. Gary Wyss assisted the analytical session. The results, summarized in Appendix B, characterize ore minerals found at the McDonald deposit, including electrum, acanthite, and Au-Ag-Hg-sulfides. In the second project, the author produced a pan concentrate from a high-grade, drill-core intercept from McDonald (PCM-94-566, at an approximate depth of 710 ft.), and a number of reflected light photomicrographs were taken. Results from this second study can also be found in Appendix B.

# 6. Conclusions

Resource modelling and simulation of gold at West Butte was conducted to better characterize modes of mineralization at West Butte described by company geologists. Preliminary resource estimates produced by Newmont suggest the existence of a 500 koz gold orebody at West Butte with a grade of 0.21 troy ounces per ton (Newmont Mining Corporation, 2014). A conservative, ordinary-kriged estimate of West Butte delineated a 470 koz gold orebody at an average grade of 0.171 opt. The corresponding simulated model highlighted regions of relatively-high uncertainty within the grade shell where data are sparse.

## 6.1. Recommendations

These recommendations are written in conjunction with the recommendations provided by Ken Paul and Marion Guimard in the 2011 Newmont relogging report.

### 6.1.1. Improvement of the Resource Model at West Butte

It has been demonstrated that downhole contamination exists in the majority of reverse circulation drilling at the McDonald deposit. If the McDonald deposit is to further be developed, it is recommended to replace all contaminated reverse circulation drilling with core drilling. Core drilling should prioritize replacing reverse circulation drillholes that contain the largest proportion of gold intercepts greater than 0.02 opt. Replacement of contaminated reverse circulation drilling by core drilling may also warrant the removal of the high-yield limit, which will likely increase estimated tonnages at higher grades outside the grade shell. Additional core drilling at West Butte would also likely lead to the estimation of a larger-tonnage orebody. The estimated model contains high-grade tonnages partially-restricted by their proximity to core data, and the addition of more core data may expand the grade shell and subsequently increase estimated, higher-grade tonnages.

Future iterations of the resource estimate at West Butte should eventually discard the grade shell, and domains should be defined based on a geologic attribute. Grade shells have been used in previous resource models of McDonald, but grade shelling is not an ideal method of defining domains.

### 6.1.2. Future Exploration and Improvement of the Geologic Model

Logged geologic data on the McDonald deposit failed to provide a means of separating high-grade, subvertical mineralization from lower-grade stratabound mineralization. It is recommended that future exploration programs at the McDonald deposit include a logging program focused on delineating high-grade, subvertical mineralization. Oriented, angled-core drilling may be utilized to log vein orientations, which may assist in characterizing high-grade mineralization.

High-grade mineralization at West Butte is interpreted to follow along the 9800' E-W fault. While the fault is poorly documented, it is known that high-grade mineralization has east-west and vertical continuity. It is recommended to continue the angled-core drilling program started by Echo Bay Mining towards East Butte along a 100° azimuth. A digitized surface of the 9800' E-W fault should also be created and updated as more core drilling takes place.

Additional exploration drilling should also take place below known mineralized zones at East Butte and West Butte to test the possible extent of high-grade mineralization at depth. Most drillholes at McDonald terminated within the andesite unit (Ta). Newmont geologists evaluating the deposit have drawn comparisons to a "sandwich model", described by Hedenquist (2000), which shows the preferred location of vein and disseminated ore in a permeable lithology (Figure 37). If this model is followed, there is potential for high-grade vein deposits in the footwall.
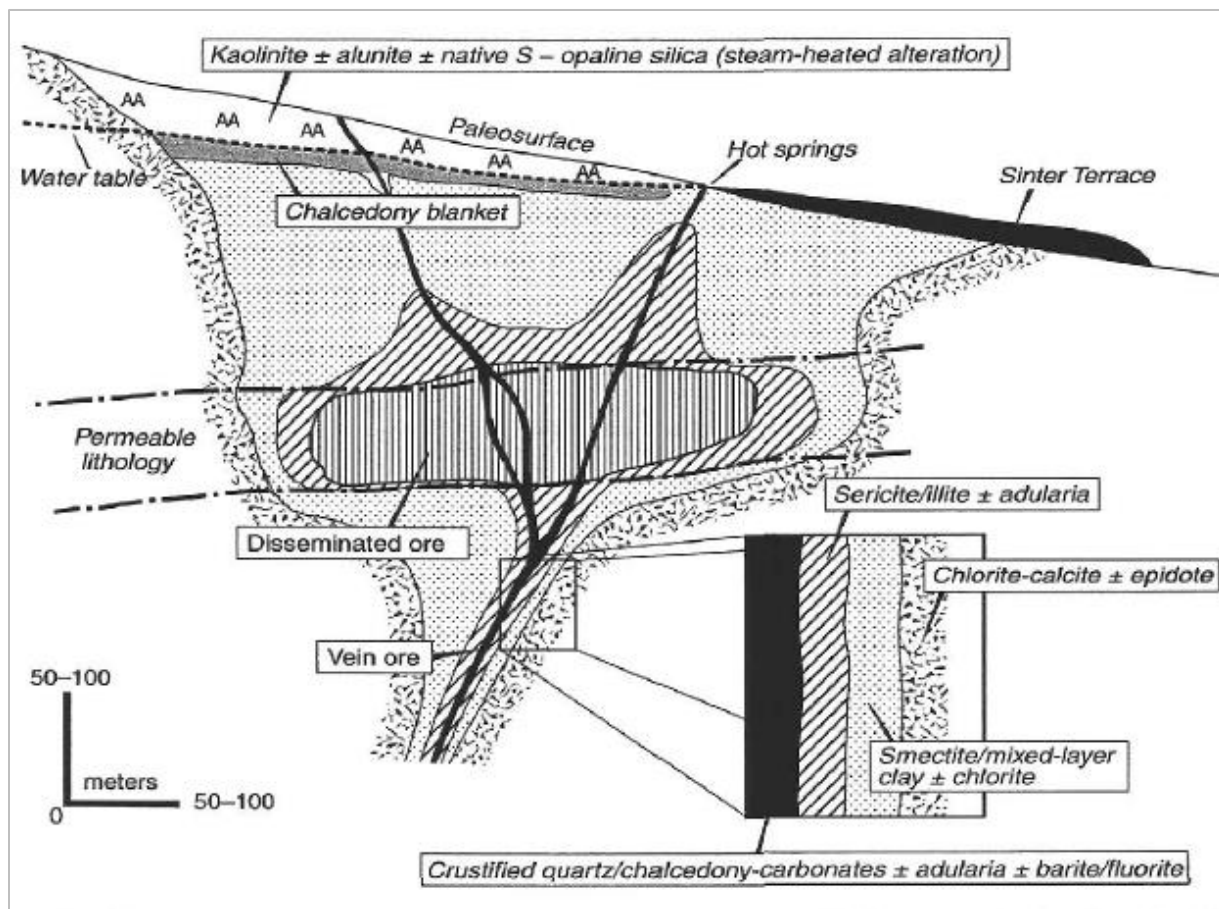
**Figure 37: "Sandwich model" low-sulfidation epithermal gold system. Taken from (Hedenquist, Arribas, & Gonzalez-Urien, 2000)**

Faulting at the McDonald deposit is poorly characterized, and may have some controls on mineralization. Faulting bounds gold mineralization on the north and west flanks of West Butte, and the 9800' E-W fault is interpreted to be a mineralizing structure for higher-grade mineralization. It is recommended that faults at the McDonald deposit be investigated using geophysical methods and intercepts from core drilling. Digitized surfaces of the faults should be produced, as they will be necessary inputs during resource modeling and mine planning. Offset and age of faults relative to mineralization should also be documented.

The paragenetic sequence of mineralization at the McDonald deposit has not been investigated in detail, at least not in the literature available to this study. Preliminary work performed by the author (Appendices B and C) shows a rich and interesting assemblage of Au-Ag minerals in the deposit. It is recommended that a complete ore and alteration mineral study be conducted to better understand the McDonald deposit. Such a study should aim to document differences in chemistry and mineralogy, e.g., using hyperspectral imaging, that could provide vectors to high-grade mineralization and application to future core logging programs.

# 7. References Cited

Bartlett, M. W., Enders, M. S., Volberding, J. E., & Wilkinson, W. H. (1995). The Geology of the McDonald Gold Deposit, Lewis and Clark County, Montana. In A. R. Coyner, & P. L. Fahey (Ed.), *Geology and Ore Deposits of the American Cordillera* (pp. 981 - 1000). Reno, Nevada: Geological Society of Nevada.

CAM. (2003). *2003 Cam Study - Section-04 (Resources).* Unpublished Report.

Deutsch, C. V. (2017, June 29). *Checking Simulated Realizations - Mining*. Retrieved from Geostatistics Lessons: http://geostatisticslessons.com/lessons/checkingmin

Deutsch, C. V., & Journel, A. G. (1992). *Geostatistical Software Library and User's Guide.* New York Oxford: Oxford University Press.

Deutsch, J. L. (2019). *Geostatistics Lessons.* Retrieved from Experimental Variogram Tolerance Parameters: http://www.geostatisticslessons.com/lessons/variogramparameters

Fuller, S. (1998). *Bulk Density Tests.* Unpublished Report.

Goovaerts, P. (1997). *Goestatistics for Natural Resources Evaluation.* New York Oxford: Oxford University Press.

Hedenquist, J. W., Arribas, A. R., & Gonzalez-Urien, E. (2000). Exploration for Epithermal Gold Deposits. *SEG Reviews, 13*, 245 - 277.

Jewbali, A., Elenbaas, T., & Roos, C. (2015). What happened to my gold? Questions to ask. *Mining Engineering*, 61-66.

Knudsen, H. P. (1988). *A Short Course on Geostatistical Ore Reserve Estimation.* Butte: Montana Tech.

Leuangthong, O., McLennan, J. A., & Deutch, C. V. (2004, September). Minimum Acceptance Criteria for Geostatistical Realizations. *Natural Resources Research, 13*(3), 131 - 141. Retrieved from Centre for Computational Geostatistics.

Newmont Mining Corporation. (2014). *McDonald Management Presentation.* Unpublished Presentation.

Paul, K., & Guimard, M. (2011). *2011 Core, RC Relogging, and Field Mapping Program.* Unpublished Report.

Rosenthal, S., & Rosenthal, S. (2017, May 11). *Keeping the McDonald Candle Lit.* Retrieved from Montana Tech: https://www.mtech.edu/mwtp/2017_presentations/thursday/sonya-rosenthal.pdf

Rossi, M. E., & Deutch, C. V. (2014). *Mineral Resource Estimation.* Dordrecht Heidelberg New York London: Springer.

## 8. Appendix A



**Figure 38: North-South section (left-to-right) of drilling data on the 50,400 ft. easting. Gold grade is displayed along the lengths of the drillholes. Grid spacing is 100 ft.**

**Figure 39: North-South section (left-to-right) of drilling data on the 50,600 ft. easting. Gold grade is displayed along the lengths of the drillholes. Grid spacing is 100 ft.**
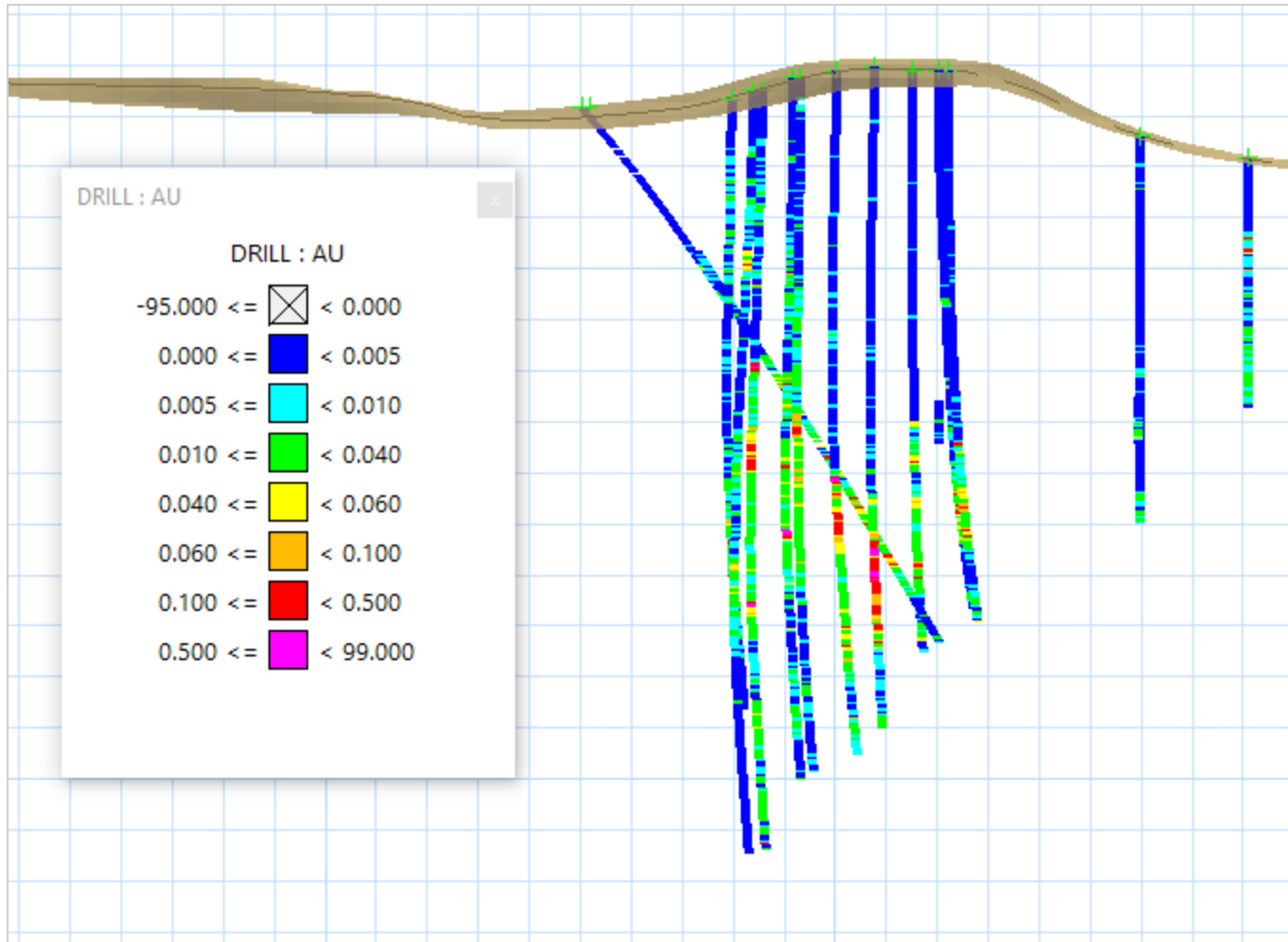
**Figure 40: North-South section (left-to-right) of drilling data on the 50,800 ft. easting. Gold grade is displayed along the lengths of the drillholes. Grid spacing is 100 ft.**
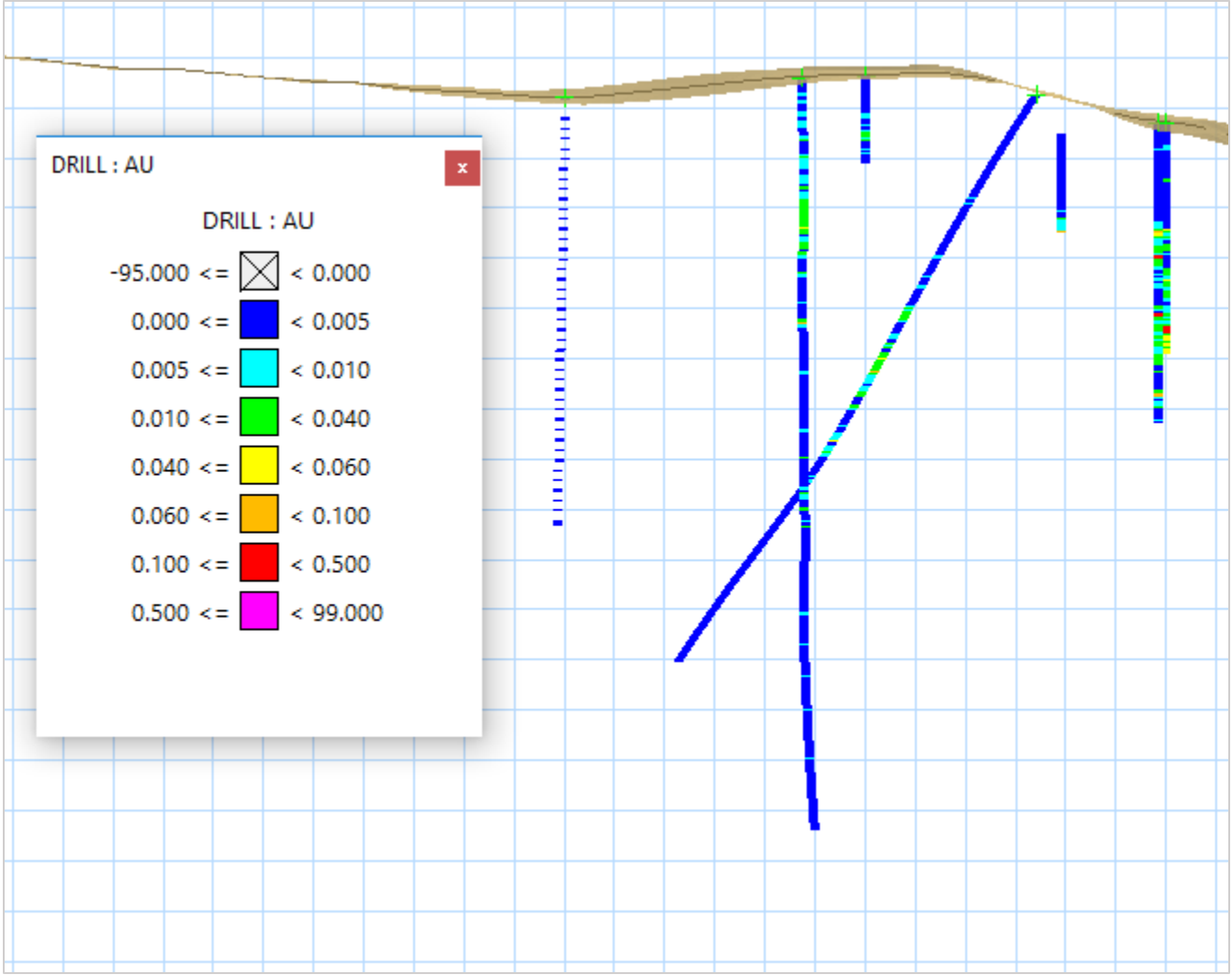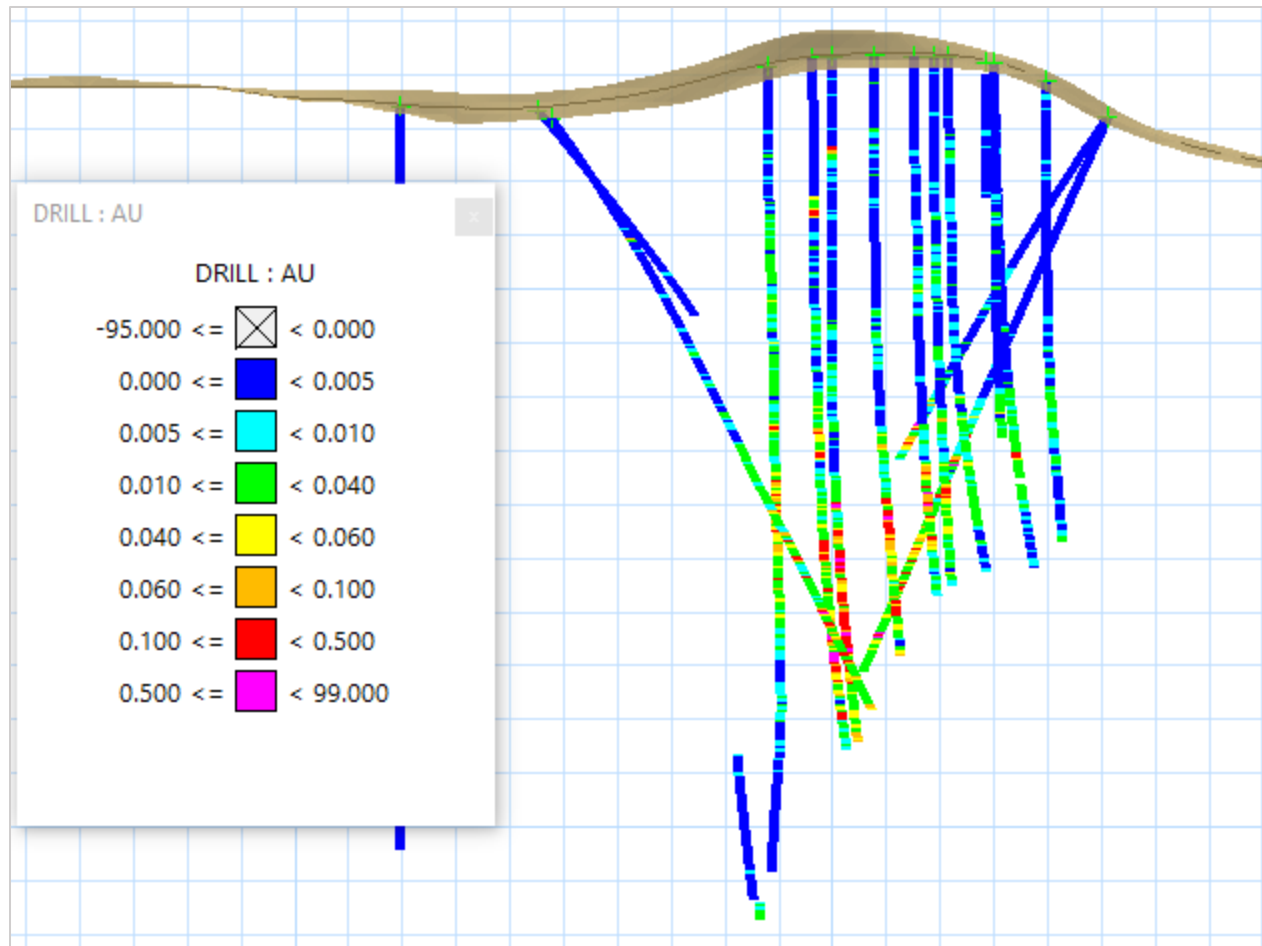
**Figure 41: North-South section (left-to-right) of drilling data on the 51,000 ft. easting. Gold grade is displayed along the lengths of the drillholes. Grid spacing is 100 ft.**

**Figure 42: North-South section (left-to-right) of drilling data on the 51,200 ft. easting. Gold grade is displayed along the lengths of the drillholes. Grid spacing is 100 ft.**

**Figure 43: North-South section (left-to-right) of drilling data on the 51,400 ft. easting. Gold grade is displayed along the lengths of the drillholes. Grid spacing is 100 ft.**
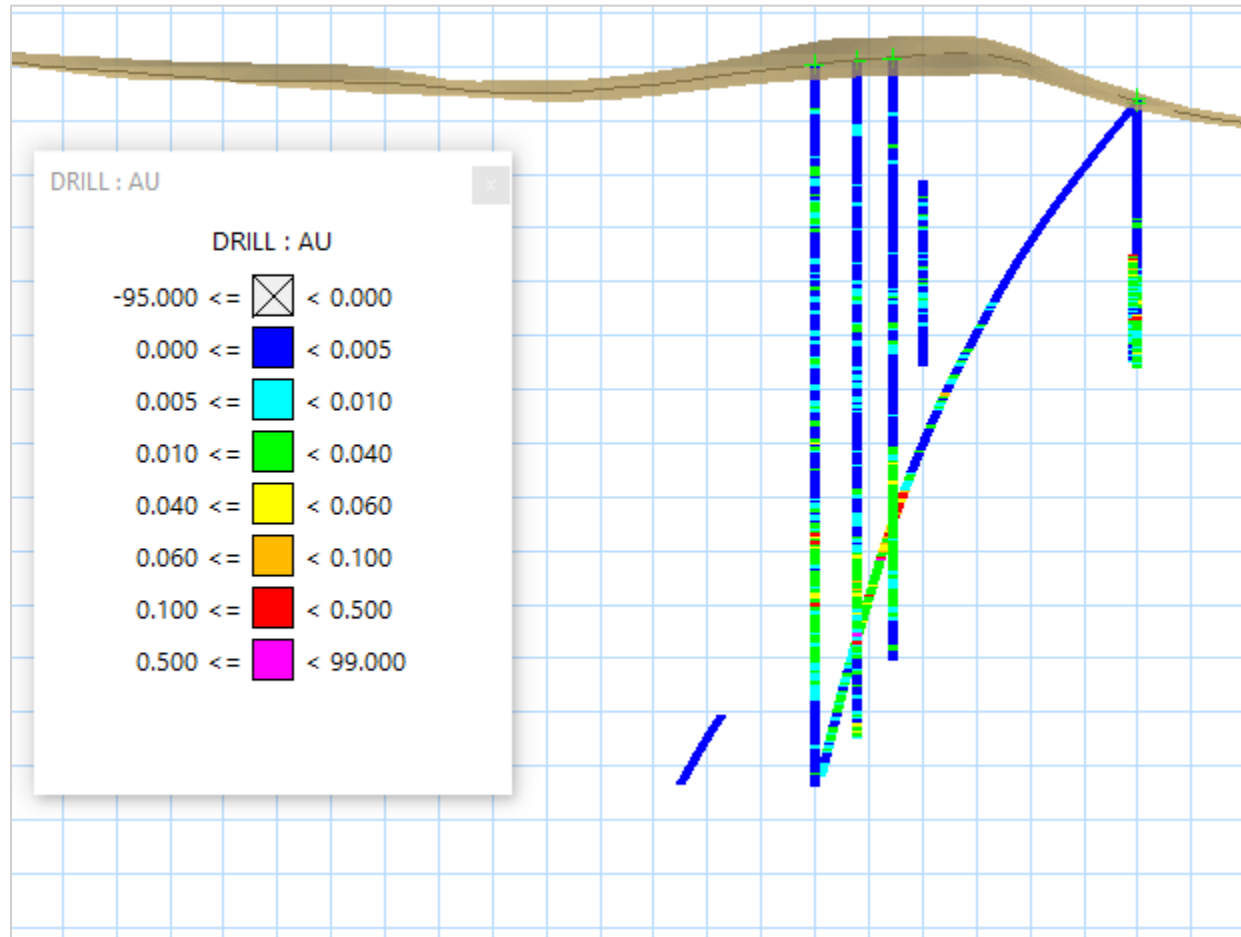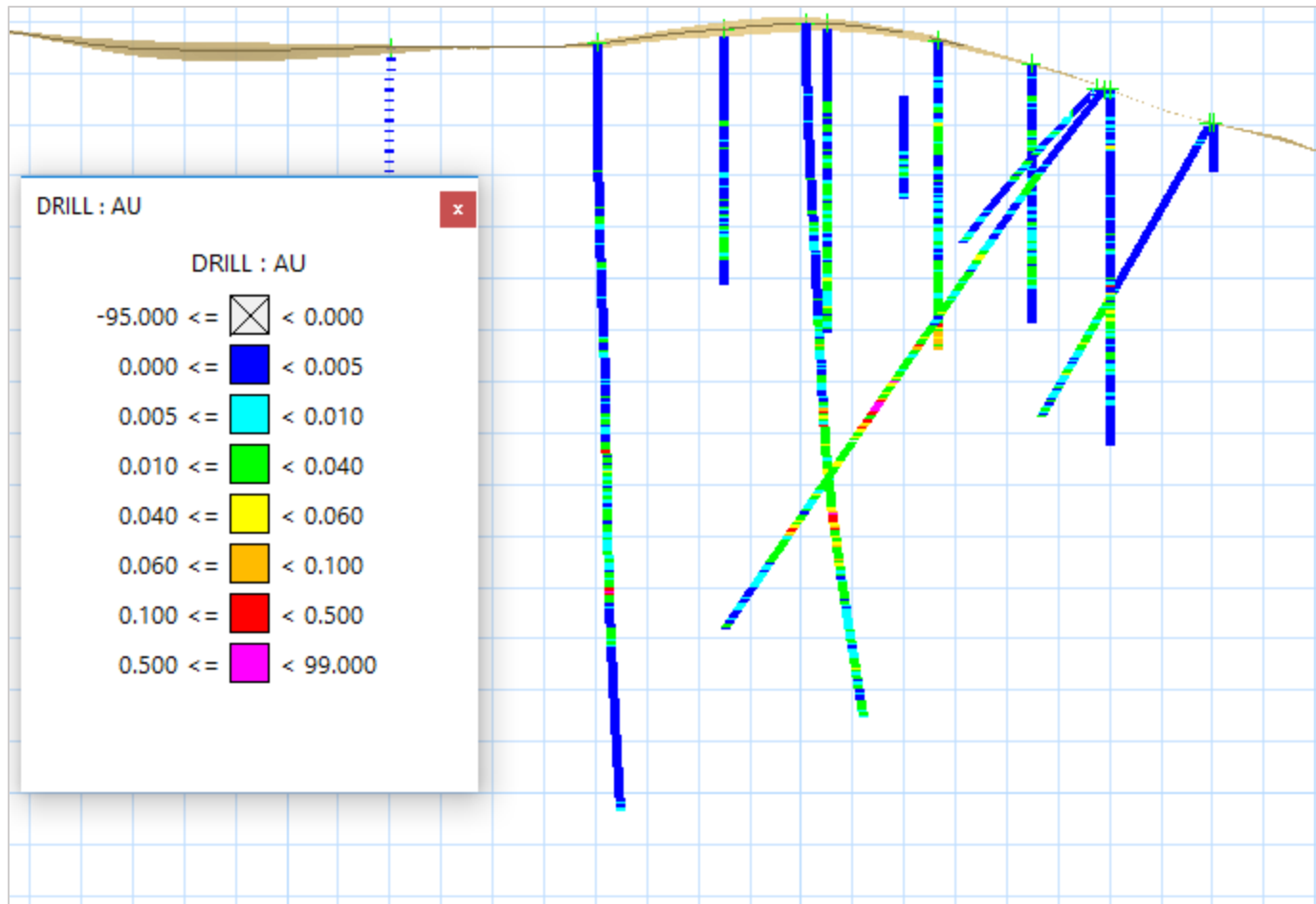
**Figure 44: North-South section (left-to-right) of drilling data on the 51,600 ft. easting. Gold grade is displayed along the lengths of the drillholes. Grid spacing is 100 ft.**
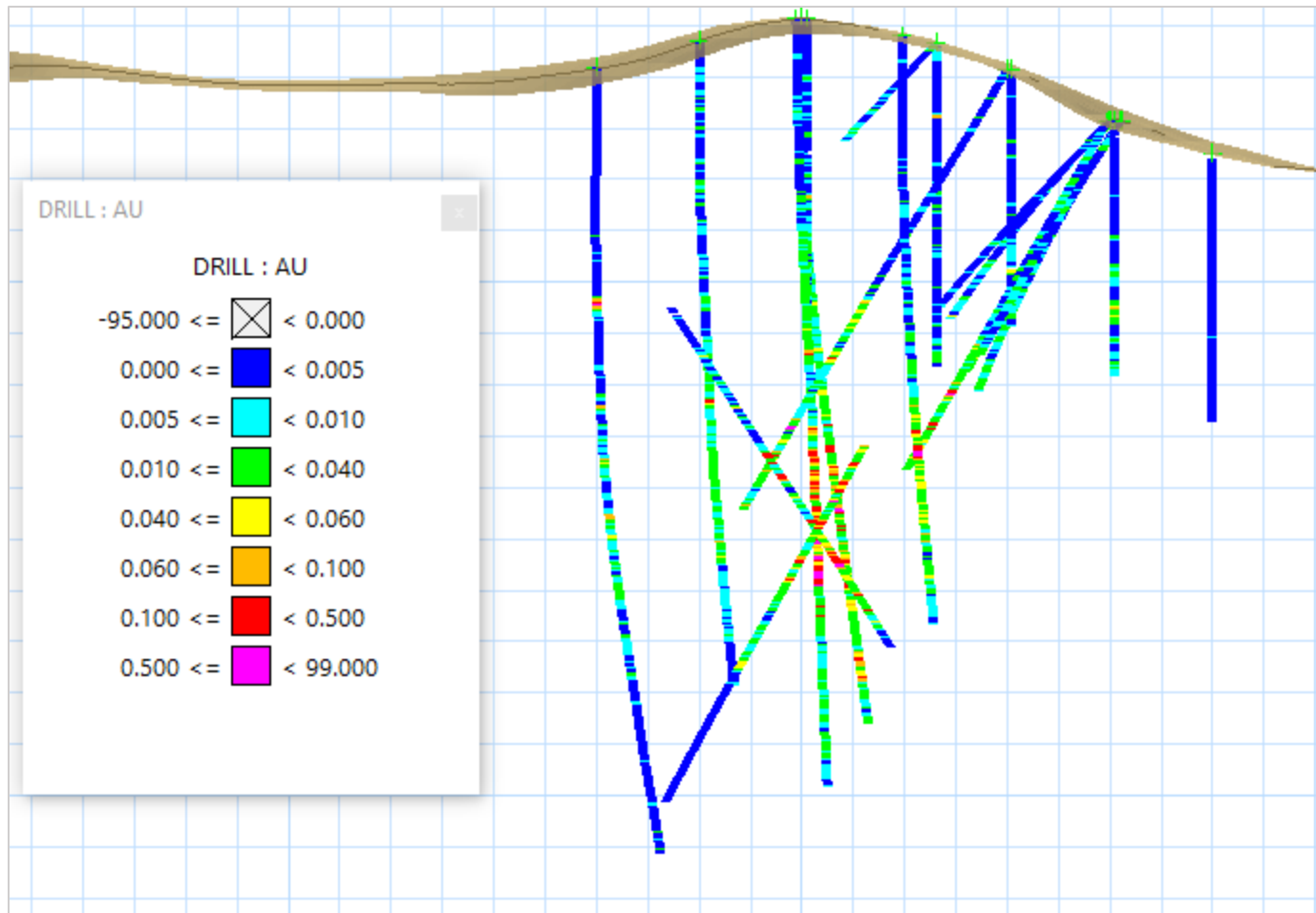
**Table XXXII: Geologic codes for the McDonald Deposit drilling database**

| FM (Formation) | LTH (Lithology) |
|---|---|
| -9 no sample | -9 no sample |
| 0: unconsolidated | 0: undifferentiated<br>1: pad material<br>2: alluvium |
| 1: rhyolite | 0: unknown<br>1: xtal poor tuff (Trtcp) |
| 2: dacite | 0: undifferentiated |
| 3: andesite | 0: undifferentiated<br>1: aphanitic flow (Taf)<br>2: amphibole prphy (Tap)<br>3: andesite agglom. (Tag) |
| 4. Sedimentary (Tvs-l) | 1: conglomerate<br>2: sandstone<br>3: siltstone |
| 5. Sedimentary (other) sediments between Trtl and Ta | 4: mudstone<br>5: calcareous siltstone |
| 6: sinter | 0: undifferentiated<br>1: geyserite |
| 7: Precambrian Belt Group | 1: undifferentiated<br>2: Helena Fm.<br>3: Empire Fm. |
| 8: Sedimentary (Tvs-u) | 1: conglomerate<br>2: sandstone<br>3: siltstone |

**Table XXXIII: Statistics of gold grade (Au opt) by alteration type**

| Alteration Type | Count | Mean | Variance | Standard deviation | Max | Upper quartile | Median | Lower quartile |
|---|---|---|---|---|---|---|---|---|
| All | 12456 | 0.016 | 0.009 | 0.093 | 6.826 | 0.011 | 0.004 | 0.002 |
| Silicic | 10419 | 0.019 | 0.01 | 0.101 | 6.826 | 0.013 | 0.005 | 0.002 |
| Argillic | 1387 | 0.004 | 0 | 0.013 | 0.232 | 0.002 | 0.001 | 0.001 |
| Fresh | 258 | 0.002 | 0 | 0.005 | 0.078 | 0.001 | 0 | 0 |
| Potassic | 20 | 0.007 | 0 | 0.006 | 0.024 | 0.008 | 0.005 | 0.003 |
| Propylitic | 35 | 0.003 | 0 | 0.004 | 0.022 | 0.004 | 0.002 | 0.001 |
| Sericitic | 18 | 0.006 | 0 | 0.002 | 0.008 | 0.008 | 0.007 | 0.003 |
| No Sample | 319 | 0.003 | 0 | 0.005 | 0.051 | 0.002 | 0.001 | 0.001 |

**Table XXXIV: Statistics of gold grade (Au opt) by hole type**

| Hole Type | Count | Mean | Variance | Standard deviation | Max | Upper quartile | Median | Lower quartile |
|---|---|---|---|---|---|---|---|---|
| All | 12456 | 0.016 | 0.009 | 0.093 | 6.826 | 0.011 | 0.004 | 0.002 |
| Core | 1409 | 0.027 | 0.005 | 0.074 | 1.105 | 0.023 | 0.008 | 0.003 |
| Reverse circulation | 10434 | 0.016 | 0.01 | 0.098 | 6.826 | 0.01 | 0.004 | 0.002 |
| Monitoring well | 613 | 0.006 | 0 | 0.012 | 0.186 | 0.006 | 0.003 | 0.001 |

**Table XXXV: Statistics of gold grade (Au opt) by lithology**

| Lithology | Count | Mean | Variance | Standard deviation | Max | Upper quartile | Median | Lower quartile |
|---|---|---|---|---|---|---|---|---|
| All | 12456 | 0.016 | 0.009 | 0.093 | 6.826 | 0.011 | 0.004 | 0.002 |
| Alluvium | 35 | 0.001 | 0 | 0.001 | 0.003 | 0.001 | 0 | 0 |
| Andesite agglomerate | 9 | 0.025 | 0.001 | 0.024 | 0.07 | 0.031 | 0.012 | 0.008 |
| Undifferentiated andesite | 89 | 0.009 | 0 | 0.013 | 0.066 | 0.009 | 0.004 | 0.002 |
| Aphanitic flow | 172 | 0.008 | 0 | 0.018 | 0.164 | 0.007 | 0.003 | 0.001 |
| Ash fall tuff | 4 | 0.003 | 0 | 0.001 | 0.004 | 0.004 | 0.003 | 0.002 |
| Calcareous mudstone | 5 | 0.004 | 0 | 0.003 | 0.009 | 0.003 | 0.002 | 0.002 |
| Conglomerate | 350 | 0.002 | 0 | 0.007 | 0.082 | 0.001 | 0.001 | 0 |
| Geyserite | 1 | 0.007 | NaN | NaN | 0.007 | 0.007 | 0.007 | 0.007 |
| Glacial till | 29 | 0.001 | 0 | 0 | 0.001 | 0.001 | 0.001 | 0 |
| Lithic tuff | 8360 | 0.022 | 0.013 | 0.112 | 6.826 | 0.015 | 0.006 | 0.002 |
| Mudstone | 89 | 0.004 | 0 | 0.005 | 0.025 | 0.004 | 0.002 | 0.001 |
| No Sample | 47 | 0.003 | 0 | 0.008 | 0.051 | 0.003 | 0.001 | 0 |
| Pad material | 36 | 0.002 | 0 | 0.002 | 0.011 | 0.001 | 0.001 | 0.001 |
| Plagioclase hornblende porphyry | 3 | 0.003 | 0 | 0.002 | 0.006 | 0.003 | 0.002 | 0.002 |
| Plagioclase porphyry | 23 | 0.005 | 0 | 0.003 | 0.011 | 0.006 | 0.004 | 0.002 |
| Sandstone | 47 | 0.008 | 0 | 0.014 | 0.076 | 0.009 | 0.003 | 0.001 |
| Siltstone | 121 | 0.011 | 0 | 0.018 | 0.078 | 0.009 | 0.003 | 0.001 |
| Undifferentiated Sinter | 238 | 0.003 | 0 | 0.004 | 0.031 | 0.004 | 0.002 | 0.001 |
| Undifferentiated unconsolidated | 41 | 0.001 | 0 | 0.001 | 0.005 | 0.001 | 0.001 | 0.001 |
| Unknown | 3 | 0.001 | 0 | 0 | 0.001 | 0.001 | 0.001 | 0 |
| Volcaniclastic sandstone | 1 | 0.001 | NaN | NaN | 0.001 | 0.001 | 0.001 | 0.001 |
| Crystal poor tuff | 230 | 0.004 | 0 | 0.008 | 0.072 | 0.004 | 0.002 | 0.001 |
| Crystal rich tuff | 2523 | 0.005 | 0.001 | 0.024 | 0.895 | 0.005 | 0.002 | 0.001 |

**Table XXXVI: Statistics of gold grade (Au opt) by oxidation intensity**

| Oxidiation Intensity | Count | Mean | Variance | Standard deviation | Max | Upper quartile | Median | Lower quartile |
|---|---|---|---|---|---|---|---|---|
| All | 12456 | 0.016 | 0.009 | 0.093 | 6.826 | 0.011 | 0.004 | 0.002 |
| Strong | 676 | 0.037 | 0.079 | 0.28 | 6.826 | 0.014 | 0.006 | 0.002 |
| Moderate | 5851 | 0.02 | 0.007 | 0.087 | 3.175 | 0.014 | 0.005 | 0.002 |
| Weak | 5038 | 0.012 | 0.002 | 0.042 | 1.354 | 0.009 | 0.004 | 0.001 |
| Not present | 854 | 0.006 | 0.002 | 0.041 | 1.068 | 0.003 | 0.001 | 0.001 |
| No sample | 35 | 0.004 | 0 | 0.009 | 0.051 | 0.003 | 0.002 | 0.001 |
| Unknown | 2 | 0.001 | 0 | 0 | 0.001 | 0.001 | 0.001 | 0.001 |

**Table XXXVII: Statistics of gold grade (Au opt) by pyrite abundance**

| Pyrite Abundance | Count | Mean | Variance | Standard deviation | Max | Upper quartile | Median | Lower quartile |
|---|---|---|---|---|---|---|---|---|
| All | 12456 | 0.016 | 0.009 | 0.093 | 6.826 | 0.011 | 0.004 | 0.002 |
| 0% | 9262 | 0.012 | 0.003 | 0.053 | 3.175 | 0.009 | 0.004 | 0.001 |
| 0 - 2% | 2815 | 0.025 | 0.008 | 0.089 | 1.945 | 0.017 | 0.006 | 0.002 |
| 2 - 5% | 286 | 0.065 | 0.195 | 0.441 | 6.826 | 0.02 | 0.008 | 0.003 |
| 5 - 10% | 65 | 0.044 | 0.021 | 0.146 | 0.904 | 0.02 | 0.006 | 0.003 |
| > 10% | 23 | 0.067 | 0.06 | 0.245 | 1.17 | 0.015 | 0.002 | 0.001 |
| No sample | 4 | 0.014 | 0.001 | 0.025 | 0.051 | 0.004 | 0 | 0 |

**Table XXXVIII: Statistics of gold grade (Au opt) by pyrite type**

| Pyrite Type | Count | Mean | Variance | Standard deviation | Max | Upper quartile | Median | Lower quartile |
|---|---|---|---|---|---|---|---|---|
| All | 12456 | 0.016 | 0.009 | 0.093 | 6.826 | 0.011 | 0.004 | 0.002 |
| Fractures or veins | 3014 | 0.028 | 0.011 | 0.103 | 2.723 | 0.019 | 0.007 | 0.003 |
| Groundmass | 589 | 0.011 | 0.002 | 0.043 | 0.749 | 0.007 | 0.002 | 0.001 |
| Both | 777 | 0.037 | 0.081 | 0.285 | 6.826 | 0.014 | 0.006 | 0.002 |
| Not present | 8006 | 0.011 | 0.001 | 0.036 | 1.008 | 0.008 | 0.003 | 0.001 |
| No sample | 49 | 0.004 | 0 | 0.008 | 0.051 | 0.003 | 0.002 | 0.001 |

**Table XXXIX: Statistics of gold grade (Au opt) by vein abundance**

| Vein Abundance | Count | Mean | Variance | Standard deviation | Max | Upper quartile | Median | Lower quartile |
|---|---|---|---|---|---|---|---|---|
| All | 12456 | 0.016 | 0.009 | 0.093 | 6.826 | 0.011 | 0.004 | 0.002 |
| 0 - 2% | 3761 | 0.02 | 0.006 | 0.077 | 2.723 | 0.015 | 0.006 | 0.002 |
| 2 - 5% | 1595 | 0.023 | 0.039 | 0.198 | 6.826 | 0.013 | 0.005 | 0.002 |
| 5 - 10% | 375 | 0.027 | 0.014 | 0.118 | 1.945 | 0.015 | 0.006 | 0.003 |
| 10 - 25% | 509 | 0.031 | 0.011 | 0.105 | 1.105 | 0.014 | 0.007 | 0.003 |
| 25 - 50% | 158 | 0.04 | 0.013 | 0.113 | 0.904 | 0.02 | 0.007 | 0.002 |
| 50 - 75% | 36 | 0.042 | 0.038 | 0.194 | 1.17 | 0.013 | 0.004 | 0.001 |
| 75 - 100% | 17 | 0.077 | 0.044 | 0.209 | 0.816 | 0.013 | 0.004 | 0.002 |
| Veinlets | 2808 | 0.012 | 0.001 | 0.036 | 0.749 | 0.009 | 0.004 | 0.002 |
| Not present | 3153 | 0.008 | 0.001 | 0.033 | 0.952 | 0.005 | 0.002 | 0.001 |
| No sample | 44 | 0.004 | 0 | 0.009 | 0.051 | 0.003 | 0.002 | 0.001 |

**Table XL: Statistics of gold grade (Au opt) by vein type**

| Vein Type | Count | Mean | Variance | Standard deviation | Max | Upper quartile | Median | Lower quartile |
|---|---|---|---|---|---|---|---|---|
| All | 12456 | 0.016 | 0.009 | 0.093 | 6.826 | 0.011 | 0.004 | 0.002 |
| Chalcedonic | 2292 | 0.019 | 0.008 | 0.091 | 3.175 | 0.01 | 0.004 | 0.002 |
| Limonite-goethite and Mn-oxide | 305 | 0.047 | 0.162 | 0.403 | 6.826 | 0.014 | 0.005 | 0.002 |
| Massive quartz | 3674 | 0.017 | 0.005 | 0.068 | 1.945 | 0.013 | 0.005 | 0.002 |
| Quartz and adularia | 8 | 0.01 | 0 | 0.016 | 0.049 | 0.007 | 0.002 | 0.002 |
| Quartz and pyrite | 1119 | 0.025 | 0.012 | 0.109 | 2.723 | 0.016 | 0.006 | 0.003 |
| Quartz, specularite, and pyrite | 375 | 0.037 | 0.01 | 0.1 | 1.354 | 0.029 | 0.011 | 0.005 |
| Amethystine quartz and other | 16 | 0.004 | 0 | 0.004 | 0.012 | 0.003 | 0.003 | 0.002 |
| Not present | 3319 | 0.008 | 0.001 | 0.032 | 0.952 | 0.006 | 0.002 | 0.001 |
| Unknown | 1307 | 0.013 | 0.001 | 0.033 | 0.55 | 0.011 | 0.004 | 0.002 |
| No Sample | 41 | 0.004 | 0 | 0.009 | 0.051 | 0.003 | 0.001 | 0.001 |
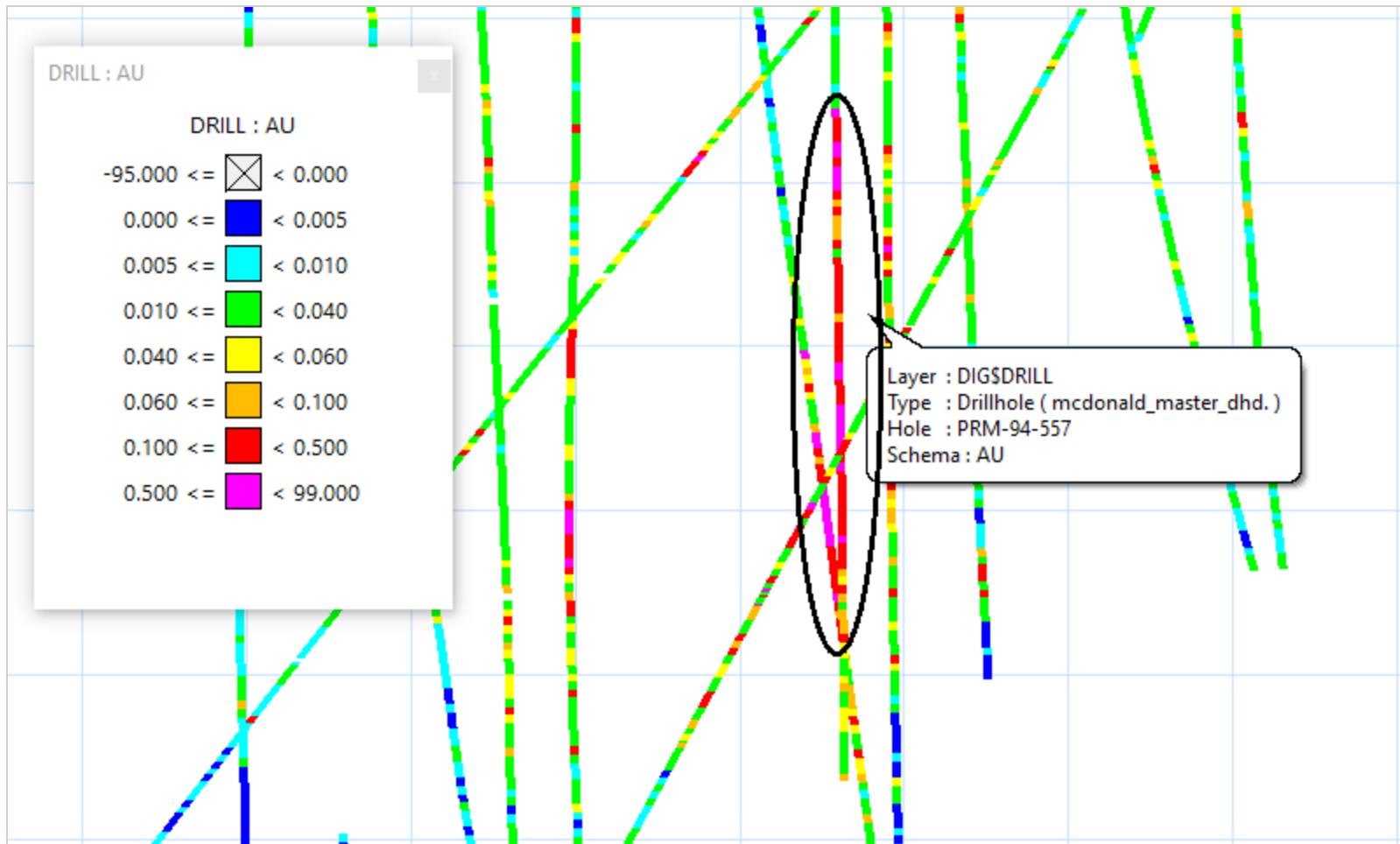
**Figure 45: North-South section (left-to-right) of reverse circulation drilling at West Butte along the 51,360 ft. easting. Grid spacing is 100 ft. Gold grades are displayed along the lengths of the drillholes. Note PRM-94-557, which appears to show downhole contamination of high grade values over a length of roughly 300 ft.**

| | FROM | TO | INT | AU |
|---|---|---|---|---|
| **PRM-94-557** ⌄ | | | | |
| COLLAR SURVEY **ASSAY** | | | | |
| **151** | 750.000 | 755.000 | 5.000 | 0.026 |
| **152** | 755.000 | 760.000 | 5.000 | 1.213 |
| **153** | 760.000 | 765.000 | 5.000 | 0.329 |
| **154** | 765.000 | 770.000 | 5.000 | 0.162 |
| **155** | 770.000 | 775.000 | 5.000 | 0.297 |
| **156** | 775.000 | 780.000 | 5.000 | 1.113 |
| **157** | 780.000 | 785.000 | 5.000 | 0.813 |
| **158** | 785.000 | 790.000 | 5.000 | 0.376 |
| **159** | 790.000 | 795.000 | 5.000 | 0.628 |
| **160** | 795.000 | 800.000 | 5.000 | 1.387 |
| **161** | 800.000 | 805.000 | 5.000 | 1.102 |
| **162** | 805.000 | 810.000 | 5.000 | 0.113 |
| **163** | 810.000 | 815.000 | 5.000 | 0.069 |
| **164** | 815.000 | 820.000 | 5.000 | 0.360 |
| **165** | 820.000 | 825.000 | 5.000 | 0.088 |
| **166** | 825.000 | 830.000 | 5.000 | 0.062 |
| **167** | 830.000 | 835.000 | 5.000 | 0.069 |
| **168** | 835.000 | 840.000 | 5.000 | 0.147 |
| **169** | 840.000 | 845.000 | 5.000 | 0.036 |
| **170** | 845.000 | 850.000 | 5.000 | 0.134 |
| **171** | 850.000 | 855.000 | 5.000 | 0.127 |

**Figure 46: Sample intervals from 750 ft. to 855 ft. in RC drillhole PRM-95-557. Potentially contaminated intervals are boxed in gray and show decreasing gold grade with depth**
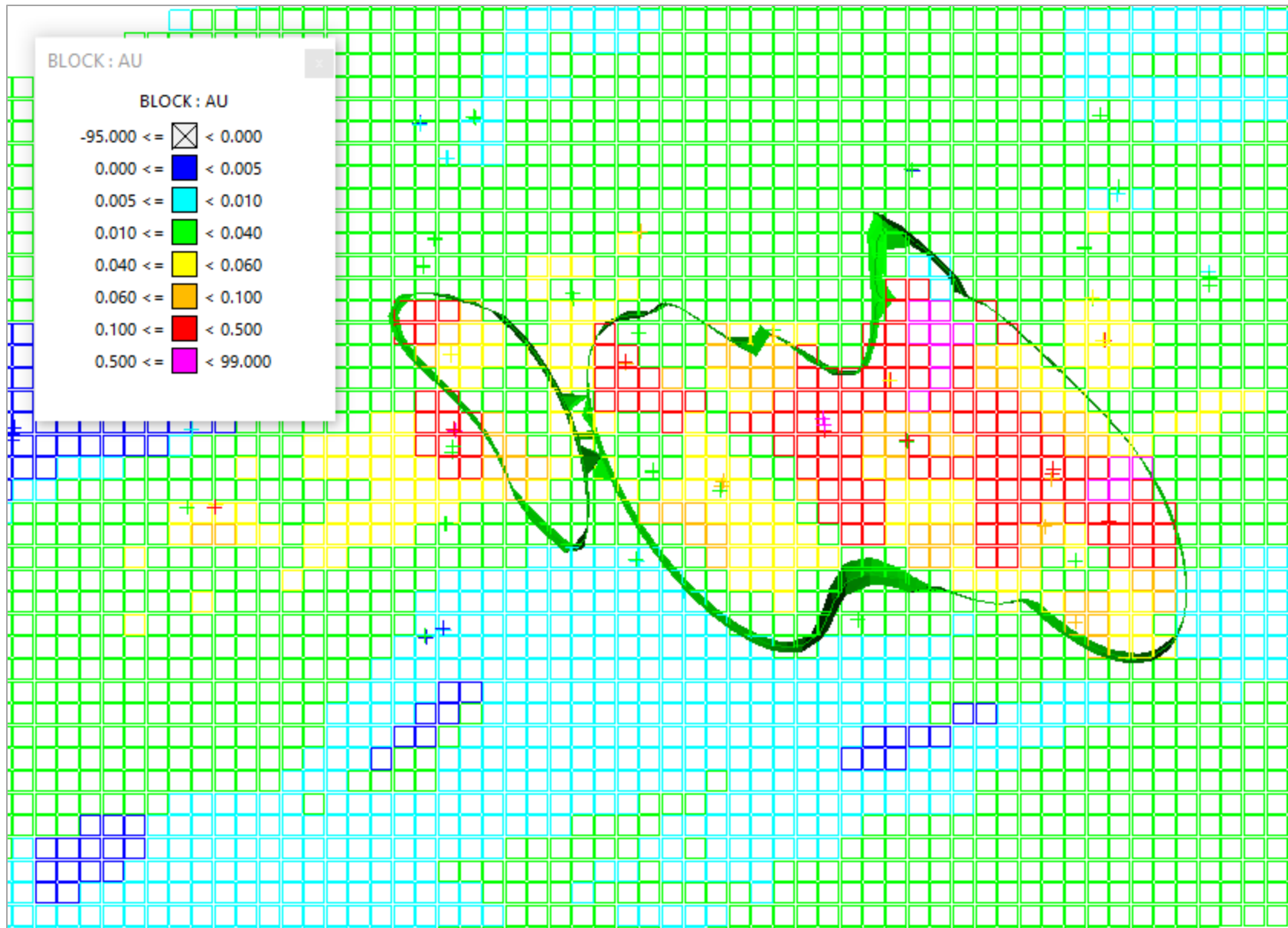
**Figure 47: Plan view section on the 4450 ft. elevation of sample grades (crosses) and estimated grades (boxes). Ordinary Kriging estimate is shown.**
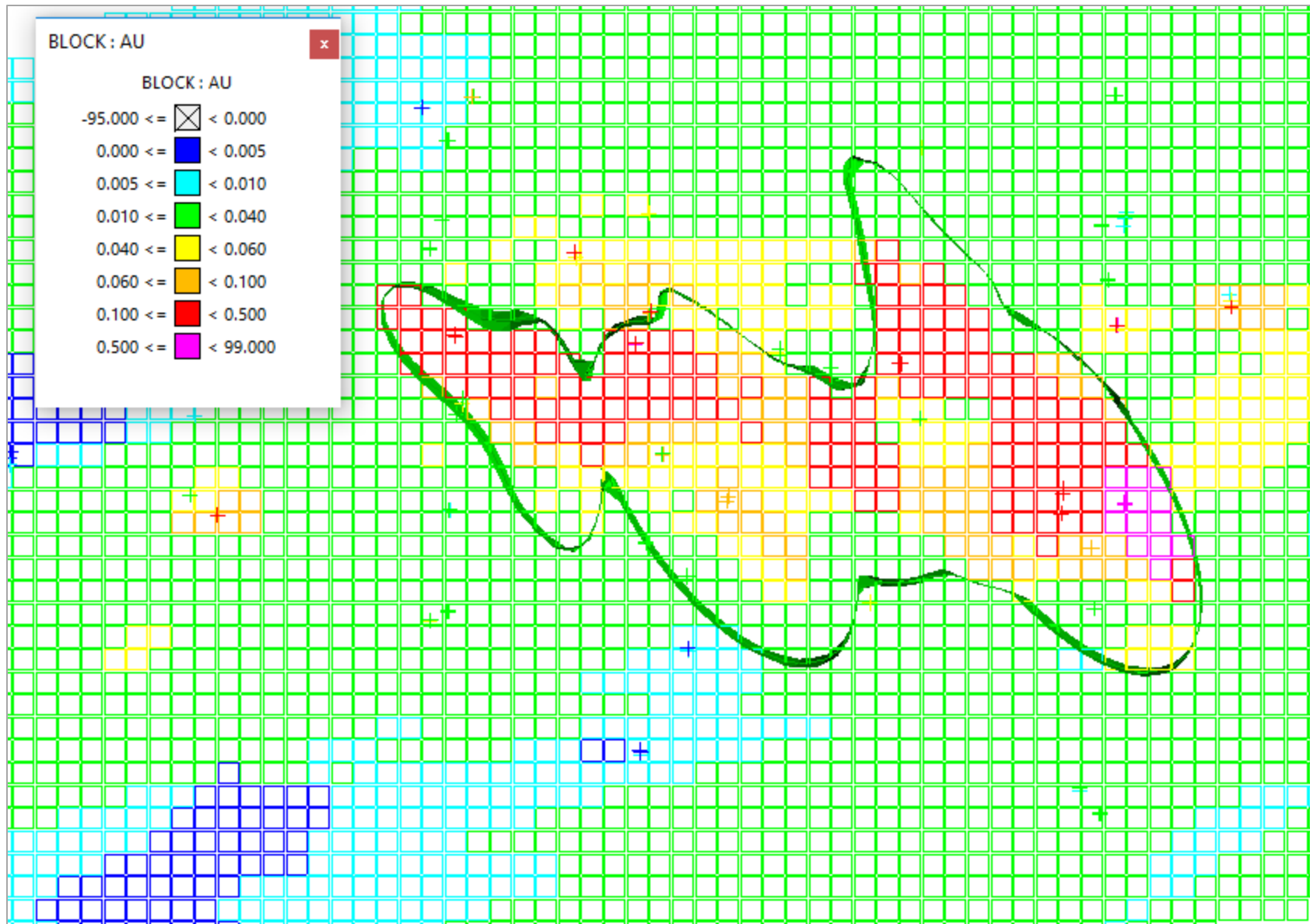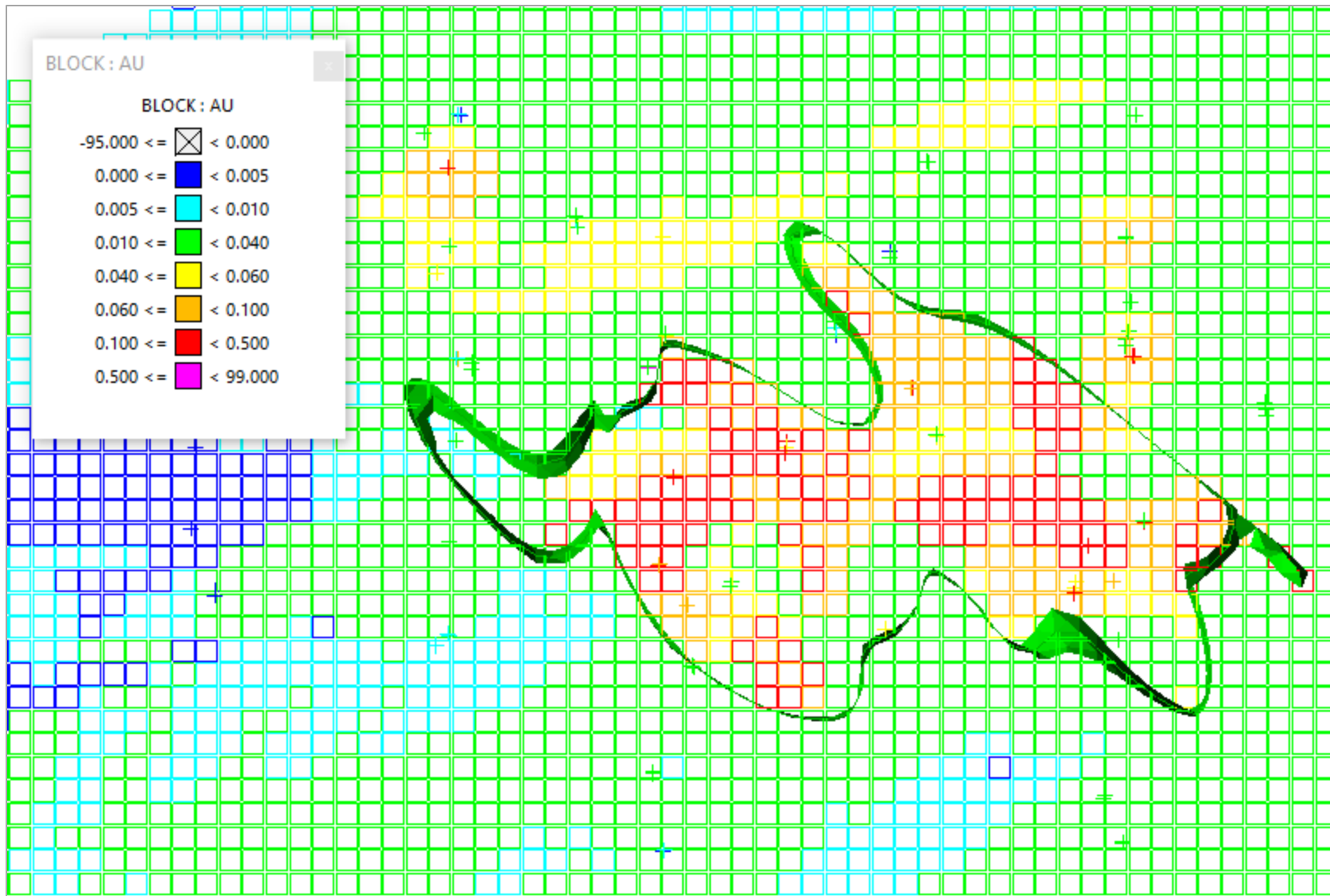
**Figure 48: Plan view section on the 4500 ft. elevation of sample grades (crosses) and estimated grades (boxes). Ordinary Kriging estimate is shown.**
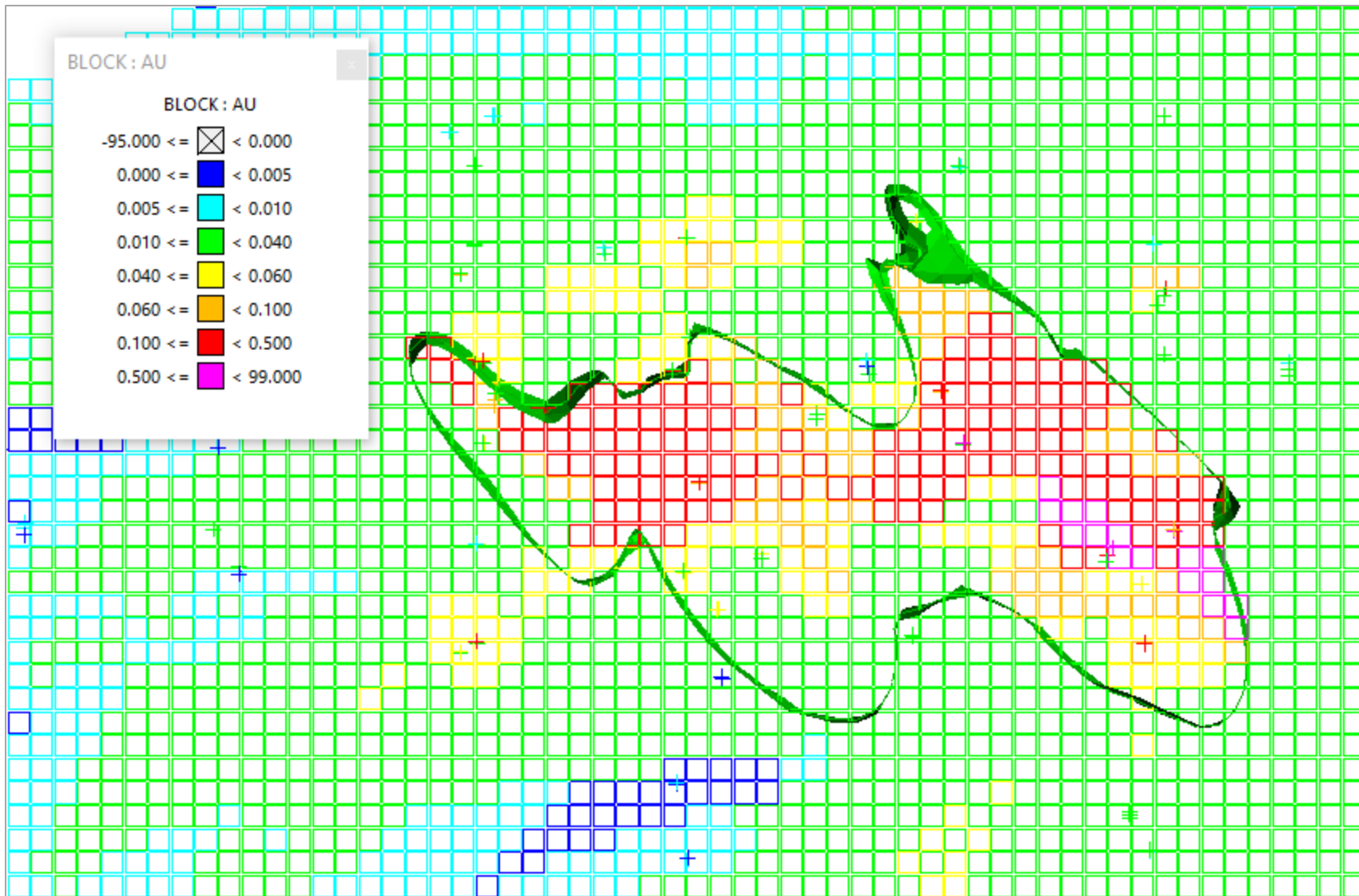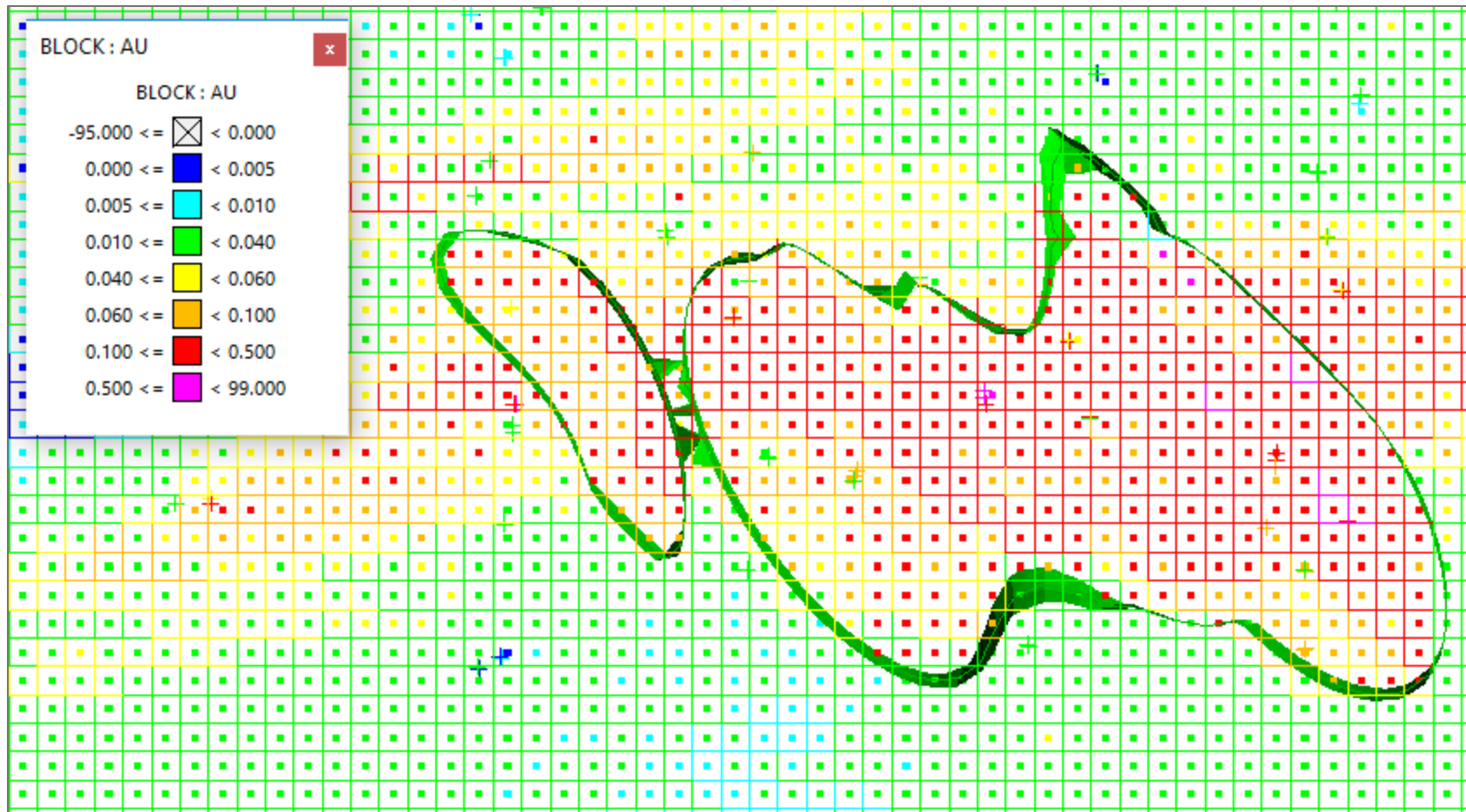
**Figure 49: Plan view section on the 4550 ft. elevation of sample grades (crosses) and estimated grades (boxes). Ordinary Kriging estimate is shown.**

**Figure 50: Plan view section on the 4600 ft. elevation of sample grades (crosses) and estimated grades (boxes). Ordinary Kriging estimate is shown.**

**Figure 51: Plan view section on the 4450 ft. elevation of sample grades (crosses), simulated grades (solid small boxes), and estimated grades (boxes). 30 realization E-type and ordinary kriged estimate shown.**
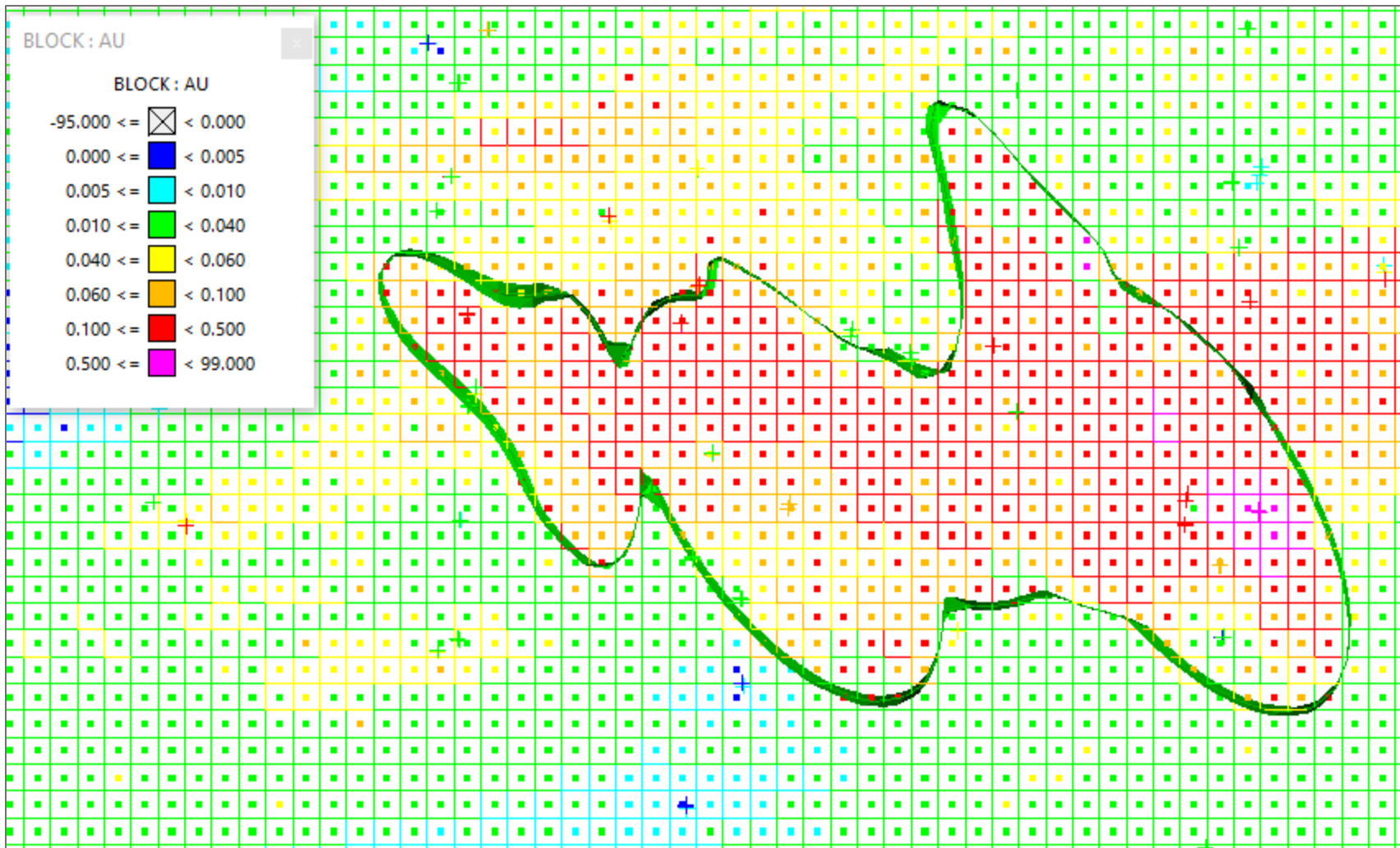
**Figure 52: Plan view section on the 4500 ft. elevation of sample grades (crosses), simulated grades (solid small boxes), and estimated grades (boxes). 30 realization E-type and ordinary kriged estimate shown.**
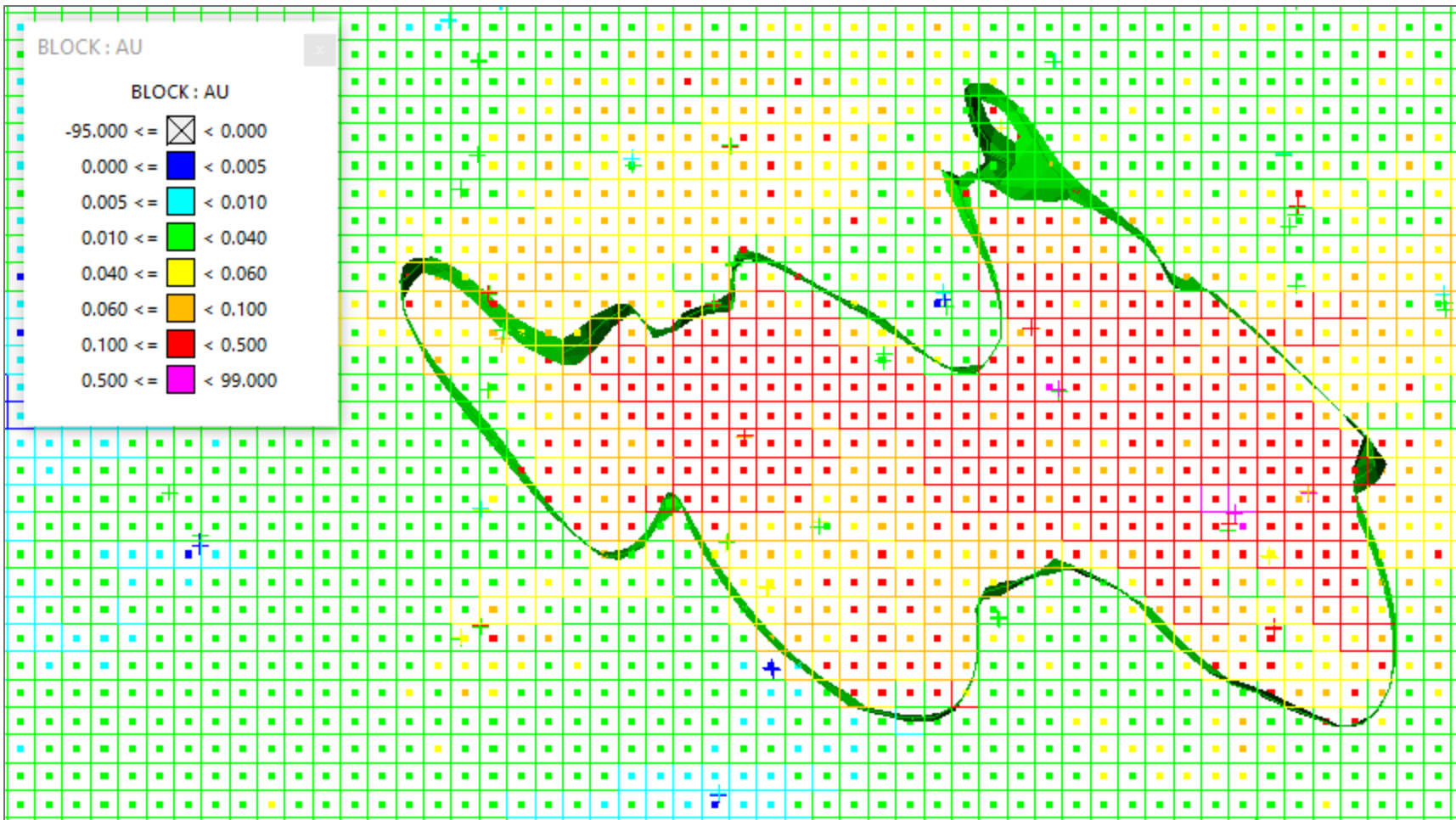
**Figure 53: Plan view section on the 4550 ft. elevation of sample grades (crosses), simulated grades (solid small boxes), and estimated grades (boxes). 30 realization E-type and ordinary kriged estimate shown.**
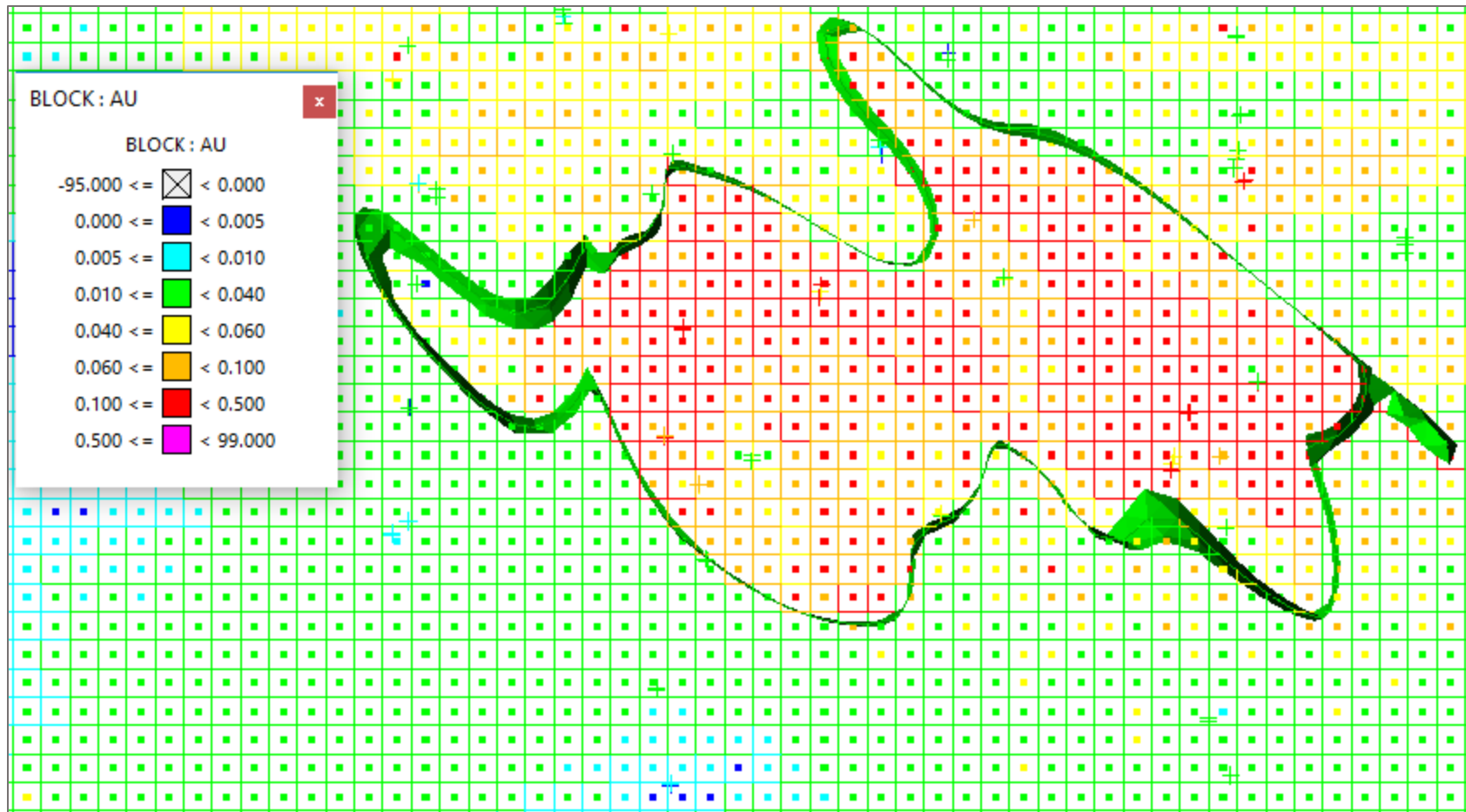
**Figure 54: Plan view section on the 4600 ft. elevation of sample grades (crosses), simulated grades (solid small boxes), and estimated grades (boxes). 30 realization E-type and ordinary kriged estimate shown.**
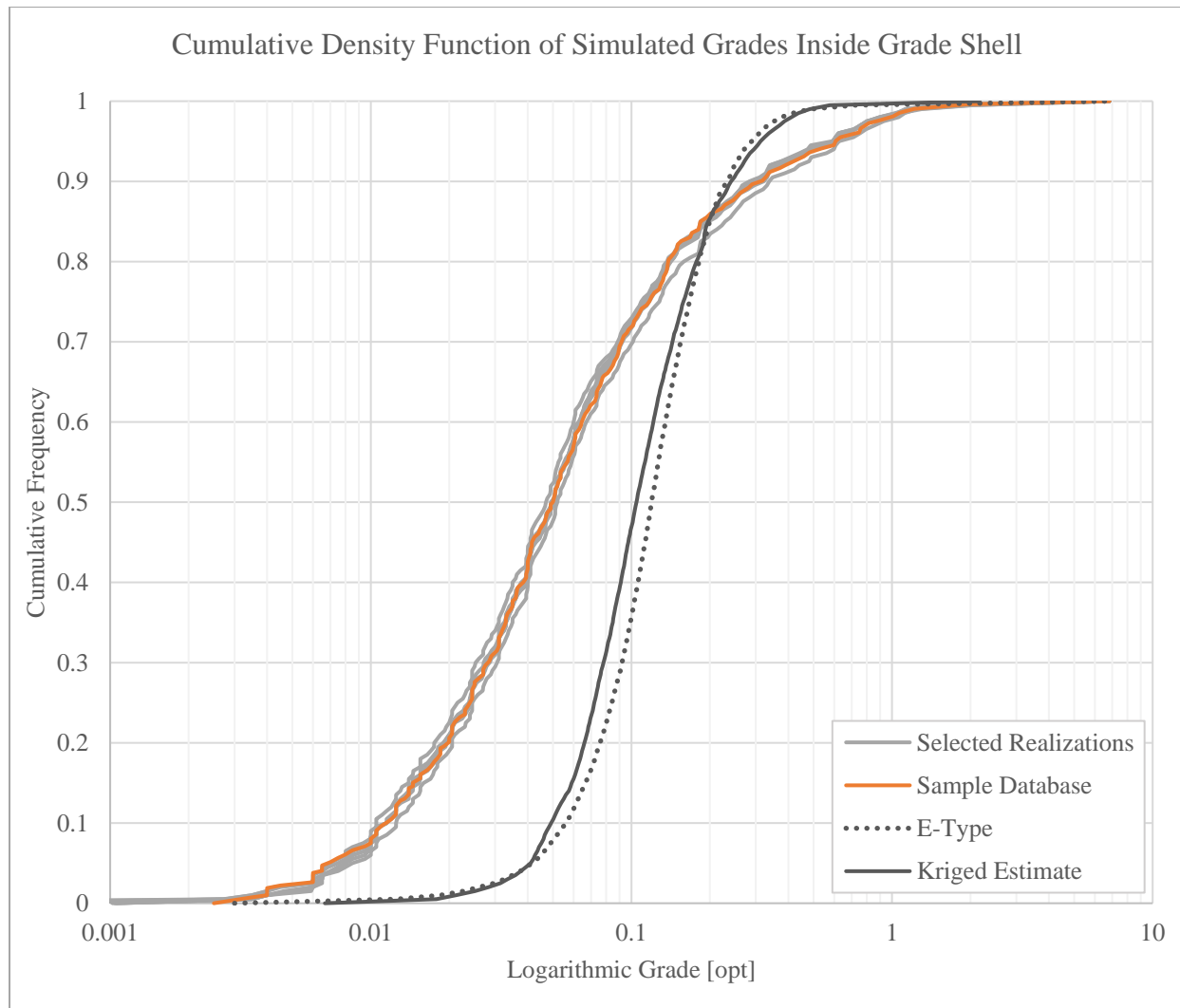
**Figure 55: Logarithmic cumulative density function of simulated grades inside the grade shell**
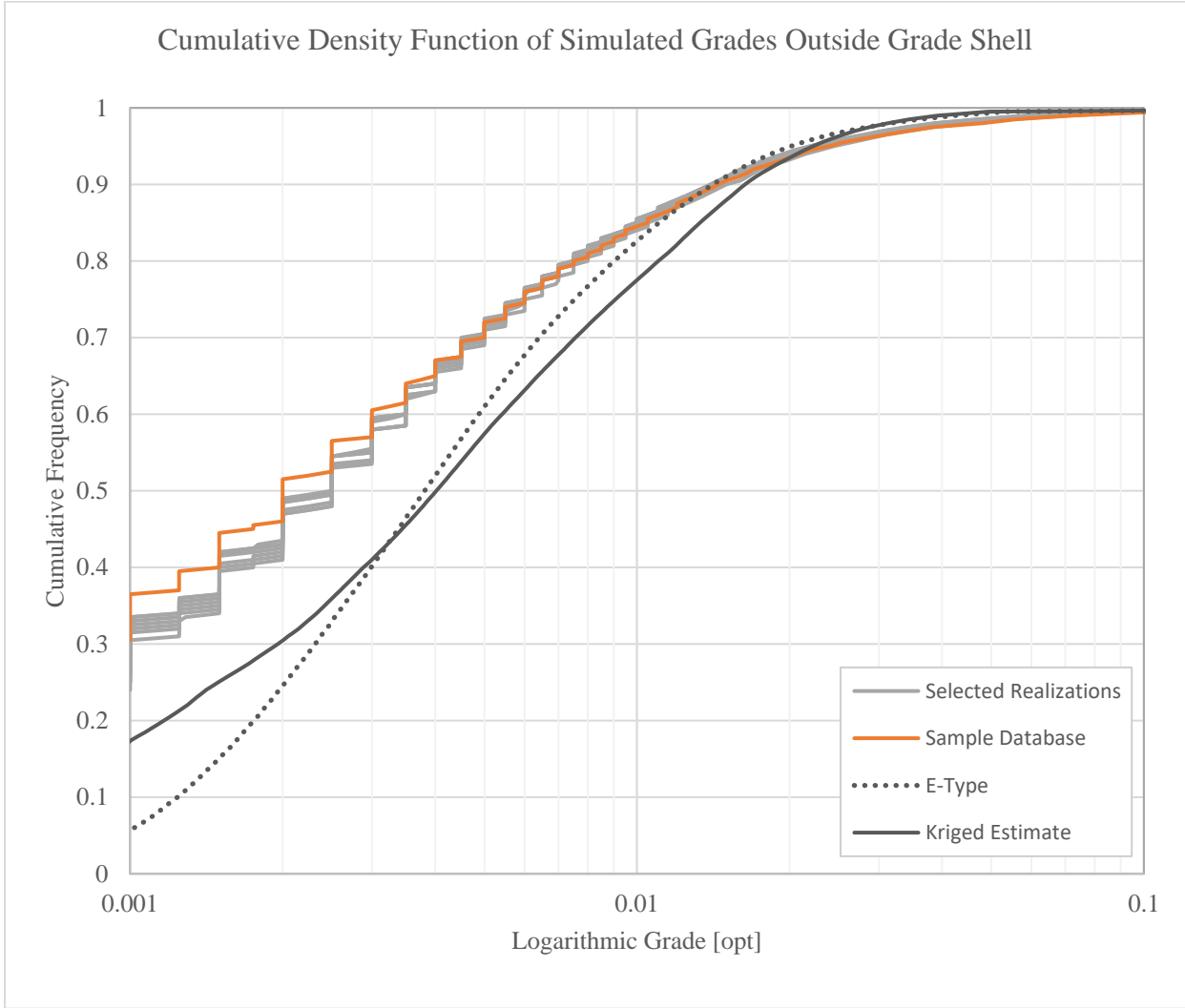
**Figure 56: Logarithmic cumulative density function of simulated grades outside the grade shell**

# 9. Appendix B

The following is a short mineralogy report put together by the author and Prof. Chris Gammons.

Fe-stained clay was sampled from a box of drill core (Box 117) from the West Butte ore body (drill hole PCM-94-566, approximately 710' depth). The interval in question (707.5 to 717') was reported to assay 3.64 opt Au and 1.485 opt Ag. Some of the clay-rich material was physically panned and produced an impressive amount of silt-sized gold grains. The sample was then homogenized, crushed to < 0.5 mm, and sent to Gary Wyss at CAMP for further processing. Mr. Wyss first separated the clay from the clastic material by repeated rinsing and decanting the suspended solids. The clastic material was then separated using di-iodomethane (density of ~3.3 g/ml). The fraction that sank through the heavy liquid (that is, particles with density > 3.2 $g/cm^3$) was cleaned with acetone, dried in an oven, and used for preparation of polished epoxy plugs.

A series of photo-micrographs was taken (following pages) using a reflected light microscope. In these photos, gold (and/or electrum) grains are the bright, yellowish-white grains. The photo-micrographs mostly show grains of gold/electrum that are angular in shape and are attached to particles of gangue minerals. The grains range in size from < 1 µm to > 200 µm in diameter. Additional gold grains were found that occurred as isolated, rounded grains that probably were abraded during crushing. These grains were not photographed because the gold-gangue relationships are no longer shown.

Most of the light gray material in the photographs is thought to be hematite, goethite, and/or Mn-oxides. Some grains of partially oxidized pyrite were found in the samples (not shown here), but none of the pyrite grains had inclusions of gold. Darker gray particles (only slightly brighter than the epoxy) are probably a mix of quartz and other non-reflective gangue minerals such as muscovite, adularia, clays, and carbonate minerals. Further mineral ID is not possible without SEM-EDS.

The most significant finding of this small study is that high-grade intercepts in the oxidized portion of the McDonald deposit may contain significant fractions of relatively coarse-grained gold that could yield relatively-high gold recoveries with gravitational separation methods.

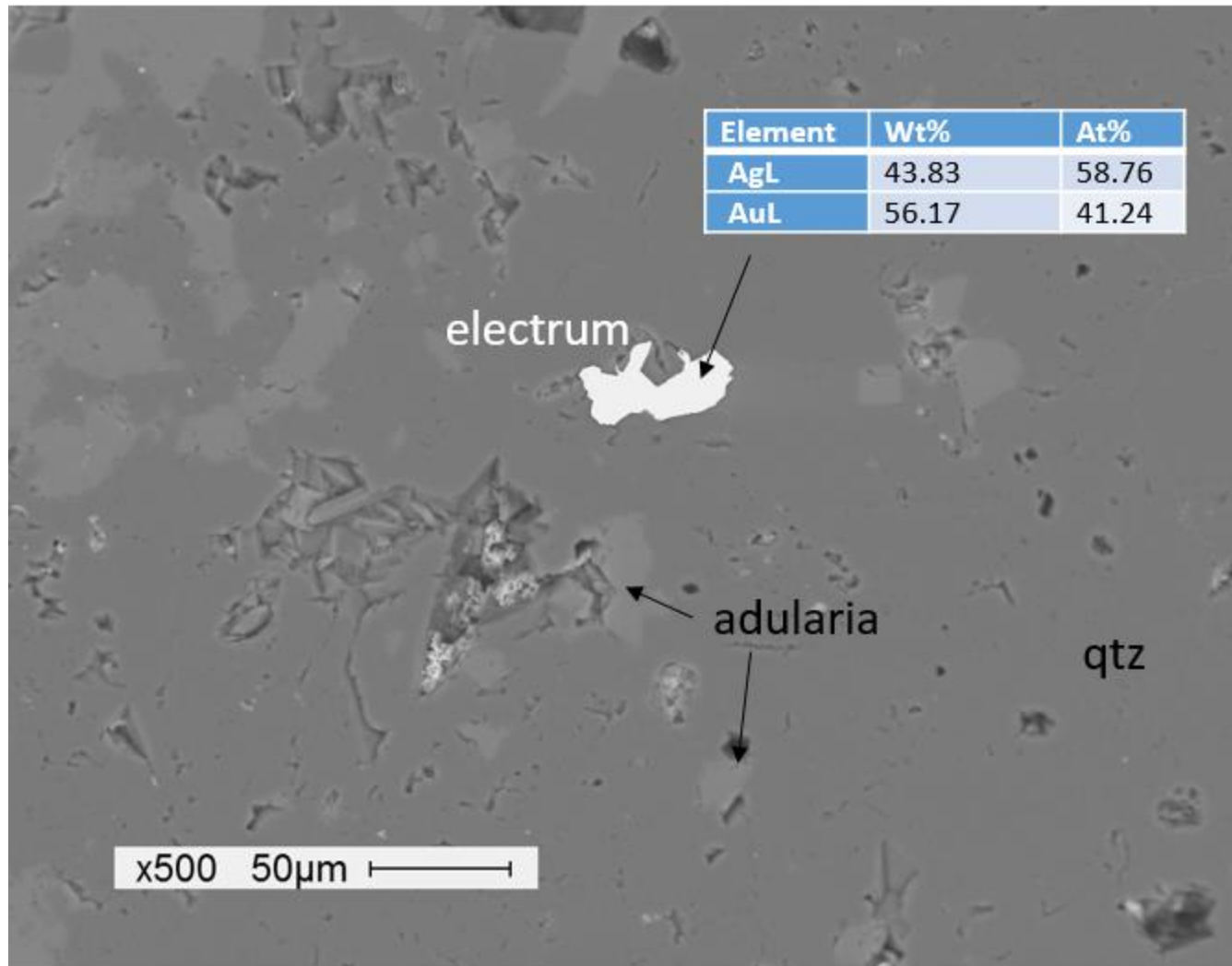| Element | Wt% | At% |
|---------|-------|-------|
| AgL | 43.83 | 58.76 |
| AuL | 56.17 | 41.24 |

Figure B1: SEM-BSE image of a sample taken at 790.4 ft. in drillhole PCM-91-173, showing electrum grains (white) surrounded by a matrix of quartz (qtz) and adularia.
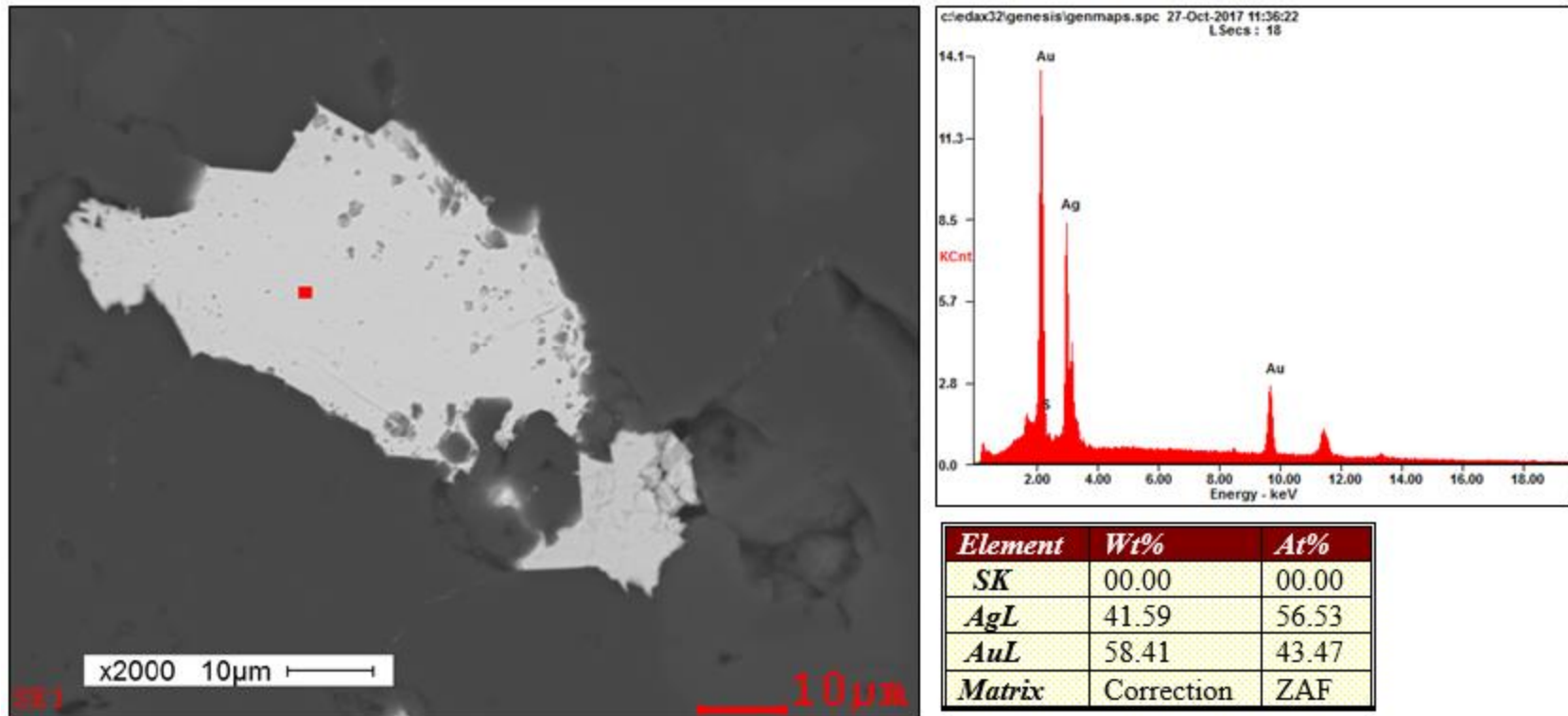
Figure B2: SEM-BSE image of a sample taken at 790.4 ft. in drillhole PCM-91-173, showing an electrum grain (white) surrounded by a matrix of quartz. The red box denotes the area analyzed for composition.
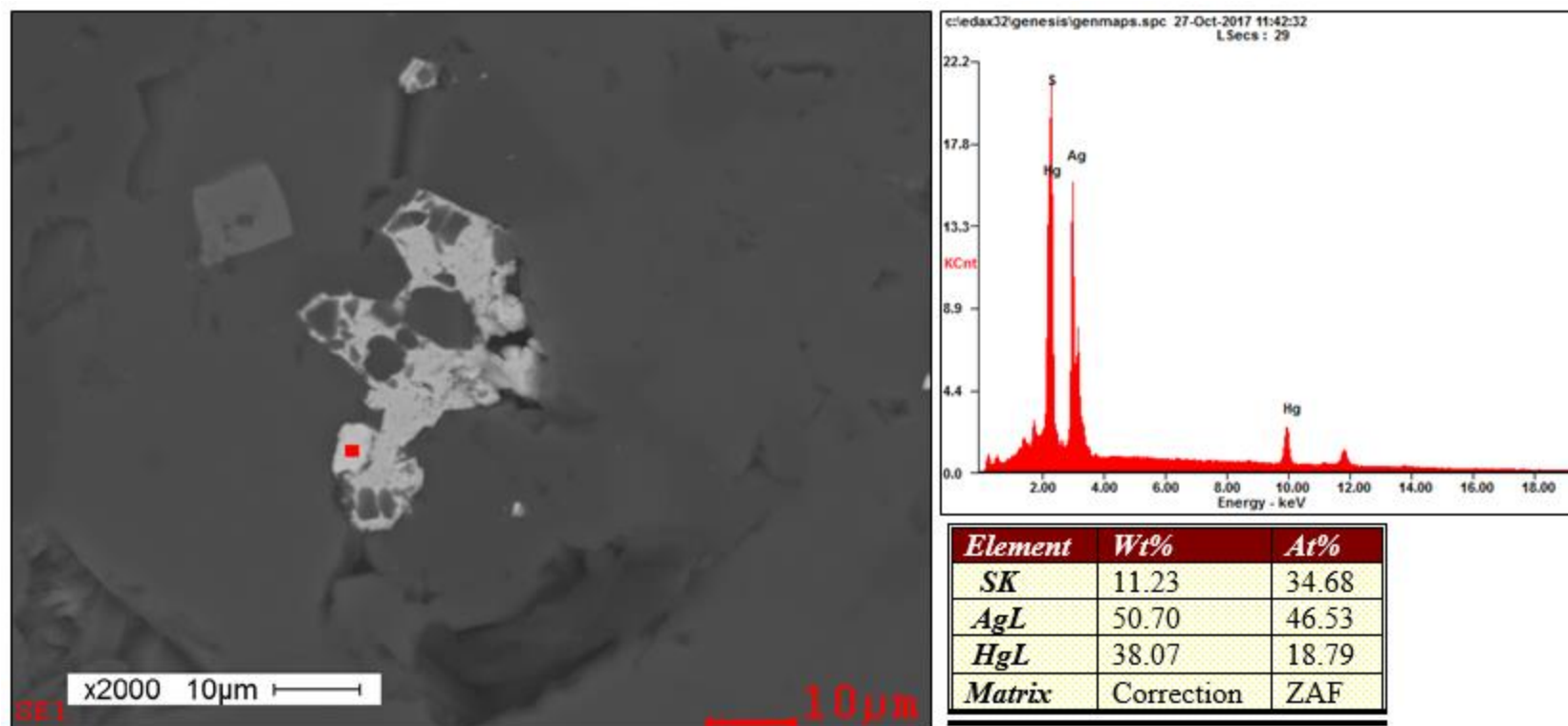
| Element | Wt% | At% |
|---------|-----|-----|
| SK | 00.00 | 00.00 |
| AgL | 41.59 | 56.53 |
| AuL | 58.41 | 43.47 |
| Matrix | Correction | ZAF |

Figure B3: SEM-BSE image of a sample taken at 790.4 ft. in drillhole PCM-91-173 showing acanthite (light gray) and a Ag-Hg sulfide (bright-gray), possibly imiterite ($Ag_2HgS_2$), surrounded by a matrix of quartz (darkest gray). The square (medium gray) mineral to the left is rutile.  The red box denotes the area analyzed for composition.
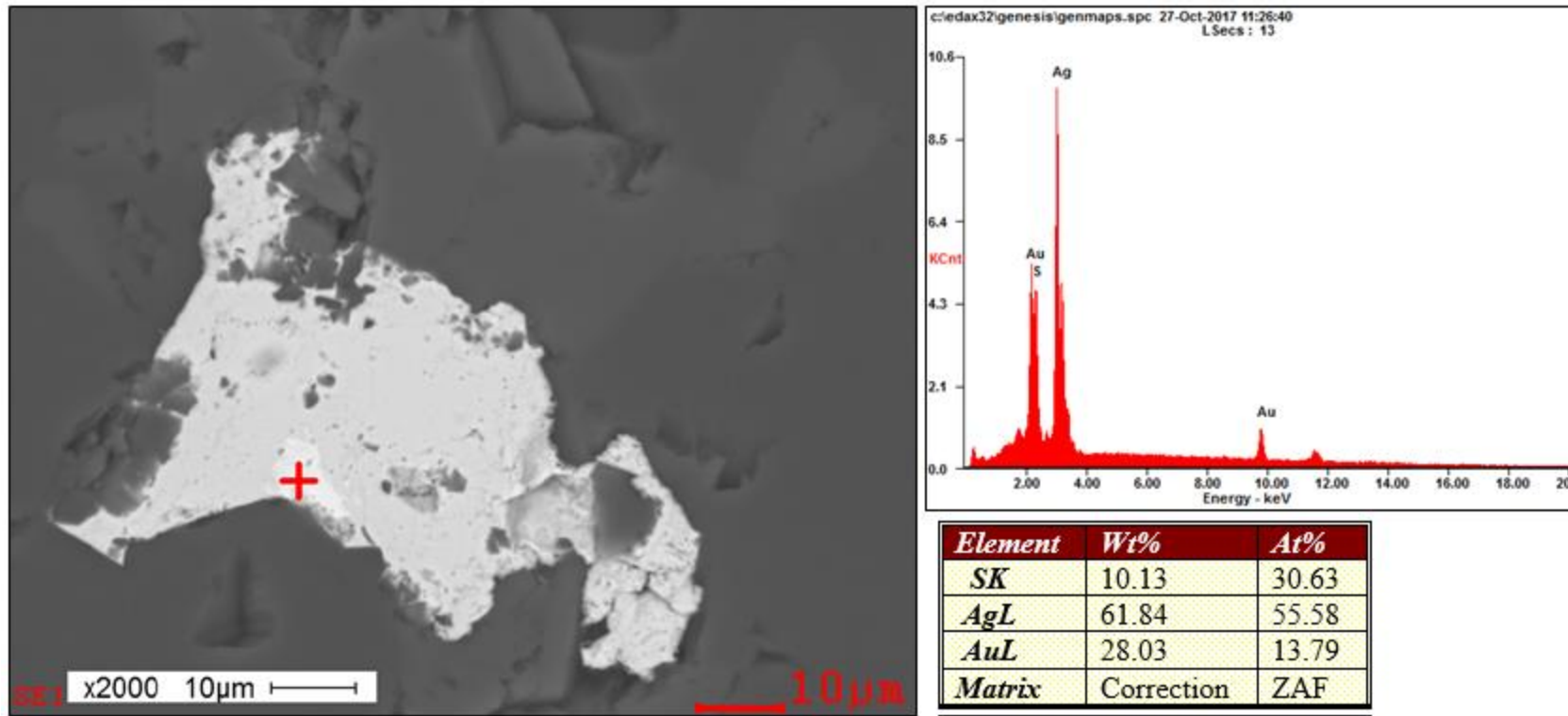
Figure B4: SEM-BSE image of a sample taken at 790.4 ft. in drillhole PCM-91-173 showing acanthite and an Au-Ag sulfide (bright), possibly uytenbogaarditite ($Ag_3AuS_2$), surrounded by a matrix of quartz. The red cross denotes the area analyzed for composition.
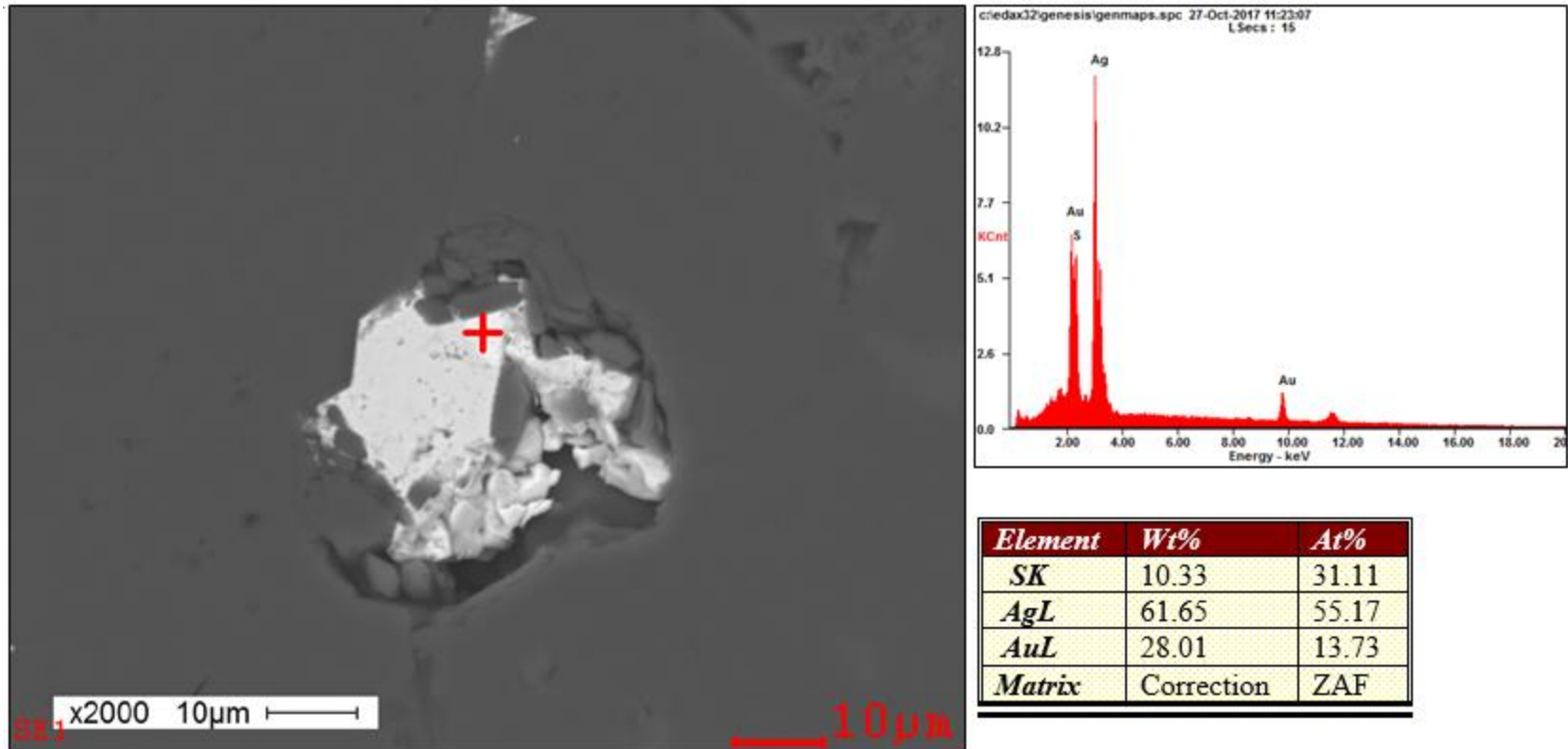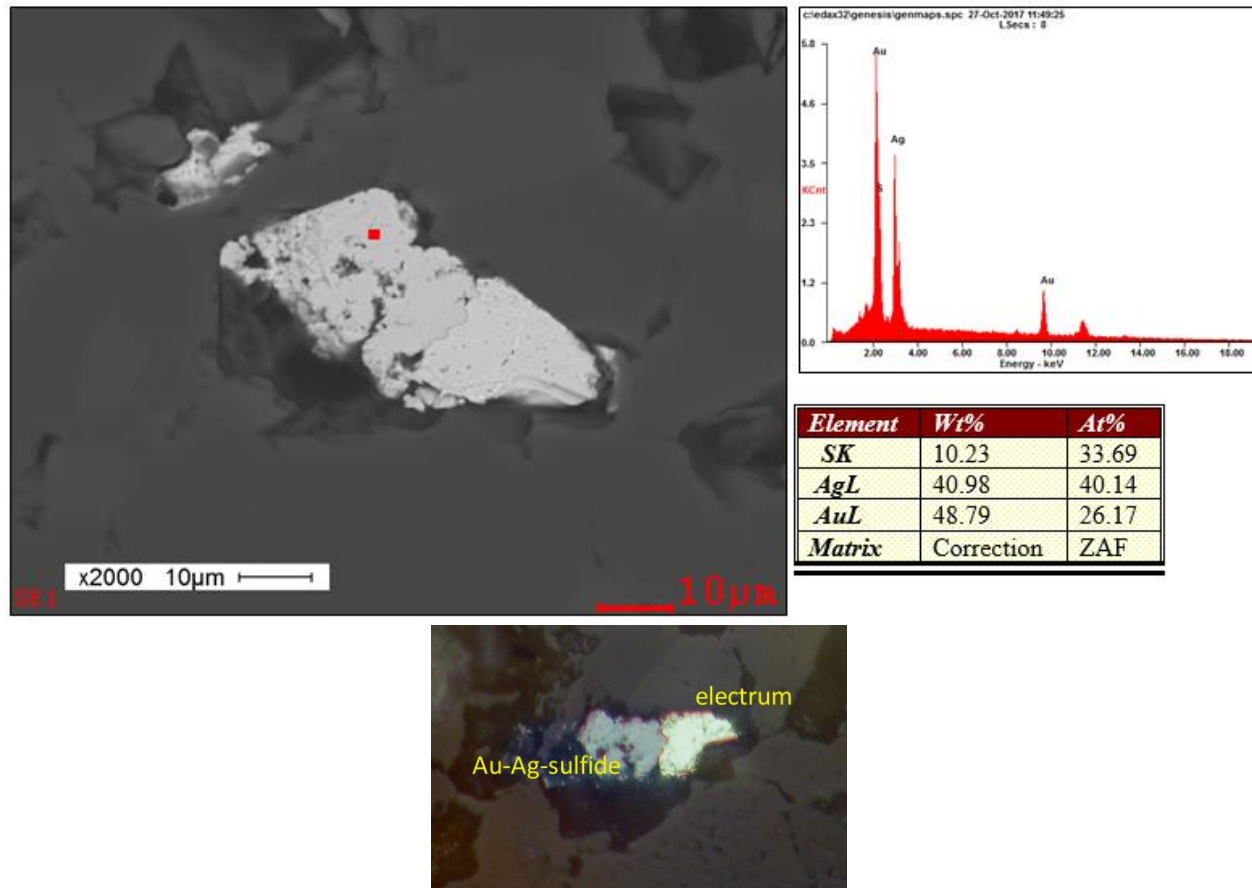
Figure B5: SEM-BSE image of a sample taken at 790.4 ft. in drillhole PCM-91-173 showing acanthite and an Au-Ag sulfide (bright triangular crystal), possibly uytenbogaarditite ($Ag_3AuS_2$), surrounded by a matrix of quartz. The red cross denotes the area analyzed for composition.

Figure B6: SEM-BSE image of a sample taken at 790.4 ft. in drillhole PCM-91-173 showing two electrum grains (light-gray) of varying composition (46 – 56 wt% Au) and an Au-Ag sulfide (red dot, slightly darker than electrum). The EDS analysis suggests a stoichiometry of $Ag_4Au_3S_3$, which is not a known mineral. More work (e.g., electron microprobe) would be needed to confirm the composition of this phase. The color image is a photograph of the same grain cluster taken in reflected light.
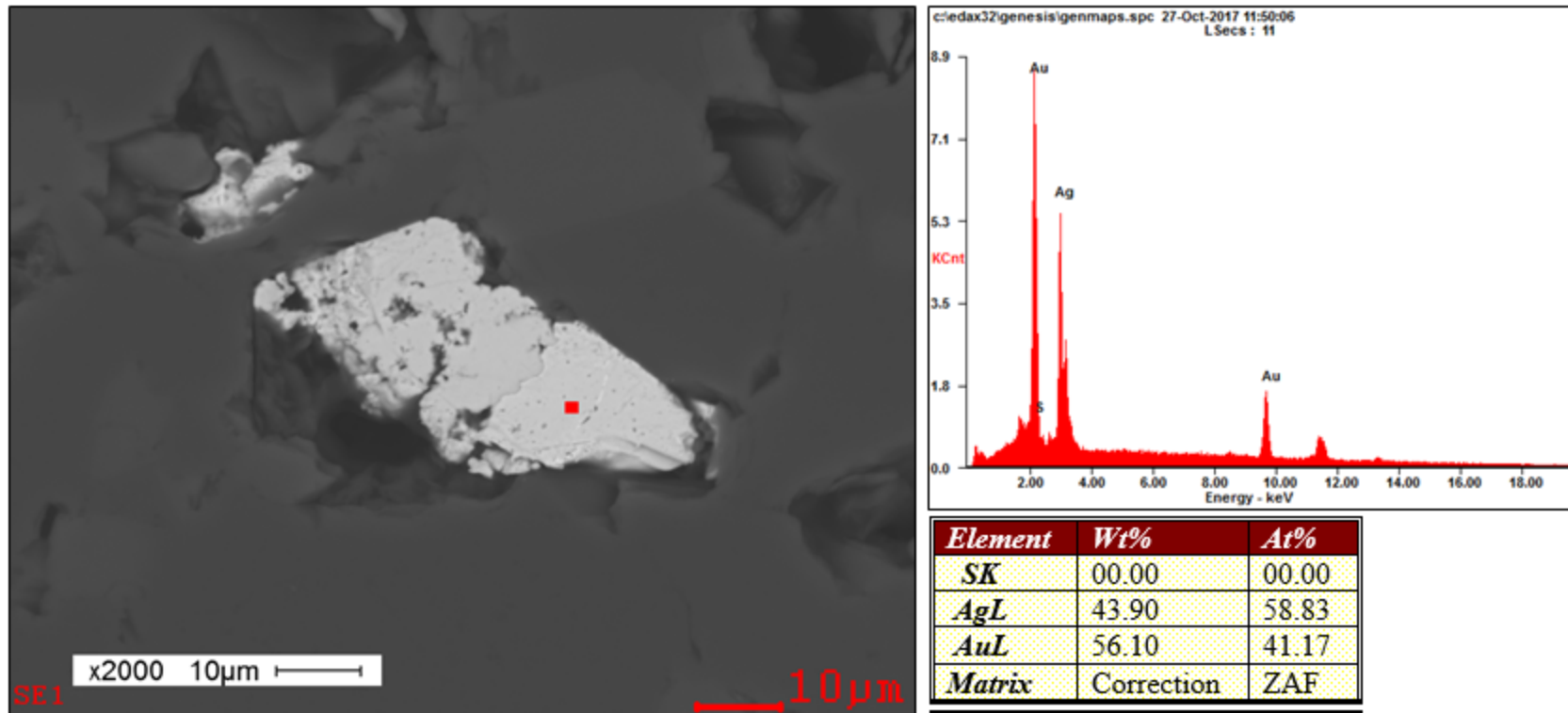
| Element | Wt% | At% |
|---------|-----|-----|
| SK | 00.00 | 00.00 |
| AgL | 43.90 | 58.83 |
| AuL | 56.10 | 41.17 |
| Matrix | Correction | ZAF |

Figure B7: SEM-BSE image of the same sample from as previous page showing analysis of electrum.
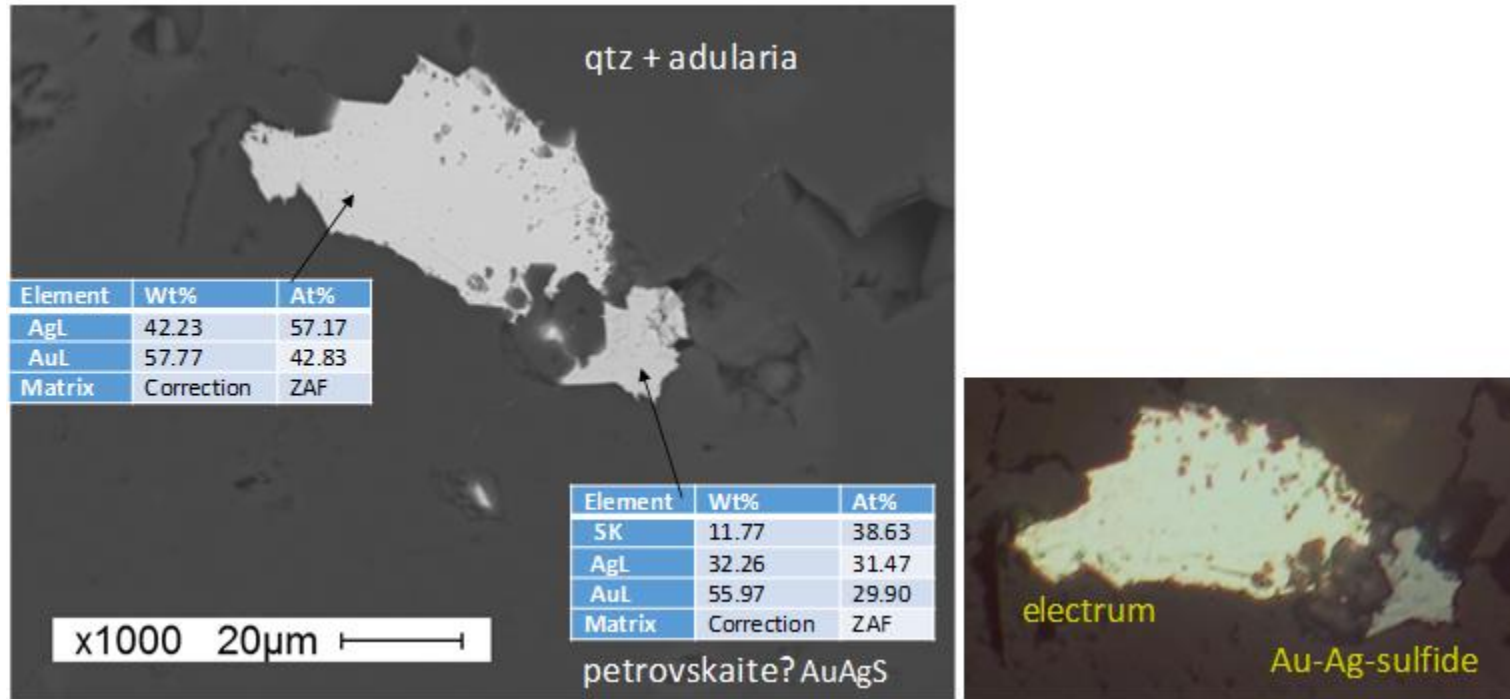
Figure B8: SEM-BSE image (left) and reflected light image (right) of a sample taken at 790.4 ft. in drillhole PCM-91-173 showing a large electrum grain and an Au-Ag sulfide, most likely petrovskaite (AuAgS).
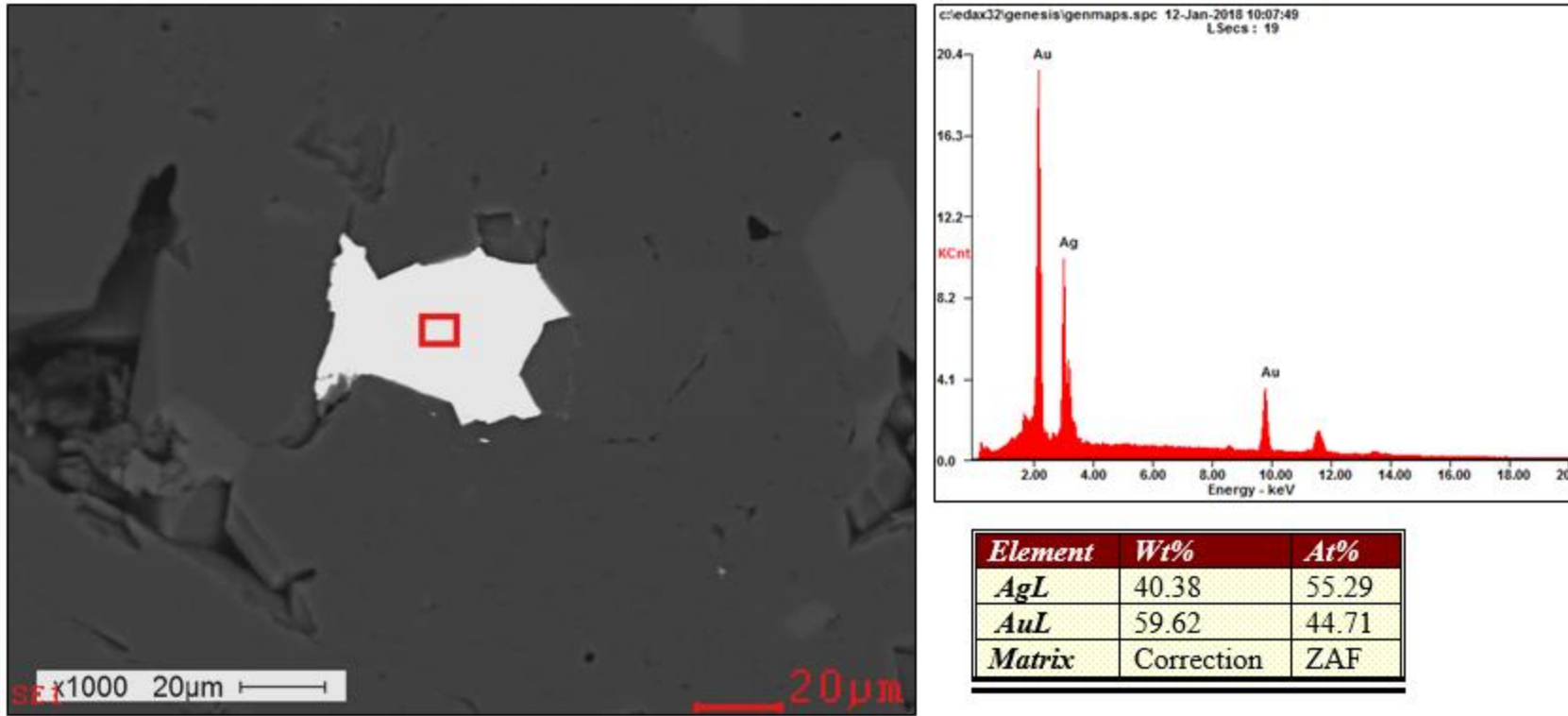
Figure B9: Photomicrograph of a sample taken at 790.4 ft. in drillhole PCM-91-173 using scanning electron microscopy/energy-dispersive X-ray spectroscopy (SEM-EDS). Photomicrograph shows an electrum grain (white) surrounded by a matrix of quartz and adularia. The red box denotes the area analyzed for composition.
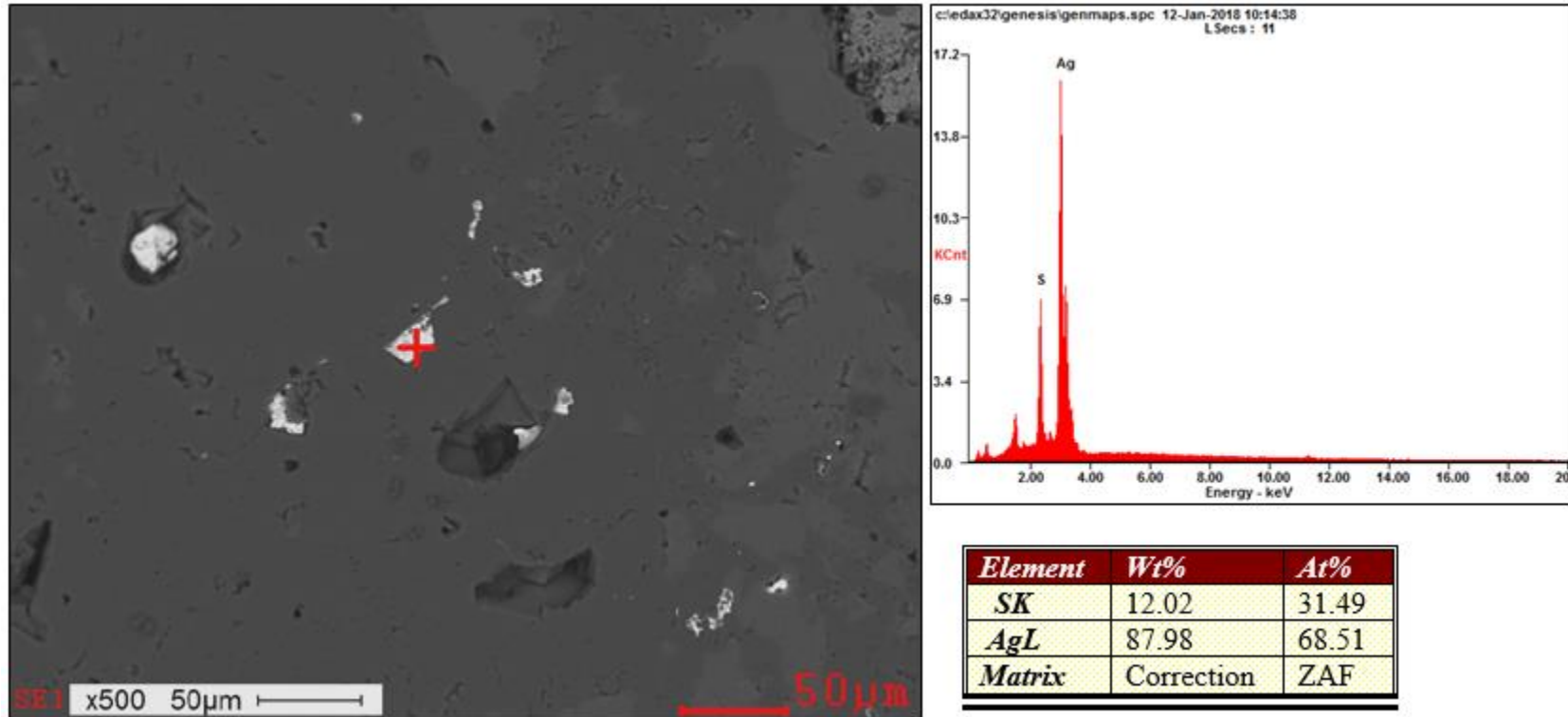
Figure B10: Photomicrograph of a sample taken at 790.4 ft. in drillhole PCM-91-173 using scanning electron microscopy/energy-dispersive X-ray spectroscopy (SEM-EDS). Photomicrograph shows grains of acanthite (white) surrounded by a matrix of quartz and adularia. The red cross denotes the area analyzed for composition
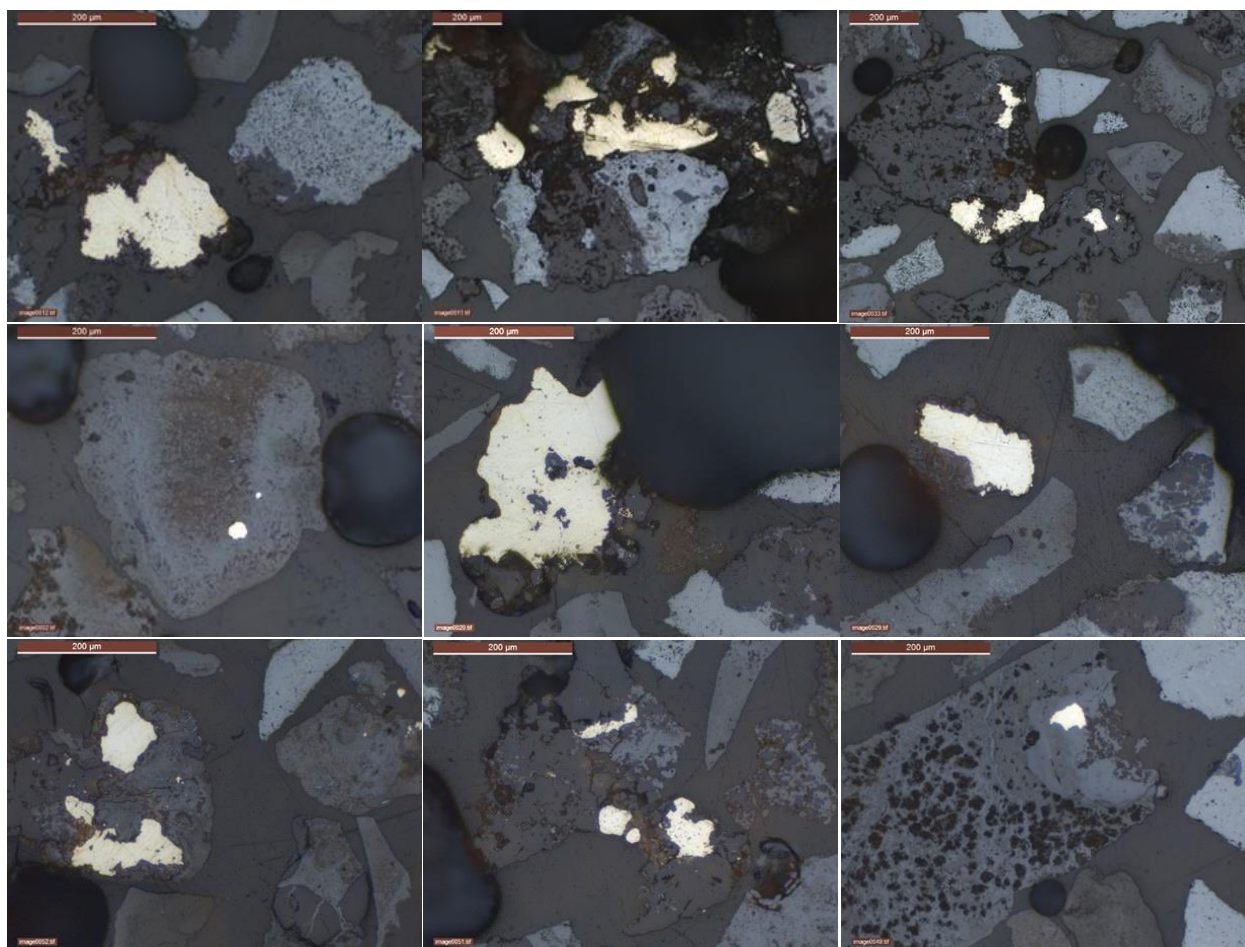
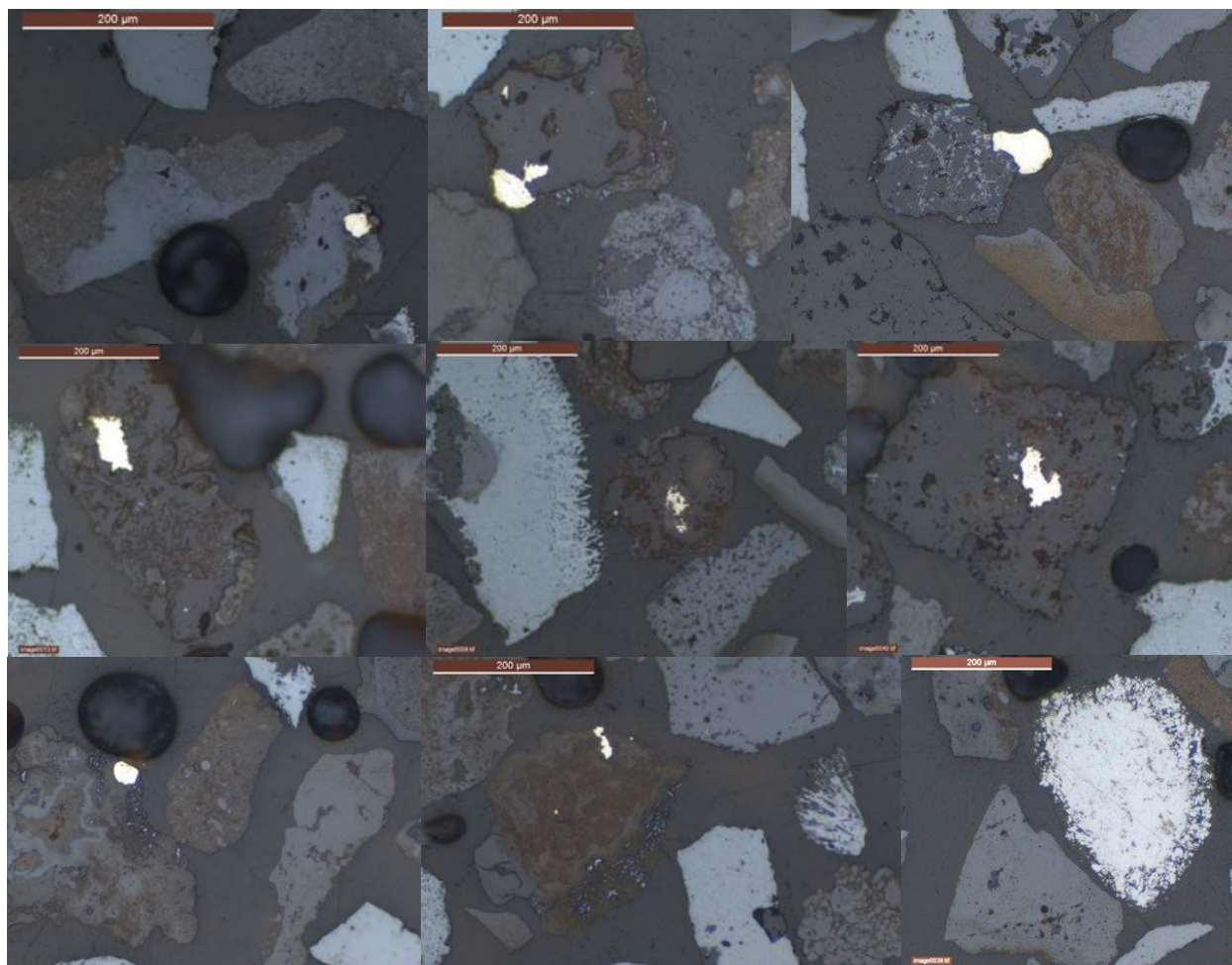Figure B11: Gold and electrum grains from McDonald (drillhole PCM-94-566, 710' depth).
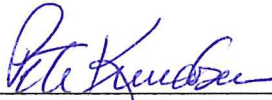
Figure B12: Additional photographs of gold and electrum grains from the same sample (drillhole PCM-94-566, 710' depth). The bright grain in lower right panel is an unknown mineral (not gold).

# SIGNATURE PAGE

This is to certify that the thesis prepared by Jonathan Szarkowski entitled "Resource Estimation and Simulation at West Butte in the McDonald Gold Deposit near Lincoln, Montana" has been examined and approved for acceptance by the Department of Geological Engineering, Montana Technological University, on this 26th day of April, 2019.

Christopher Gammons, PhD, PG, Professor
Department of Geological Engineering
Chair, Examination Committee

Pete Knudsen, PhD, PE, Professor Emeritus
Department of Mining Engineering
Member, Examination Committee

Christopher Roos, MS, PE, Assistant Professor
Department of Mining Engineering
Member, Examination Committee